POÇOS DE CALDAS PROJECT

NAGRA NTB 90-33
SKB TR 90-24
UK DOE WR 90-055

Poços de Caldas Report No. 15

Summary and implications for radioactive waste management

JANUARY 1991

An international project with the participation of Brazil, Sweden (SKB), Switzerland (NAGRA), United Kingdom (UK DOE) and USA (US DOE). The project is managed by SKB, Swedish Nuclear Fuel and Waste Management Co.

POÇOS DE CALDAS PROJECT

NAGRA NTB 90-33
SKB TR 90-24
UK DOE WR 90-055

Poços de Caldas Report No. 15

Summary and implications for radioactive waste management

JANUARY 1991

An international project with the participation of Brazil, Sweden (SKB), Switzerland (NAGRA), United Kingdom (UK DOE) and USA (US DOE). The project is managed by SKB, Swedish Nuclear Fuel and Waste Management Co.

"You can't always get what you want,
but if you try, sometimes,
you might find you get what you need".

M. Jagger & K. Richards

****

The Poços de Caldas Project: Summary and implications for radioactive waste management

N.A. Chapman[1], I.G. McKinley[2], M.E. Shea[3], J.A.T. Smellie[4]

[1]INTERA Sciences, Geosciences Group, Park View House, 14B Burton Street, Melton Mowbray, Leicestershire LE13 1AE (England)

[2]Nagra, Hardstrasse 73, 5430 Wettingen (Switzerland)

[3]University of Chicago, Dept. of Geological Sciences, 5734 S. Ellis Avenue, Chicago, IL 60615 (USA)

[4]Conterra AB, P.O. Box 493, 75106 Uppsala (Sweden)

Abstract

This report provides an overview of the Poços de Caldas natural analogue study, aspects of which have been described in detail in the previous 14 reports of this series.

The first part of this report provides the historical background to the project, describes the research programme developed at the Osamu Utsumi and Morro do Ferro sites and summarises the main findings of the geological, hydrologic and geochemical characterisation work.

This is followed by reviews of the four analogue sub-projects - testing geochemical models of trace element solubility and speciation, evaluation of models of redox front development and movement, examining the rôle of natural colloids as a vector for transport of trace elements and appraisal of a modelling approach to quantifying hydrothermal alteration and solute transport processes.

Finally, the direct implications of the project to radioactive waste management are discussed along with some valuable spin-off which was identified. Such a large multi-disciplinary study proved a very valuable focus for forging contacts between specialists from different disciplines in a manner closely analogous to that required for an integrated site assessment. The iterative development of the modellers' wish lists and the field/lab analytical programme was a key to the success of this Project and provides guidelines for site-specific performance assessment.

Zusammenfassung

Dieser Bericht gibt einen Ueberblick über die Poços de Caldas Analogstudie, deren verschiedene Forschungsaspekte in den 14 vorangegangenen Berichten dieser Serie im Detail beschrieben wurden.

Der erste Teil dieses Berichtes informiert über den historischen Hintergrund des Projektes, beschreibt die Untersuchungsprogramme für die Orte Morro do Ferro und Osamu Utsumi U-Mine und fasst die wichtigsten Erkenntnisse zur Geologie, Hydrologie und Geochemie dieser zwei Untersuchungsstellen zusammen.

Es folgt ein Ueberblick über die vier Analog-Unterprojekte: Prüfung geochemischer Modelle zur Löslichkeit und Speziation von Spurenelementen, Bewertung von Modellen zur Entstehung und Fortbewegung von Redoxfronten, Beurteilung der Rolle von Kolloiden für den Transport von Spurenelementen und Bewertung eines Näherungsmodells zur Quantifizierung von Gesteinsveränderungen und Lösungstransportprozessen unter hydrothermalen Bedingungen.

Zum Abschluss werden die direkten Folgerungen aus dem Projekt für die Lagerung radioaktiver Abfälle diskutiert und einige zusätzliche Erkenntnisse mitgeteilt. Dieses grosse, multidisziplinäre Projekt erwies sich als sehr nützlich, um Kontakte zwischen Fachspezialisten verschiedener Disziplinen zu knüpfen, ähnlich wie das für eine integrierte Standortbeurteilung erforderlich wäre. Die iterative Entwicklung der Wunschliste der Modellierer und des analytischen Feld-/Laborprogramms war für den Erfolg des Projektes mitentscheidend und kann Richtlinien für die standortspezifische Sicherheitsanalyse geben.

Résumé

Ce rapport présente une vue générale des études effectuées au site d'analogies naturelles de Poços de Caldas. Ces études sont décrites dans les 14 premiers rapports de la présente série.

Dans sa première partie, ce rapport présente un historique du projet, décrit le programme des recherches entreprises sur les sites de Osamu Utsumi et de Morro do Ferro, et résume les principaux résultats des travaux géologiques, hydrologiques et géochimiques.

Ensuite, il passe en revue les quatre sous-projets d'analogies naturelles, à savoir le contrôle de modèles géochimiques sur la solubilité et la spéciation d'éléments trace, l'évaluation de modèles sur le développement et le déplacement de fronts redox, l'examen du rôle joué par des colloïdes naturels comme vecteur de transport d'éléments trace, et le bien-fondé d'une approche par modèles pour la quantification de l'altération hydrothermale et des processus de transport de soluté.

Enfin, le rapport examine les implications directes du projet pour la gestion des déchets radioactifs, et commente quelques voies nouvelles identifiées. Une étude multi-disciplinaire d'aussi grande envergure s'est avérée extrêmement utile pour développer des contacts entre spécialistes de différentes disciplines, de manière semblable à ce qui devrait se faire pour la qualification intégrée d'un site. La réalisation itérative des souhaits des modéliseurs et du programme analytique sur le terrain et en laboratoire fut une clé du succès de ce projet et peut servir de guide pour la définition du processus d'évaluation d'un site particulier.

Preface

The Poços de Caldas Project was designed to study processes occurring in a natural environment which contains many features of relevance for the safety assessment of radioactive waste disposal. The study area, in the State of Minas Gerais, Brazil, is a region of high natural radioactivity associated with volcanic rocks, geothermal springs and uranium ore deposits. It contains two sites of particular interest on which the project work was focussed: the Osamu Utsumi uranium mine and the Morro do Ferro thorium/rare-earth ore body. The first site is notable in particular for the prominent redox fronts contained in the rock, while Morro do Ferro was already well-known as one of the most naturally radioactive locations on the surface of the Earth, owing to the high thorium ore grade and the shallow, localised nature of the deposit.

The features displayed by these two sites presented the opportunity to study a number of issues of concern in repository performance assessment.

The project ran for three and a half years from June 1986 until December 1989 under the joint sponsorship of SKB (Sweden), NAGRA (Switzerland), the Department of the Environment (UK) and the Department of Energy (USA), with considerable support from a number of organisations in Brazil, notably Nuclebrás (now Urânio do Brasil). The first-year feasibility study was followed by two and a half years of data collection and interpretation.

This report is one of a series of 15; a complete list of reports is given below. Those in series A present data and interpretations of the sites, while those in series B present the results of modelling the data with performance assessment objectives in mind. The main findings of the project are summarised in detail in this report (no. 15).

Poços de Caldas Project Report Series

Series A: Data, Descriptive, Interpretation

Report No.	Topic	Authors (Lead in Capitals)
1.	The regional geology, mineralogy and geochemistry of the Poços de Caldas alkaline caldera complex, Minas Gerais, Brazil.	SCHORSCHER, Shea.
2.	Mineralogy, petrology and geochemistry of the Poços de Caldas analogue study sites, Minas Gerais, Brazil. I: Osamu Utsumi uranium mine.	WABER, Schorscher, Peters.
3.	Mineralogy, petrology and geochemistry of the Poços de Caldas analogue study sites, Minas Gerais, Brazil. II: Morro do Ferro.	WABER.
4.	Isotopic geochemical characterization of selected nepheline syenites and phonolites from the Poços de Caldas alkaline complex, Minas Gerais, Brazil.	SHEA.
5.	Geomorphological and hydrogeological features of the Poços de Caldas caldera and the Osamu Utsumi mine and Morro do Ferro analogue study sites, Brazil.	HOLMES, Pitty, Noy.
6.	Chemical and isotopic composition of groundwaters and their seasonal variability at the Osamu Utsumi and Morro do Ferro analogue study sites, Poços de Caldas, Brazil.	NORDSTROM, Smellie, Wolf.
7.	Natural radionuclide and stable element studies of rock samples from the Osamu Utsumi mine and Morro do Ferro analogue study sites, Poços de Caldas, Brazil.	MacKENZIE, Scott, Linsalata, Miekeley, Osmond, Curtis.
8.	Natural series radionuclide and rare-earth element geochemistry of waters from the Osamu Utsumi mine and Morro do Ferro analogue study sites, Poços de Caldas, Brazil.	MIEKELEY, Coutinho de Jesus, Porto da Silveira, Linsalata, Morse, Osmond.
9.	Chemical and physical characterisation of suspended particles and colloids in waters from the Osamu Utsumi mine and Morro do Ferro analogue study sites, Poços de Caldas, Brazil.	MIEKELEY, Coutinho de Jesus, Porto da Silveira, Degueldre.
10.	Microbiological analysis at the Osamu Utsumi mine and Morro do Ferro analogue study sites, Poços de Caldas, Brazil.	WEST, Vialta, McKinley.

Series B: Predictive Modelling and Performance Assessment

Summary Report

Contents

CHAPTER 1. INTRODUCTION

Over very long time periods, buried radioactive wastes will come to behave as an integral part of their surrounding geological environment. Predicting what this future behaviour will be is considerably facilitated by comparison with the evolution of parallel natural geochemical systems, particularly those that are rich in radioelements. The geochemical processes that are included in performance assessment models for waste repositories can be found in nature, where they have been active over long periods of time. It should be made clear that no natural system represents an entire repository concept. However, detailed characterisation of such occurrences helps to refine models and give confidence in their predictions. This approach, namely seeking similar circumstances in nature (so-called natural analogues), has developed considerably in profile since 1984 when the first guidelines were sketched out (Chapman *et al.*, 1984; Côme and Chapman, 1985).

Although many important natural analogue findings have arisen from detailed studies of specific occurrences of a particular process or material, it was clear that interpreting radionuclide mobilisation and transport from ore deposits would involve so many technical aspects that a complete picture could only be gained through large-scale international effort. In 1984, the Poços de Caldas region of the state of Minas Gerais in Brazil was identified as potentially highly instructive with respect to the geochemical behaviour of U/Th-series radionuclides and rare-earth elements (REEs; chemically analogous in some respects to transuranic elements). At that time the potential importance of the geochemical behaviour of redox fronts in fractured rocks, and of colloid/particulate materials as radionuclide complexing or transport agents in groundwaters, was being recognised in safety assessments of high-level waste and spent fuel disposal.

The Poços de Caldas area had been the subject of long-term studies, particularly focussed on the Th/REE ore deposit of Morro do Ferro, since the early seventies. The Poços de Caldas region, and Morro do Ferro in particular, had been identified as amongst the most naturally radioactive places on the surface of the Earth. In 1977, an international conference on areas of high natural radioactivity was held in Poços de Caldas. (Cullen and Penna Franca, 1977).

A considerable amount of research on the biological uptake of U/Th series daughter elements was performed by the New York University Medical Center's Institute of

Environmental Medicine (see, for example, Linsalata *et al.*, 1986). This work looked in detail at the thorium deposit of Morro do Ferro, and the uptake of Ra-228 by plants, cattle and humans in the vicinity and downstream areas of the catchment / drainage area.

Later work in this project looked specifically at the mobility of thorium in solution and particulate form in near-surface waters (Eisenbud *et al.*, 1984). In early 1984, representatives from NYU and SKB (Sweden) met in Poços de Caldas to evaluate the geological potential of Morro do Ferro as an analogue for the burial of high-level radioactive waste. This resulted in a report compiled by a research group at the University of São Paulo (IPT Report, 1984). In late 1984, a group representing SKB, NAGRA (Switzerland) and the Department of Energy (USA) visited the area to assess the possibilities for extending the work, under international sponsorship, to look at other aspects of direct relevance to repository performance assessment. In addition to considering further work at Morro do Ferro, this pilot group noted that the very prominent natural oxidation fronts (redox fronts) displayed in the nearby Osamu Utsumi uranium mine could provide information vital to near-field repository models where such fronts were thought likely to occur in either the near-field (Nagra, 1985) or in the far-field (KBS, 1983). The fact that the redox fronts in the mine so clearly influence the mobility and distribution of uranium in the fractured rock mass made this an obvious site for study.

Over the next 12 months a project was formulated in outline to look at trace element chemistry, evolution of the redox fronts, colloids and elevated temperature hydrothermal element transport aspects in particular, and the UK Department of the Environment also became involved as a co-sponsor. A three-year project was devised, of which the first year (June 1986 – June 1987) was to be a feasibility study designed to obtain sufficient information to test the viability of the analogues and, if necessary, to revise or redirect the subsequent work programme. This early work involved drilling and rock/water sampling at both Morro do Ferro and the Osamu Utsumi mine, and received considerable support from Nuclebrás (now Urânio do Brasil), the mine operators.

At the end of the feasibility study year, both the data gathered and the growing awareness of other critical issues in performance assessment enabled the project technical committee to draw up a list of four main objectives:

1. Assisting in the validation of equilibrium thermodynamic codes and databases used to evaluate rock/water interactions and solubility/speciation of elements.

2. Determining interactions of natural groundwater colloids, radionuclides and mineral surfaces with respect to radionuclide transport processes and colloid stability.

3. Producing a model of the geochemical evolution of redox fronts, specifically with the aim of understanding long-term, large-scale movements of redox-sensitive natural series radionuclides (including, if possible, natural Pu and Tc).

4. Modelling the migration of REE/U-Th series radionuclides during hydrothermal activity similar to that anticipated in the very near-field of some spent-fuel repositories.

These objectives have remained as the focus of the project throughout its existence, and the results presented in this summary and in the associated technical reports are structured so as to present the advances made in these areas.

It should be emphasised that only certain components of the "performance assessment model chain" have been tested in the project and that these tests vary in rigour. Objectives (1) and (3) have involved quantitative testing (partial validation) of mathematical models (and databases) which are used regularly by performance assessors. The code used in (4) is similar in structure to assessment codes, but has not yet been used in such applications. No comprehensive mathematical model of the effects of colloid transport exists and hence objective (2) involves qualitative testing of the conceptual models which are currently under development.

From the outset, the project profited from the involvement of a range of laboratories and technical investigators covering many disciplines, including hydrogeology, radiochemistry, rock and water analysis, geomorphology, microbiology, and chemical modelling. One of the great successes of the project has been to bring together an excellent spectrum of expertise for the purpose of studying a common set of problems and achieving consensus on the geochemical evolution of the two study sites. This, in itself, constitutes a form of multidisciplinary group development with internal peer review that would have useful parallels in repository site characterisation. A list of all the laboratories and individuals involved, together with the technical management structure of the project, is provided in Appendix 1, and a list of presentations/ publications resulting from the project is given in Appendix 2.

Time restrictions and the volume of data to be reported gave rise to logistic problems. The technical reports thus incorporate the interpretations of the authors based predominantly on their own data, and there may naturally be inconsistencies between various reports. It is the intention of this summary report to provide an overview of all the information available, although it is expected that further analysis of the project database will give rise to a series of future publications.

This report is a detailed summary of the whole of the Poços de Caldas project. It begins by describing the area, and then focusses on detailed descriptions of the two study sites. In order to put the sites into context, a limited programme of regional petrological, geochronological and geomorphological studies was carried out, and these are described in the next Chapter. Chapters 3 and 4 describe the detailed geology and geochemistry of the Osamu Utsumi mine and Morro do Ferro respectively, concentrating on the operative geochemical processes. Chapters 5 – 8 cover the four performance assessment-related technical objectives of the project, and draw conclusions specific to these topics.

Finally, Chapter 9 presents a more general overview of the information derived in this project, with emphasis on how it could be applied in particular waste management programmes. This Chapter also highlights areas which may be worth further study, and suggests ways in which the experience gained could be used to improve similar studies in the future.

CHAPTER 2. GEOMORPHOLOGY, SURFACE FEATURES AND GEOLOGY OF THE POÇOS DE CALDAS PLATEAU

The Poços de Caldas plateau lies in the highland savanna region of the state of Minas Gerais, about 300 km north of São Paulo. A detailed description of the geomorphological and hydrogeological features of the plateau and the two main study sites, together with information on vegetation and climate, is given in Holmes *et al.* (this report series; Rep. 5).

2.1. Geomorphology

The plateau is formed by a volcanic caldera that is roughly circular in outline, about 35 km in diameter along its NW-SE axis, 30 km along its NE-SW axis, and some 800 km^2 in area (Fig. 2.1). Its altitude is between 1300 and 1600 m.a.s.l. It has an elevated rim and undulating topography within this confining chain of higher peaks. Within the main caldera structure fourteen circular structures have been identified, based mainly upon topography, and appear to be minor intrusions (Loureiro and Santos, 1988). Despite its dissected nature, it is misleading to think of the present plateau as being deeply eroded. The areal and cross-sectional configurations are typical of a collapsed caldera. Although there is a large volume of ejecta derived from such volcanic activity, it is far less than the volume of the depression, which can be accounted for by the collapse of the deep underlying volcanic structure. Based upon these considerations, it was concluded that the Poços de Caldas caldera assumed a comparatively low relief very early in its evolution. The highest points of the pre-erosional volcanic edifice may have been little more than 500 m above the present plateau surface. This conclusion is potentially in conflict with some other estimated erosion rates, which would extrapolate to values of approximately 3500 to 7000 m of erosion over a 70 Ma period (see Waber *et al.*, this report series; Rep. 2). Erosion history is important with respect to the generation of the secondary ore bodies and the rate of movement of the redox and weathering fronts.

If the pre-erosional surface was around 500 m above the present-day surface then, over a period of 75 Ma (the approximate time since cessation of volcanic activity), this would represent an average erosion rate of about 6–7 m/Ma. Note again that this value differs from other estimates (see Waber *et al.*, this report series; Rep. 2).

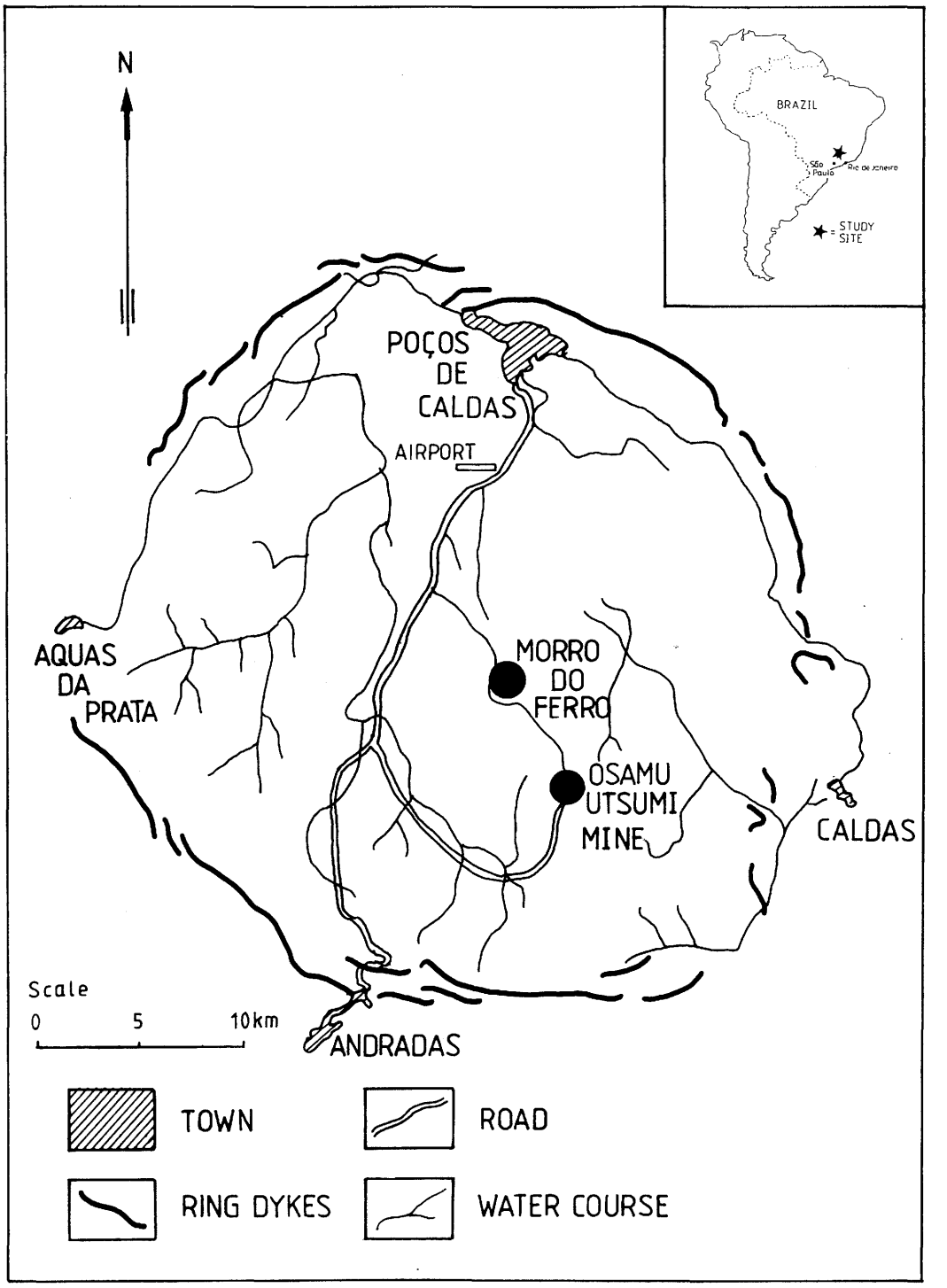

Figure 2.1. Location of the Osamu Utsumi mine and Morro do Ferro study sites.

Denudation appears to have been very slow and many of the present landforms are believed to be residual ancient features, at least in terms of several millions of years. Some evidence for this is provided by the presence of considerable bauxite deposits which form particularly on the crests of interfluves where free drainage ensures the progressive removal of silica.

Drainage patterns on the Poços de Caldas plateau have changed little over the last 5 Ma and erosion of the interfluves has kept pace with that of the valley floors. Rates of denudation are an average of 12 m per Ma, and weathering processes are thought to have remained similar over the last 10 Ma.

There are three principal fault systems within the caldera, which are an important control on the planform of local drainage patterns. The first strikes N60°W, extends beyond the caldera, and was reactivated during uplift. The second strikes N40°E and is related to caldera collapse. Thirdly, there are radial and sub-circular faults related to various intrusions.

The rim of the Poços de Caldas caldera is mainly defined by the metamorphic induration of the surrounding country rock and does not represent a worn-down perimeter of volcanic material.

2.2. Climate, vegetation and soils

The average annual temperature of the Poços de Caldas plateau is 19°C. The maximum is around 36°C and the minimum is approximately 1°C. The 30-year average precipitation is 1700 mm, with more than 120 days of rain each year. Alternating wet and dry seasons are typical, with >80% of the annual precipitation occurring between October and March.

Four main vegetation types are found in the Poços de Caldas plateau. These are campo cerrado (shrub), mata (evergreen forest), savanna (grass), and agreste (woodland savanna). The plateau experienced extensive deforestation due to logging activity approximately 100 years ago. The current distribution of vegetation comprises mainly grass and shrubs on the hill tops and plains of the plateau interior, with thick stands of trees in many of the river and stream valleys.

The soils of the plateau are predominantly silts and clays which, due to the intense weathering, consist predominantly of kaolinite, gibbsite and limonite. This soil is excavated by mammals, lizards and various insects, particularly termites. Stone lines, a

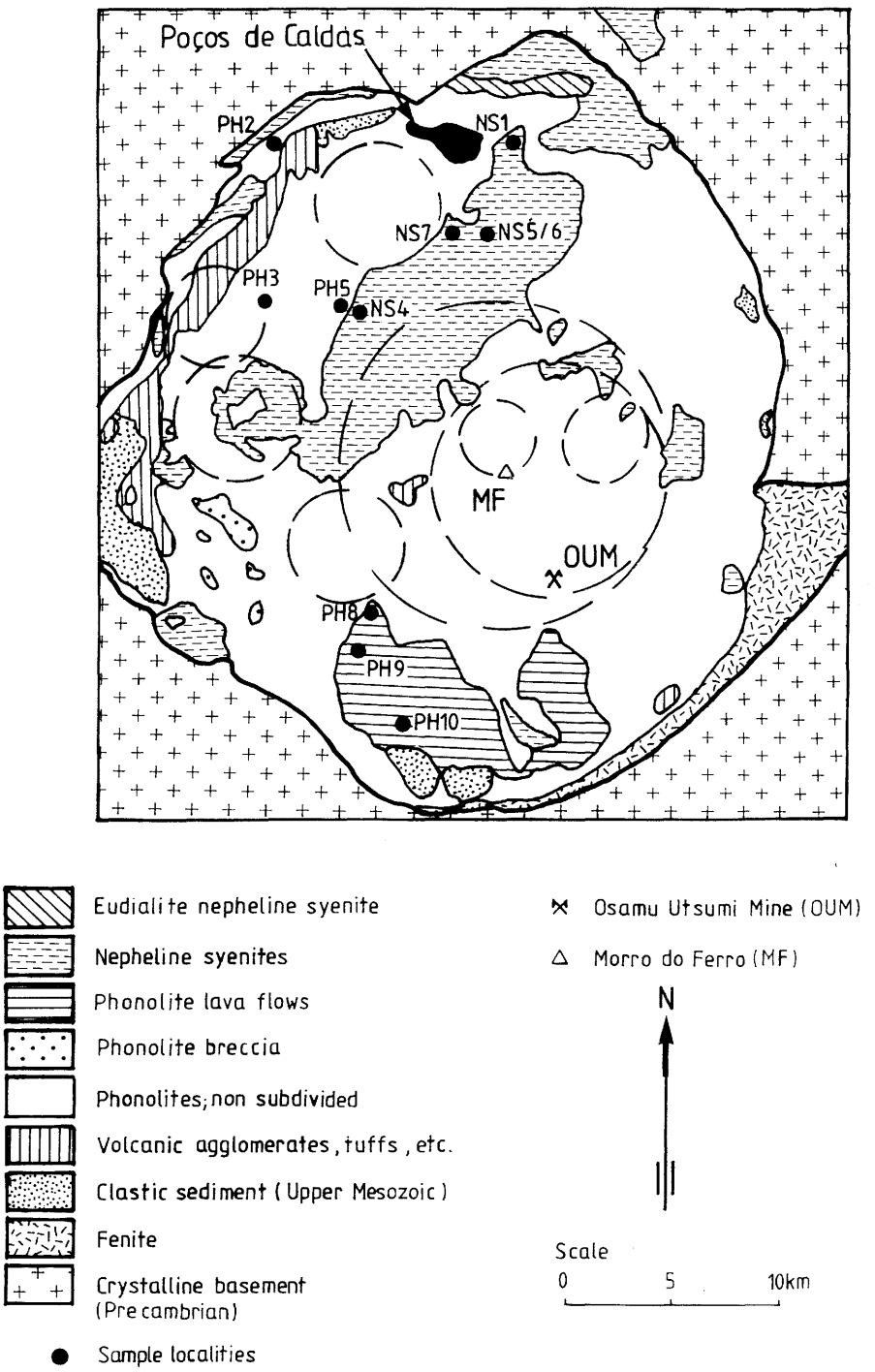

Figure 2.2. Main geological subdivisions of the Poços de Caldas caldera.

distinctive tropical feature caused by resistant residual material accumulating at a shallow depth, are clearly noted in sections of the plateau.

Land use in the Poços de Caldas plateau includes a variety of activities. A major bauxite (aluminium) mining and processing facility is operated by Alcoa. Other significant operations include the Osamu Utsumi uranium mine. Truck farming is carried on by many of the small land-owners, but cattle grazing is restricted mainly to large land-owners. There is some limited coffee growing. Quarrying for building and pavement stone (nepheline syenite and phonolite) is done for local use.

2.3. Geology and geological evolution

The Poços de Caldas caldera complex is a ring structure of late Cretaceous age comprising a suite of alkaline volcanic and plutonic rocks (Fig. 2.2), generally containing normal background amounts of U, Th, and rare-earth elements (REEs). Detailed accounts of the geology can be found in Schorscher and Shea, Waber *et al.*, Waber, and Shea (this report series; Reps. 1-4). Hydrothermal water/rock interactions of local extent led to the formation of several ore deposits of economic importance. Two of these, the Osamu Utsumi uranium deposit (with subsidiary Th and REEs) and the Morro do Ferro thorium and rare-earth deposit (with subsidiary U), formed the two main study sites of the Poços de Caldas Project.

The Poços de Caldas caldera is one of a number of alkaline igneous complexes in Brazil (Ulbrich and Gomes, 1981) and, with a surface extent of about 800 km^2, is the largest alkaline complex in South America.

The evolutionary history of the caldera (Fig. 2.3) began with major volcanism involving phonolite lavas and volcanoclastics, followed by caldera subsidence and nepheline syenite intrusions forming ring dykes and minor circular structures, and, finally, intrusions of eudialite-bearing nepheline syenites and extrusions of nepheline phonolites.

The latest stages of caldera volcanism also included the formation of breccia pipes caused by violent outgassing and defluidisation of the volatile-rich alkaline magma bodies. This was accompanied by hydrothermal activity, which persists to a minor extent to this day in parts of the caldera. Lamprophyric dykes appear to be the last form of igneous activity.

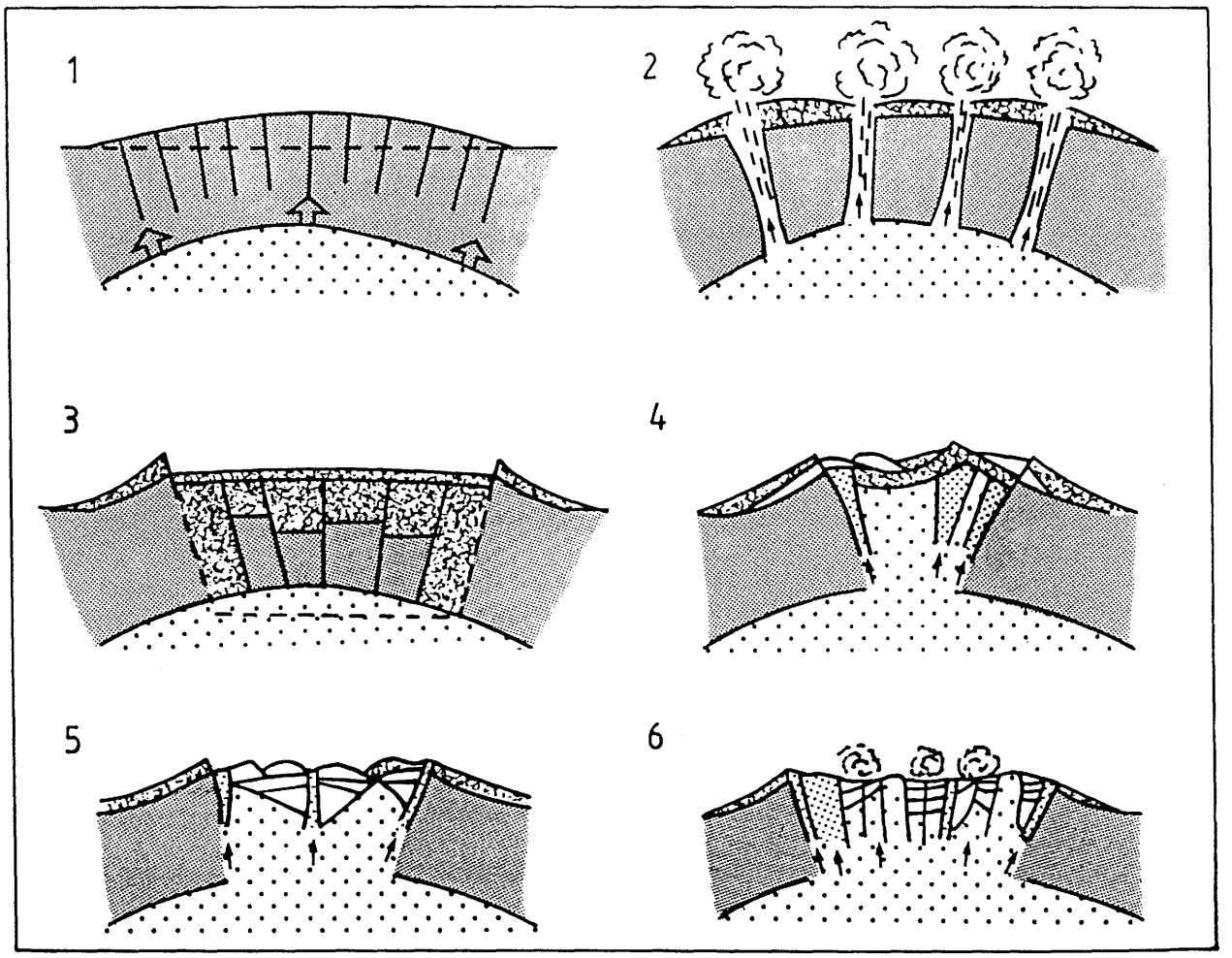

Figure 2.3. Evolutive model of the Poços de Caldas alkaline igneous complex (after Ellert, 1959).

1. Basement elevation, distension, fracturing and erosion.
2. Volcanism: phonolites, volcanoclastics.
3. Caldera subsidence.
4. ⎫ Nepheline intrusions: phonolites, nepheline syenites, in ring dykes and minor
5. ⎭ circular structures, plus nepheline phonolites.
6. Intrusion of eudialite-bearing nepheline syenite, plus nepheline phonolites.

The earliest radiometric age determinations (K-Ar) suggested that the Poços de Caldas volcanic activity occurred between 80 and 62 Ma (Amaral *et al.*, 1967). Kawashita *et al.* (1984) derived ages of 85 to 90 Ma for some nepheline syenites.

Current Rb-Sr analyses (Shea, this report series; Rep. 4) for the central nepheline syenite body of the caldera, representing one of the earlier stages of caldera evolution, give an internal isochron cooling age of 78($\pm$3) Ma. In the same study, Ar-Ar analysis shows the age of a lamproite dyke, possibly representing the final stage of volcanic activity, as being 76($\pm$1) Ma. The dated lamproite dyke crosscuts hydrothermal alteration and mineralisation at the Osamu Utsumi mine, thereby giving a minimum age for the hydrothermal event.

The earlier age determinations, especially the K-Ar study, have likely been disturbed by postmagmatic events such as hydrothermal alteration, contact/regional metamorphism and/or marked surficial weathering. It is therefore possible to constrain the age and span of igneous activity, with a re-evaluation of the above K-Ar data, as ranging from no more than approximately 72–82 Ma ago, and probably even less. This position is also taken by Ulbrich (1985), who felt that the interval of caldera activity may even have been as short as 1-2 Ma, based on analogy with other well-dated volcanic complexes.

The nepheline syenites and phonolites are moderately enriched, and the Osamu Utsumi mine samples extremely enriched, in potassium, as well as many incompatible elements. Petrological and geochemical studies of the regional rocks (Schorscher and Shea, this report series; Rep. 1) indicate that high-temperature alteration apparently occurred in two stages. The first stage, between approximately 700° and 350°C, was deuteric (or "autometamorphic"), and affected the mineralogy but not the bulk chemistry. The second stage, at temperatures below 350°C, was metasomatic, and introduced K while removing Na.

Chemical calculations, modelling results and preliminary laboratory experiments (Cathles and Shea, this report series; Rep. 13) suggest that the intense potassic alteration and uranium mineralisation could have been produced by the channelling of hydrothermal fluid through the breccia pipes. This fluid channelling also produced a 30 wt.% primary alteration and a 50 μg/g uranium protore.

This alteration requires a flux of approximately 10^5 kg/cm^2 of hydrothermal ($\sim$300°C) water to have passed through the Poços de Caldas breccia body. The worst-case scenario of hydrothermal flow (and thereby alteration) through a hypothetical radwaste repository is 10^3 times less.

CHAPTER 3. THE OSAMU UTSUMI URANIUM MINE

3.1. Geology

The Osamu Utsumi open pit mine (Fig. 3.1) covers an area of about two square kilometres located in the gently undulating landscape which characterises the Poços de Caldas plateau. The mine has been operated since 1975 and comprises an open-cast benched excavation up to 150 m deep. Earlier exploratory shafts and adits have been partially mined out during exploitation of the deposit.

The geology, geochronology, mineralogy and geochemistry of the mine and the regional surroundings are outlined in detail by Schorscher and Shea, Waber *et al.*, Waber, Shea and MacKenzie *et al.*, this report series; Reps. 1-4 and 7.

Drainage of the area is controlled by a network of small, shallow valleys which discharge into the main valley heading towards the north, north-west. This valley crosses the northern part of the mine area (Fig. 3.2).

The uranium deposit is defined by a primary low grade disseminated U-Zr-(REE-Mo)-mineralisation and a high grade stockwork veinlet Zr-REE-U-Th-Mo mineralisation emplaced in various host rocks that have been altered by hydrothermal solutions in a roughly concentric zonal pattern. The host rocks comprise a suite of hydrothermally and metasomatically altered intrusive bodies of nepheline syenites and flows of volcanic to subvolcanic phonolites. The hydrothermal alteration and the primary mineralisation are closely related to the intrusion of two major breccia pipes. Late-stage lamprophyric dykes, not affected by these hydrothermal events, crosscut all the existing units, including the breccia pipes.

Intense weathering under semi-tropical conditions has led to the alteration of the uppermost exposed rock, and to a secondary supergene enrichment of uranium along redox fronts, assumed to be the result of downward-migrating oxidising groundwaters (Fig. 3.3). These fronts are observed as a marked colour change from reddish-brown to bluish-grey. The transition is sharp, in the order of a few millimetres. The reddish-brown colouration results from the oxidation of pyrite and subsequent precipitation of iron oxyhydroxides. The redox fronts extend to variable depths, following deeply-plunging fracture zones and heterogeneities in physical rock properties. The secondary enrichments of uranium on the reduced side of a redox front are very much restricted in their dimensions and occur adjacent to the front over a distance of a few centimetres to decimetres at the most. The degree of weathering is strongly dependent on the intensity

Figure 3.1. Panoramic view of the Osamu Utsumi open-pit uranium mine, Poços de Caldas. Note the colour variations reflecting the heterogeneous extent of the oxidising weathering processes (yellow/buff colouration).

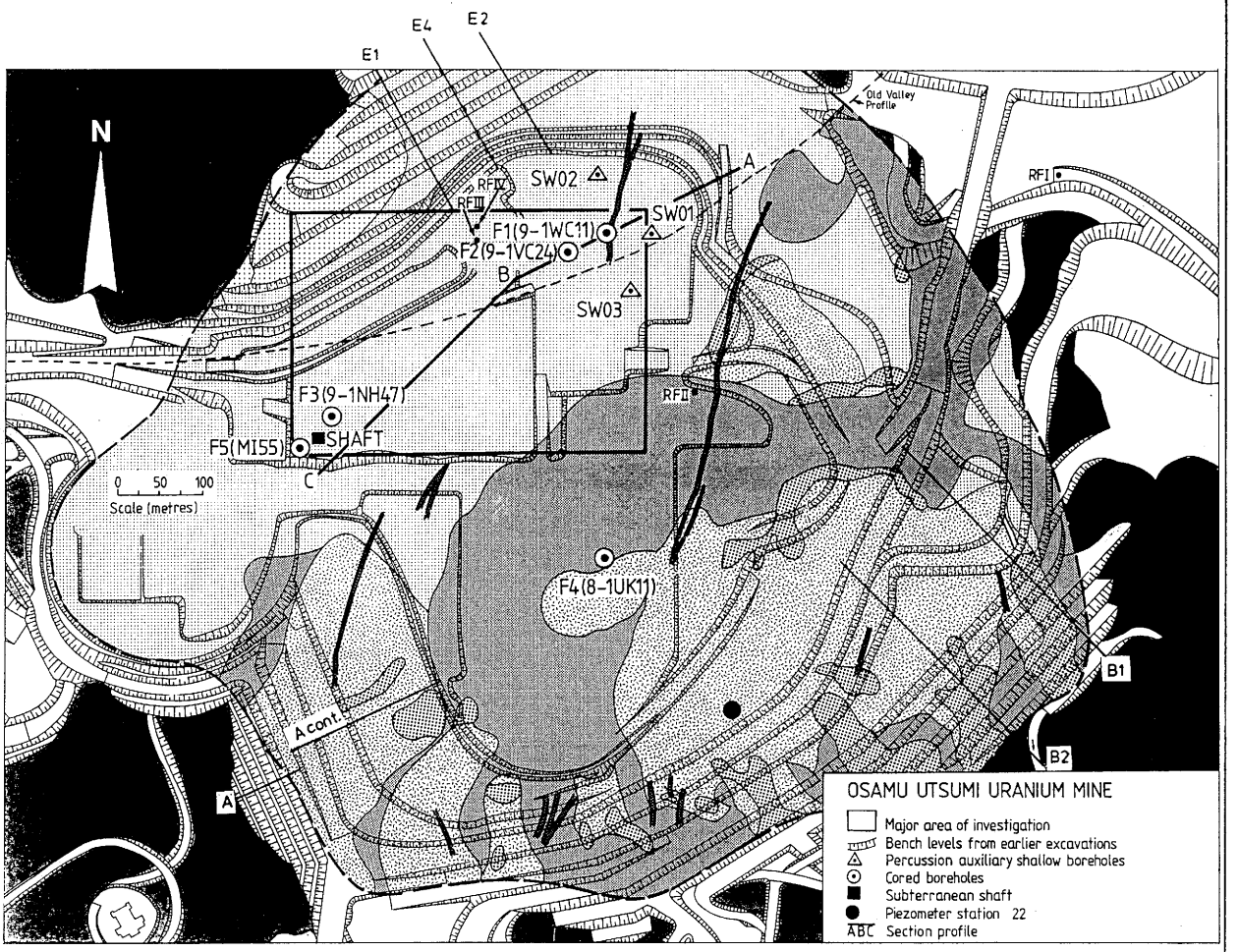

Limit of mapped area

(Oldest)

Subvolcanic phonolite with very weak hydrothermal alteration; no pyrite impregnation.

Mainly subvolcanic & minor volcanic phonolites, fractured if near 4.

Abyssal & hypabyssal intrusive nepheline syenites (intrusive in 1); fractured if near 4.

Subvolcanic pseudoleucite phonolites (intrusive in 1 and 2); fractured if near 4.

Subvolcanic conduit breccia, locally grading to extremely xenolithic ultra-fine-grained, flow-textured phonolites.

End of major hydrothermal event (formation of "potassic rock" and U-Mo-Zr-REE-pyrite hydrothermal mineralisations).

(Youngest)

Biotite-lamprophyre dykes (late-stage intrusive).

RFI, II, III, IV Location of redox fronts for detailed investigations.

E1, E2, E4 Vertical profiles in ore body 'E'.

B1, B2 Vertical profiles in ore body 'B'.

A Vertical profiles in ore body 'A'.

Figure 3.2. Osamu Utsumi mine map showing the main geological subdivisions, the borehole locations, the groundwater sampling points, and the surface rock sampling profiles.

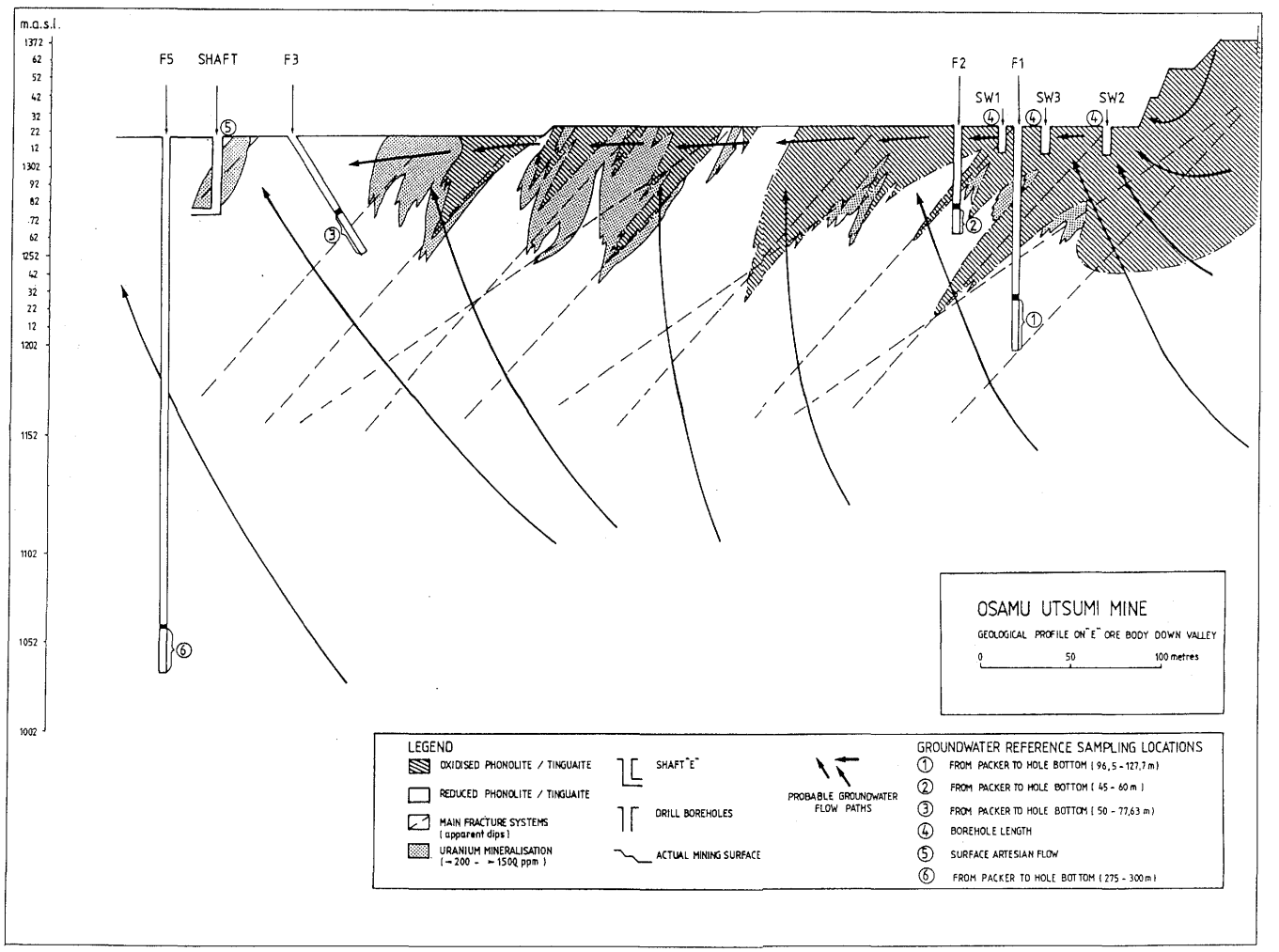

Figure 3.3. Cross-section along profile A-C of Figure 3.2 showing the relationships of the boreholes and groundwater sampling locations to the geology, geochemistry and hydrogeology of the site.

of the hydrothermal alteration and the textural and physical properties of the underlying rock types. A vertical profile within the mine area (Fig. 3.4) displays a lateritic cover (including the top-soil horizon), followed by a saprolitic horizon, oxidised hydrothermally altered rock and, finally, the reduced hydrothermally altered rock.

The part of the mine investigated in the project is predominantly phonolite, which has been hydrothermally altered throughout the complete thickness drilled. Fracturing of the bedrock is widespread, especially within the upper 50 to 80 m; at greater depths fracturing is less uniform and there is a trend towards more discrete fractures or highly porous zones which are often hydraulically conductive and lined with fresh pyrite, indicating a predominantly reducing groundwater environment. The increasing competence of the reduced rock with depth is supported by physical measurements which clearly distinguish between higher porosity (approx. 5–10%) rocks down to about 50 to 70 m, and lower porosities (<5%) below this depth.

Studies at the mine have involved the drilling of five intermediate to deep boreholes (F1-F5) and three shallow holes (SW01-SW03); their locations in the mine and relationships to the local geology, geochemistry and hydrology are illustrated in Figures 3.2 to 3.4.

Drillcore samples have been supplemented by material from surface exposures within, and from outcrops outside, the mine confines, thus providing a regional context for interpretation. Routine groundwater sampling was carried out in all boreholes. Additional artesian occurrences (i.e. piezometer station 22 and the old exploratory shaft; Fig. 3.2), together with some streams and small reservoirs around the mine periphery, were also sampled to provide a greater understanding of the recharge/ discharge hydrochemistry. Boreholes F1-F3 and F5 constitute the major reference locations where the palaeohydrology is known and groundwater sampling is from restricted depth intervals controlled by downhole packer systems. These locations form the key reference points sampled for the large volumes of water required for full hydrochemical characterisation (this Chapter; section 3.3), colloid extraction (see Chapter 7) and microbiological studies (see Chapter 6).

Two separate sites within the mine were used as the focus for investigating:

a) redox front processes and radionuclide speciation/mobility in groundwaters (analogue objectives 1–3); boreholes F1-F3 and F5 (Fig. 3.2).

b) high-temperature hydrothermal studies (analogue objective 4); borehole F4 (Fig. 3.2).

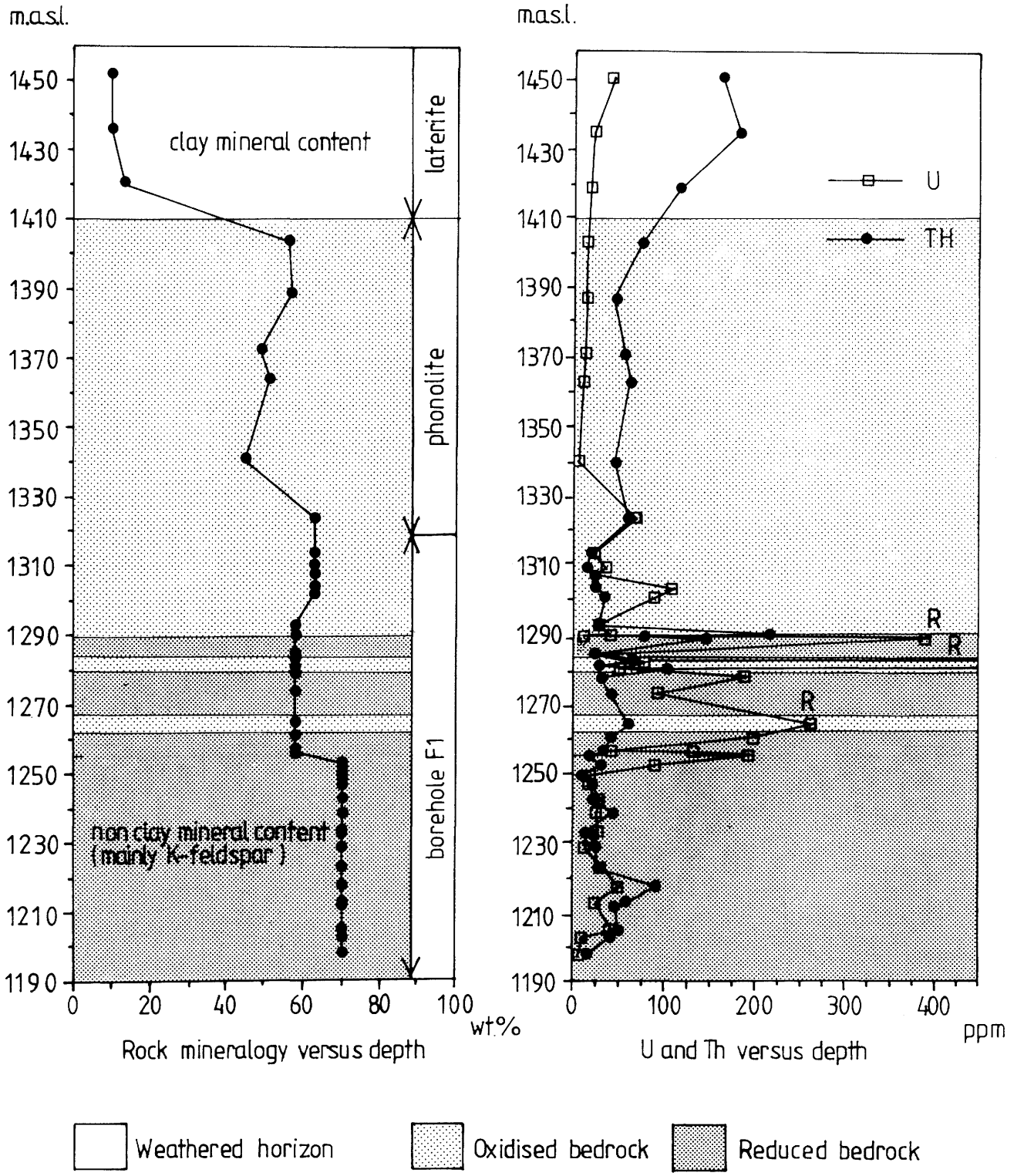

Figure 3.4. Distribution of clay mineral content, uranium and thorium extending from the original (pre-mine) ground surface to the bottom of borehole F1. Note the distinct change in mineralogy at about 1407 m.a.s.l, and the enrichment of uranium and thorium near the surface and associated with the redox fronts (denoted by 'R').

3.1.1. Mineralogy and petrology

Microscopic studies show that all the primary magmatic rocks may be generally classified as phonolites of volcanic to subvolcanic origin. Subordinate to these are minor occurrences of nepheline syenite, pipe breccia and fine-grained phonolitic dyke structures; ultramafic dykes crosscut all major rock units.

All the major rock units are extremely altered by hydrothermal and later low-temperature weathering processes. The most obvious features of the alteration are intense K-metasomatism resulting in newly formed K-feldspar and sericitisation, with subsequent kaolinisation of the rocks. Fractures, resulting from several tectonic and hydrothermal episodes, are numerous and fall mostly in the range of 1-10 mm in width. They are usually altered and filled with clay minerals, K-feldspar, zircon, fluorite, pyrite, zeolites and, in the oxidised horizons, Fe-oxyhydroxides. In a few fissures, uranium and/or molybdenum mineralisation can be observed.

Studies of the opaque phases show that the oxidised phonolites are devoid of sulphides; only hematite, goethite and less well-defined crystalline Fe-oxyhydroxides are present, mostly finely dispersed within the rock matrix. The reduced phonolites are characterised by impregnations of disseminated pyrite, partly associated with very fine-grained pitchblende. This major pyrite frequently occurs with subsidiary sphalerite (partly as inclusions). At least one generation of secondary pyrite occurs close to the redox boundary in the reduced rock.

Combining drillcore data with supplementary surface sampling from higher benches in the mine, a detailed petrographic/mineralogical and geochemical cross-section through the mine has been reconstructed (Fig. 3.4; Table 3.1).

Weathered Zone (1450–1410 m.a.s.l.). This zone is completely argillised (typical laterite), comprising material composed of clay minerals (75-90%), gibbsite (5-15%) and Fe-hydroxides (4-14%); in the lower parts of this zone relict K-feldspar may also occur. The rock chemistry, compared to the underlying rocks, is characterised by a strong decrease in SiO_2 and K_2O and an increase in Al_2O_3, Fe_{tot} and loss on ignition (LOI).

Oxidised Zone (1410–1256 m.a.s.l.). The lower end of this profile extends into the top of borehole F1. The original rocks have been porphyritic volcanic to subvolcanic phonolites; in some cases pseudoleucites are common. Of the <5% of mafic constituents only pseudomorphs are present. Nepheline and pseudoleucite are completely hydrothermally altered to illite and kaolinite; apatite and zircon occur as rare magmatic accessories. The rock consists of 40–60% K-feldspar and 40–50% clay minerals, together with Fe-oxyhydroxides and primary and secondary accessories. The oxidised phonolite

TABLE 3.1

Osamu Utsumi mine: mean bulk chemistry of the leucocratic phonolites.

Element		Reduced zone n=25	Oxidised zone a) n=18	Oxidised zone b) n=10	Saprolite n=3	Laterite n=6
SiO_2	wt.%	56.22	55.93	56.09	51.85	35.58
TiO_2		0.49	0.49	0.44	0.56	0.72
Al_2O_3		21.83	23.07	23.23	27.72	37.62
Fe_{tot}		2.89	2.86	2.43	2.21	5.61
MnO		0.03	0.00	0.00	0.03	0.34
MgO		0.05	0.04	0.04	0.08	0.06
CaO		0.14	0.00	0.00	0.01	0.00
Na_2O		0.40	0.63	0.78	0.23	0.10
K_2O		13.52	13.06	13.21	9.35	3.95
P_2O_5		0.18	0.06	0.33	6.28	14.03
LOI		3.27	3.05	2.48	0.00	0.00
F	µg/g	702	1209	383	967	262
Ba		685	919	1109	464	224
Rb		300	333	343	207	113
Sr		218	184	227	828	139
Pb		7	27	26	10	14
Th		31	51	28	54	59
U		32	112	51	4	3
Nb		223	180	142	286	365
La		262	305	324	759	364
Ce		297	564	571	384	492
Nd		57	76	76	167	87
Y		53	68	61	167	84
Zr		1040	1081	792	1395	1539
V		252	212	205	434	379
Cr		6	8	8	b.d.	b.d.
Ni		3	6	6	b.d.	b.d.
Co		5	6	6	b.d.	b.d.
Cu		b.d.	4	5	b.d.	b.d.
Zn		210	17	13	73	89
Hf		4	13	2	21	21
Ga		23	39	27	n.a.	n.a.
Sc		4	4	4	6	b.d.
S		8640	36	29	678	708

Oxidised zone: a) comprises all oxidised samples from the profile down to 33 m and the 43-66 m interval of borehole F1.
b) comprises all oxidised samples of the profile down to 33 m in borehole F1.

LOI: Lost On Ignition
b.d.: below detection limit
n.a.: not analysed

is notable for the absence of pyrite, fluorite, barite, primary U-phases and Mo-phases. The bulk rock chemistry (Table 3.1) differs little from that of the underlying reduced bedrock.

Reduced Zone (1256–1198 m.a.s.l.). Porphyritic phonolites continue to dominate, differing only from the preceding zones in textural variations; they comprise 50–75% K-feldspar and 25–40% clay minerals, with minor amounts of pyrite, fluorite and Ti-phases and accessory amounts of Zr- and REE-phases and barite. Mineralogically, the main difference between the oxidised and reduced rock is the presence of pyrite and U-phases in the reduced horizons. Bulk chemistry, in common with oxidised rocks, differs from the primary unaltered phonolites by having extremely high K_2O contents and contrastingly low Na_2O, CaO and MgO contents (Table 3.1).

Illite and kaolinite are by far the most abundant clay minerals; there are, however, no obvious trends with depth. In the reduced rocks, illite, kaolinite and the few illite-smectite mixed-layer clays are of hydrothermal origin. In the oxidised rocks, additional kaolinite and illite occur, formed from meteoric weathering processes.

3.1.2. The distribution and genesis of uranium mineralisation

The distribution of uranium (Fig. 3.4) shows some interesting trends along the measured profile. The bulk rock uranium concentration (averaging around 5 μg/g) shows a slight tendency to increase upwards through the oxidised bedrock zone from around 1370 m.a.s.l.; this is most marked at the laterite surface where values up to 10 μg/g are recorded. From 1340 to 1250 m.a.s.l. (i.e. corresponding to most of borehole F1), the uranium concentrations show considerable fluctuations. This is due to the heterogeneous nature of the early hydrothermal mineralisation coupled with a subsequent superimposed alternation of oxidised/reduced bedrock caused by an interfingering of oxidation associated with several steeply-dipping fracture/porous zones. Near the hole bottom (1250–1200 m.a.s.l.), the uranium concentrations become more uniform (averaging around 20 μg/g), with values only marginally higher than in the oxidised bedrock horizons.

Uranium mineralisation in the Osamu Utsumi mine has formed from both hypogene and supergene processes. The hydrothermal hypogene type consists mostly of pitchblende with subordinate uraninite, whilst the supergene type is predominantly of pitchblende.

Hypogene mineralisation

The hypogene mineralisation is present as: a) disseminated enrichments and b) more concentrated enrichments contained in the matrix of the breccias and in veins. In its disseminated form uranium is closely associated with pyrite, occurring as minute inclusions of uranium oxide ($UO_{2.25}$ to U_3O_7). Small aggregates of REE-bearing monazite/cheralite, also of hydrothermal origin, are commonly observed forming on the pyrite surfaces. Sometimes penetrating these pyrite/uranium disseminations are small veinlets containing pyrite (U-bearing) and clay phases. In the breccia matrix and vein-type enrichments the uranium, although still partly associated with pyrite, is additionally contained within TiO_2-bearing phases such as brannerite ($UTiO_6$) and anatase; trace amounts of uranium are present in zirconium minerals.

The relative abundances of the various hydrothermal minerals vary considerably between the matrix and vein occurrences. Mineralisation has occurred during several phases, some resulting in a zirconium-rich mineralogy, others giving rise to fluorites of different compositions (violet to green varieties). The U-rich hydrothermal phase (together with ± Ti and REEs) has permeated throughout the matrix, resulting in uraninite/pitchblende, U-Ti and U-REE disseminations, and forming more concentrated accumulations of localised pitchblende (up to 5 000 μg/g) along fissures and veinlets.

Supergene mineralisation

Supergene mineralisation at the Osamu Utsumi mine is spectacularly illustrated by the development of redox fronts (Fig. 3.5). The transition from oxidised to reduced rock is clearly seen as a sharp (mm) colour change from yellow/brown to green/blue-grey (Fig. 3.5). This colour variation reflects an Fe^{2+}/Fe^{3+} change which, together with the very sharp increase in uranium concentration immediately inside the reduced section of the rock, indicates that the redox-controlled reactions affecting uranium occur at effectively the same place as those affecting iron. This suggests that the redox potential shows a sharp variation over a very short distance (in the order of 1 cm).

Two main mass transport processes contribute to the mineralisation; advection and diffusion. Advection is the more common process, occurring when there is a preferential downward flow of oxidising water along a fracture zone, resulting in a net transfer of uranium from the oxidised to the reduced rock along the direction of groundwater flow. Diffusion occurs when the oxidising waters come into contact with the reduced rock, dissolving the uranium which diffuses away from the front into both the oxidised and

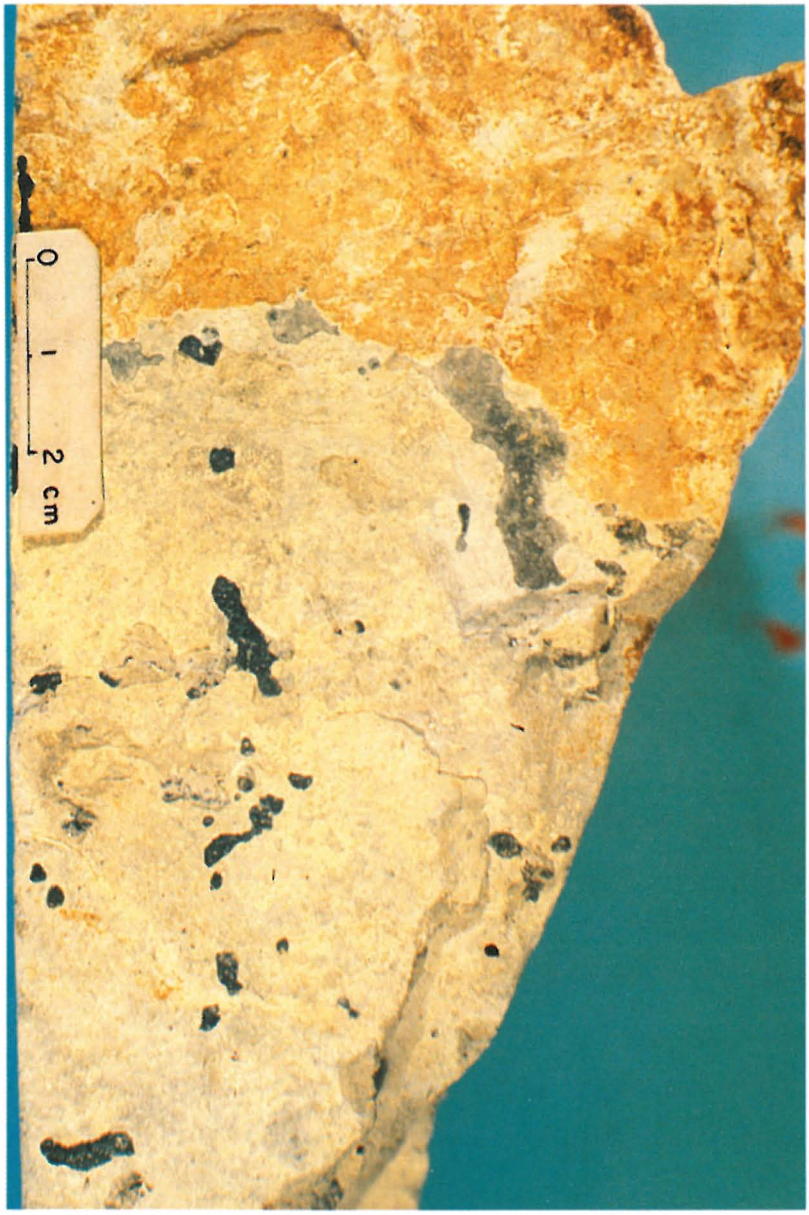

Figure 3.5. Phonolite sample illustrating the sharpness of the redox front (oxidised: yellow/buff, reduced: grey) and the small nodular pitchblende accumulations (black) on the reduced side of the front.

reduced rock. In the reduced rock, uranium as a solid phase (i.e. pitchblende) is commonly formed, whilst on the oxidised side the precipitation/sorption of uranium onto disseminations of iron and manganese oxides tends to dominate.

Mineralogically, pitchblende nodules are the most impressive products of the supergene mineralisation. In the homogeneous porous phonolite they are developed along the whole redox front (mostly mm in size); this contrasts with the breccia bodies where large nodules (>5 cm in diameter) are found mainly along the deeply penetrating tips of the oxidation fronts associated with conductive faults in the area. The nodules occur as botryoidal aggregates of pitchblende intergrown with illite, K-feldspar, pyrite and a rare Cd-bearing mineral greenockite (CdS). Two pyrite generations have been recognised, one with δS values around zero, indicating a hydrothermal origin, and the other with very low δS values (-12 to -14 ppt), suggesting supergene weathering combined with bacterial activity (Waber *et al.*, this report series; Rep. 2, Appendix 1).

As weathering proceeds and the redox fronts migrate to deeper levels, previously precipitated uranium will eventually be remobilised and reprecipitated. This downward passage of oxidising conditions has, in most cases, removed the nodules, leaving 'ghost' textures in the oxidised rock, whilst in other cases relict nodules still persist.

The main mineralogical characteristics observed at the redox fronts can be summarised as follows:

* pyrite disappears within a fraction of a millimetre from the front in the reduced rock
* fluorite and carbonates disappear when oxidised during the passage of the front
* sphalerite and other sulphides occur only on the reduced side of the front
* K-feldspar begins to disappear 0.5–1.0 cm from the front within the reduced rock
* pitchblende nodules may occur 1–3 cm from the front within the reduced rock, sympathetic with the disappearance of K-feldspar
* secondary pyrite is formed at roughly the same locations as the pitchblende nodules
* Fe-oxides and Fe-oxyhydroxides demarcate the oxidised zone
* there is a general bulk decrease of kaolinite and illite within the oxidised zone during the passage of the redox front
* crandallite group minerals are the main REE phases in the oxidised zone
* jarosite- and alunite-type minerals are formed in the vicinity of the front in the reduced rock
* sporadic greenockite (CdS) is formed in the pitchblende nodules

Measured porosities are much higher in the oxidised zones (average 18%) than in their reduced counterparts (average 10%), reflecting substantial dissolution and loss of bulk material during oxidation.

3.1.3. Natural decay series radionuclides in rock samples

Natural decay series radionuclide analyses were carried out on rock samples representing: a) large-scale oxidised, reduced and conductive horizons of borehole F1, b) smaller scale sampling (decimetre intervals) across two mine exposure redox front profiles (RFII and RFIV), and c) small-scale sampling (centimetre intervals) across redox front profiles from drillcore material (3 fronts; borehole F1) and from two mine exposures (7-1ZE23 and NM). Pitchblende nodules, both recent and old varieties, have also been analysed. All analyses have been carried out on whole-rock powdered material, with the exception of redox front profile RFIV where a set of 12 samples across the front were analysed by selective leaching techniques. Sampling and analytical protocols, together with an interpretation of the data, are detailed in MacKenzie *et al.*, this report series; Rep. 7.

The radioactive decay series work in MacKenzie *et al.* (op. cit.) has focussed on a number of specific objectives, namely:

* identification of radionuclide dissolution, transport and deposition processes within the study sites in general and at the redox fronts in particular
* attempts to establish the timescales appropriate to the above processes and to evaluate the rate of movement of the redox fronts
* provision of information relating to the long-term (10^{-5}–10^{-6} Ma) direction of the groundwater flow
* investigation of the growth rates of uranium nodules

The data are presented and discussed using the method proposed by Thiel *et al.* (1983), in conjunction with a model developed by Alexander *et al.* (1988) which provides mathematical relations for situations involving uranium removal or deposition and the associated radioactive decay and growth. Where possible, an attempt was made to relate the natural decay series to hydrogeological conditions.

Redox Fronts

Although studies of a number of redox fronts were carried out on various scales, the main emphasis was on borehole F1 (Fig. 3.4) which provided the opportunity to investigate the redox fronts at 33.4 m, 42.0 m and 66.2 m (Fig. 3.6). The analytical data for drillcore F1 are included in Table 3.2 and selected redox front profiles are illustrated in Figures 3.7 to 3.9.

The redox front at 33.4 m showed activity ratios (Figs. 3.7) which indicated: a) that dissolution and redeposition effects influenced uranium and radium over a relatively wide range of about 10 m across the redox front, b) that ^{234}U is mobile within the reduced rock, and c) that the processes involved are rapid and complex. The results were consistent with a downward rate of movement of the front at this location of between 2 and 20 m per 10^6 a.

The redox front at 42.0 m shows a very similar distribution of uranium concentration to that observed at the 33.4 m front (Fig. 3.10), despite the different orientations. Furthermore, the $^{234}U/^{238}U$ data show clearly that the uranium has been precipitated on a timescale that is recent relative to the $2.5x10^5$ a half-life of ^{234}U, and that the uranium has been very efficiently precipitated immediately inside the reduced section of the rock, with some degree of mobility extending up to 2 m into the reduced rock. Furthermore, if it is assumed that the degree of disequilibrium is taken to represent how recently the uranium was deposited, then the uranium further from the front was precipitated later than that closest to the front. The $^{231}Pa/^{235}U$ data suggest a very slow rate of movement of the front in the order of centimetres in 10^5 a at most.

In common with the other two fronts, the redox front at 66.2 m (Fig. 3.11) has a uranium minimum at the front itself and distinct maxima in both the oxidised and reduced rock on each side of the front. These maxima, however, constitute much broader peaks than those exhibited by the other two fronts. Furthermore, the isotopic disequilibrium also extends over a greater distance. This persistence of $^{234}U/^{238}U$ disequilibria over a distance of at least 8 m around the front suggests an estimated downward rate of movement in the order of 10 m in 10^6 a.

From the same front, the pattern for the $^{230}Th/^{234}U$ activity ratios in the oxidised rock is consistent with the uranium concentration profile, i.e. uranium dissolution near the front (supported by $^{230}Th/^{234}U$ values greater than unity) but uranium precipitation in the oxidised rock away from the front (supported by $^{230}Th/^{234}U$ values less than unity). If it is assumed that the return to equilibrium of the $^{230}Th/^{234}U$ activity ratio over a distance of 5 to 10 m is purely the result of ^{234}U decay and associated ingrowth of ^{230}Th after the initial

TABLE 3.2

Natural decay series analyses of rock samples from the F1 drillcore, Osamu Utsumi uranium mine.

Sample	Depth (m)	^{238}U (Bq kg^{-1})	$^{234}U/^{238}U$	$^{230}Th/^{234}U$	$^{226}Ra/^{230}Th$	$^{231}Pa/^{235}U$	^{232}Th (Bq kg^{-1})
6-1A	6.00	1167 ± 17	1.01 ± 0.02	1.06 ± 0.04	0.076 ± 0.05	n.a.	193 ± 9
10-1A	9.84	384 ± 8	1.05 ± 0.03	1.09 ± 0.04	0.68 ± 0.05	n.a.	402 ± 20
16-1A	15.07	248 ± 5	1.03 ± 0.02	0.99 ± 0.04	1.49 ± 0.09	n.a.	103 ± 5
26-1A	25.22	198 ± 7	1.10 ± 0.03	0.96 ± 0.04	3.90 ± 0.25	n.a.	213 ± 8
33-1A	32.89	1085 ± 27	1.03 ± 0.02	1.02 ± 0.03	0.61 ± 0.04	n.a.	150 ± 7
34-1B-A	33.40	227 ± 5	1.00 ± 0.02	0.95 ± 0.04	3.36 ± 0.20	n.a.	302 ± 8
34-1B-D	33.51	212 ± 7	0.97 ± 0.03	6.00 ± 0.05	3.26 ± 0.24	n.a.	320 ± 15
34-1B-F	33.65	582 ± 15	0.98 ± 0.02	0.94 ± 0.04	2.16 ± 0.15	n.a.	427 ± 22
34-1C	34.00	243 ± 8	0.94 ± 0.03	1.55 ± 0.09	2.56 ± 0.13	n.a.	642 ± 35
35-1A	34.31	503 ± 13	0.85 ± 0.02	0.81 ± 0.06	1.78 ± 0.16	n.a.	88 ± 11
41-1A	40.05	794 ± 14	1.23 ± 0.04	1.01 ± 0.04	1.05 ± 0.04	n.a.	256 ± 10
42-1A	41.85	31300 ± 1000	1.15 ± 0.03	0.94 ± 0.03	0.57 ± 0.04	0.97 ± 0.07	250 ± 10
42-1B-B	41.95	345000 ± 9000	1.08 ± 0.02	0.96 ± 0.03	0.62 ± 0.04	1.03 ± 0.06	1570 ± 200
42-1B-D	41.97	110000 ± 2300	1.10 ± 0.02	0.97 ± 0.03	0.48 ± 0.03	0.95 ± 0.06	250 ± 80
42-1B-F	42.01	52500 ± 1300	1.02 ± 0.02	0.88 ± 0.03	0.51 ± 0.03	1.06 ± 0.07	1167 ± 117
42-1B-H	42.03	2020 ± 50	0.51 ± 0.01	1.00 ± 0.03	4.43 ± 0.27	1.05 ± 0.08	327 ± 10
42-1B-I	42.04	336 ± 7	1.02 ± 0.02	1.09 ± 0.04	9.20 ± 0.59	2.84 ± 0.41	280 ± 12
42-1B-K	42.05	557 ± 18	0.93 ± 0.03	1.00 ± 0.05	6.50 ± 0.43	1.13 ± 0.10	447 ± 22
43-1A	42.10	607 ± 15	0.99 ± 0.02	1.00 ± 0.05	6.60 ± 0.38	0.97 ± 0.07	293 ± 10
45-1A	44.87	1849 ± 50	1.02 ± 0.03	1.23 ± 0.03	0.91 ± 0.06	n.a.	549 ± 30
47-1A	46.10	6891 ± 119	0.96 ± 0.04	n.a.	n.a.	n.a.	n.a.
50-1A	49.83	1085 ± 16	1.07 ± 0.04	0.94 ± 0.04	1.28 ± 0.10	n.a.	136 ± 7
55-1A	54.30	1884 ± 33	1.09 ± 0.01	0.97 ± 0.03	0.92 ± 0.06	n.a.	158 ± 15
60-1A	59.80	3741 ± 100	0.79 ± 0.02	0.81 ± 0.06	0.92 ± 0.06	n.a.	222 ± 8
65-1A	64.50	2217 ± 32	0.94 ± 0.02	0.89 ± 0.03	1.04 ± 0.06	n.a.	119 ± 6
66-1A-A	65.93	750 ± 17	0.94 ± 0.02	1.27 ± 0.03	1.03 ± 0.06	n.a.	150 ± 5
67-1A-B	66.19	1150 ± 27	0.84 ± 0.02	1.69 ± 0.08	1.69 ± 0.12	n.a.	197 ± 23
67-1A-D	66.26	1560 ± 38	0.86 ± 0.02	1.04 ± 0.04	0.79 ± 0.05	n.a.	135 ± 12
68-1A-A	67.00	2530 ± 67	0.88 ± 0.02	1.04 ± 0.03	0.76 ± 0.04	n.a.	88 ± 7
75-1A	74.25	500 ± 10	1.03 ± 0.03	1.07 ± 0.04	1.11 ± 0.07	n.a.	55 ± 7
80-1A	79.80	560 ± 13	1.01 ± 0.02	1.00 ± 0.03	0.90 ± 0.05	n.a.	87 ± 3
101-1A	100.32	428 ± 15	1.08 ± 0.03	1.35 ± 0.07	0.80 ± 0.06	n.a.	102 ± 10
110-1A	110.00	462 ± 12	1.04 ± 0.02	1.01 ± 0.03	1.09 ± 0.07	n.a.	175 ± 8
111-1B	110.13	170 ± 5	1.09 ± 0.03	0.99 ± 0.03	0.91 ± 0.06	n.a.	102 ± 5
121-1A	120.19	365 ± 8	1.00 ± 0.02	1.12 ± 0.04	0.85 ± 0.06	n.a.	153 ± 10

n.a. = not analysed.

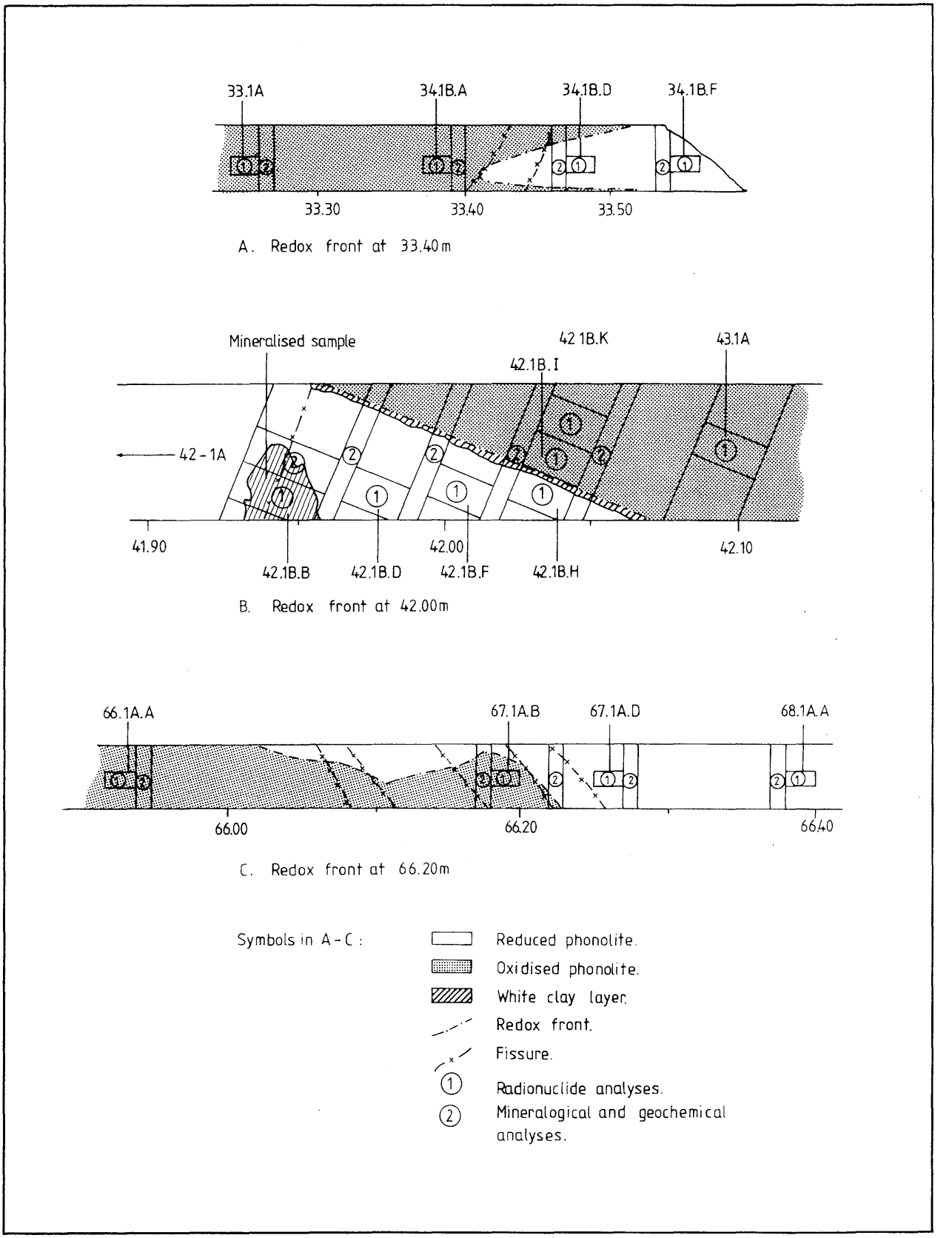

Figure 3.6. Sections of drillcore F1 showing details of sampling positions close to the redox fronts.

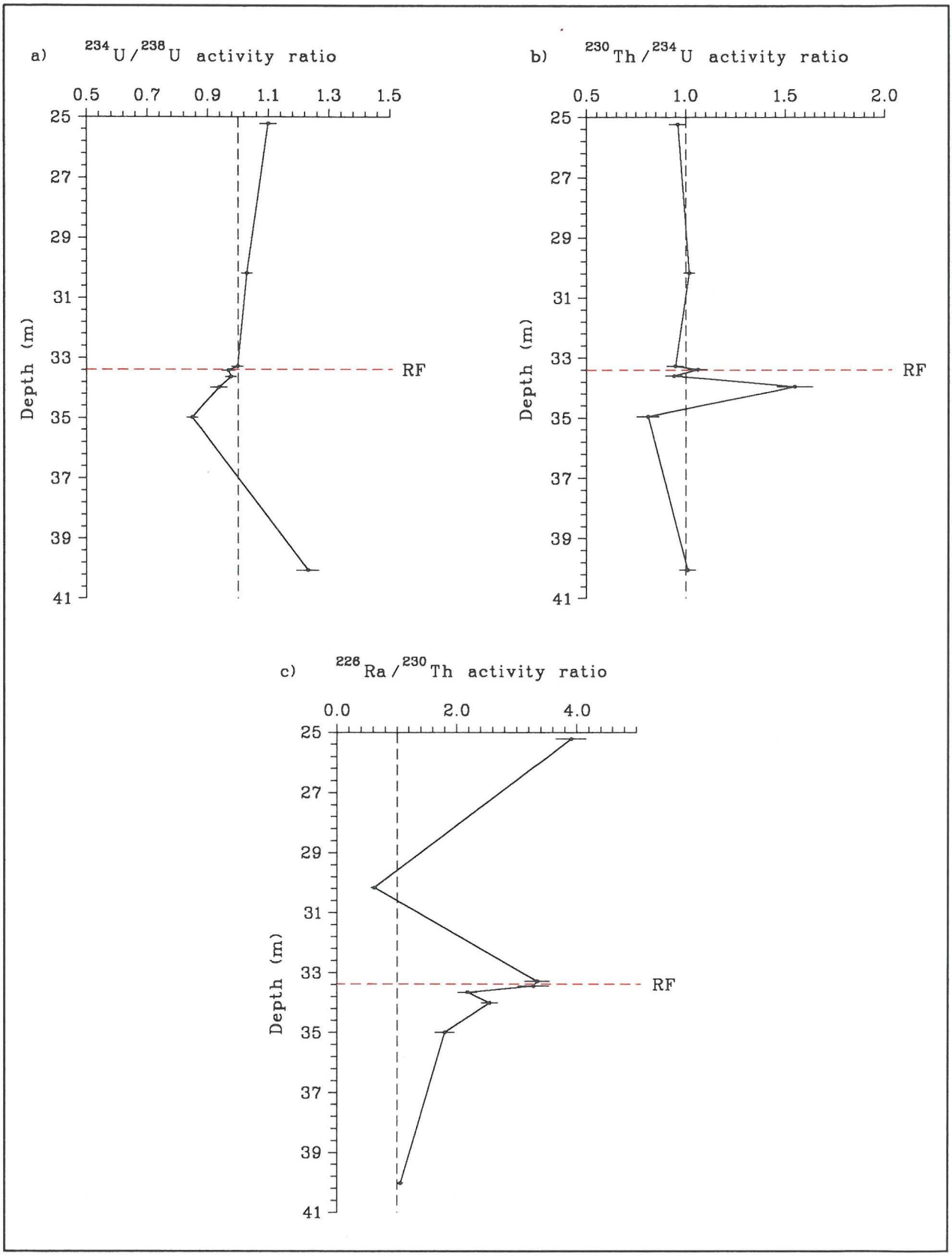

Figure 3.7. Activity ratio profiles across redox front 33.4 m for: a) $^{234}U/^{238}U$, b) $^{230}Th/^{234}U$ and c) $^{226}Ra/^{230}Th$.

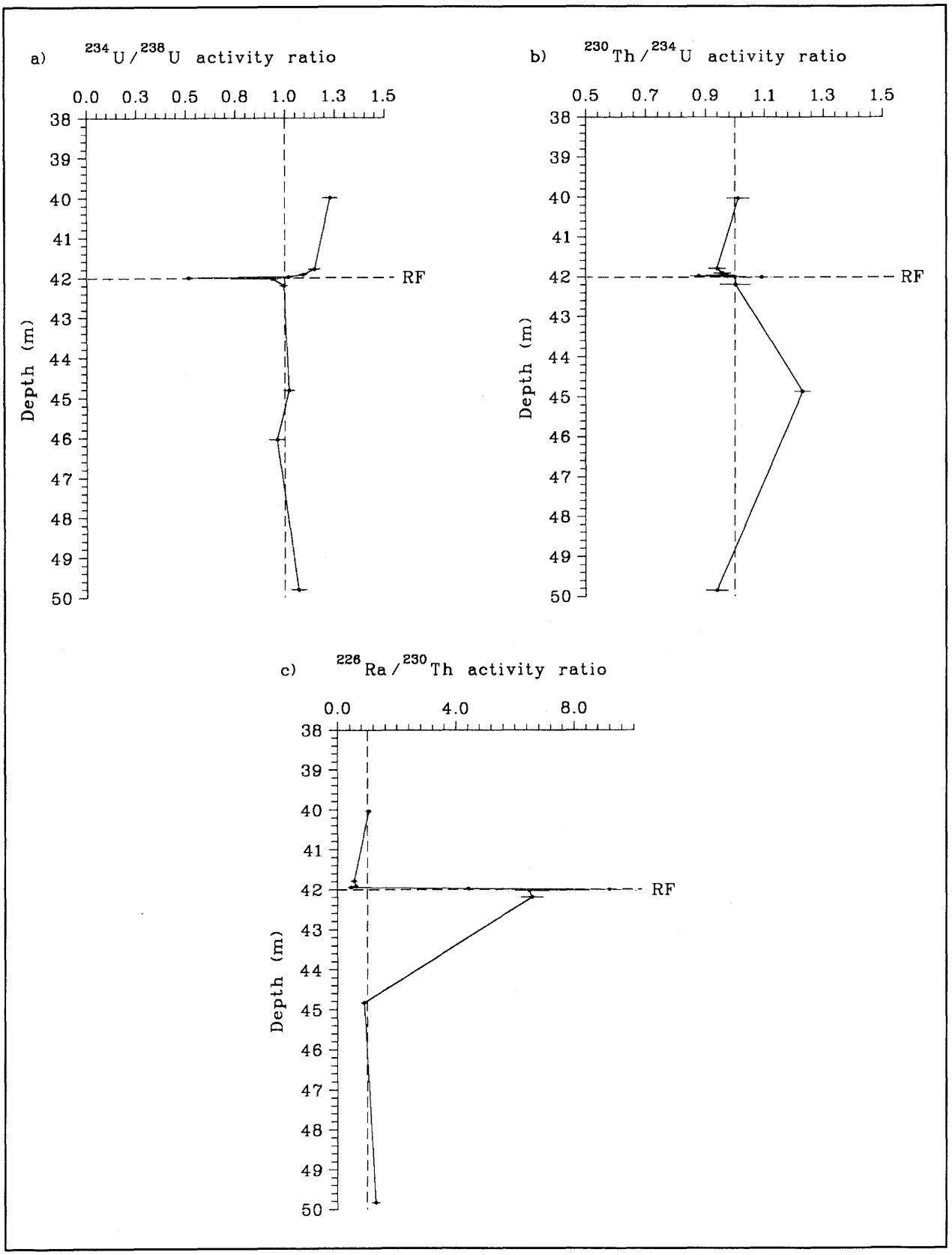

Figure 3.8. Activity ratio profiles across redox front 42.0 m for: a) $^{234}U/^{238}U$, b) $^{230}Th/^{234}U$ and c) $^{226}Ra/^{230}Th$.

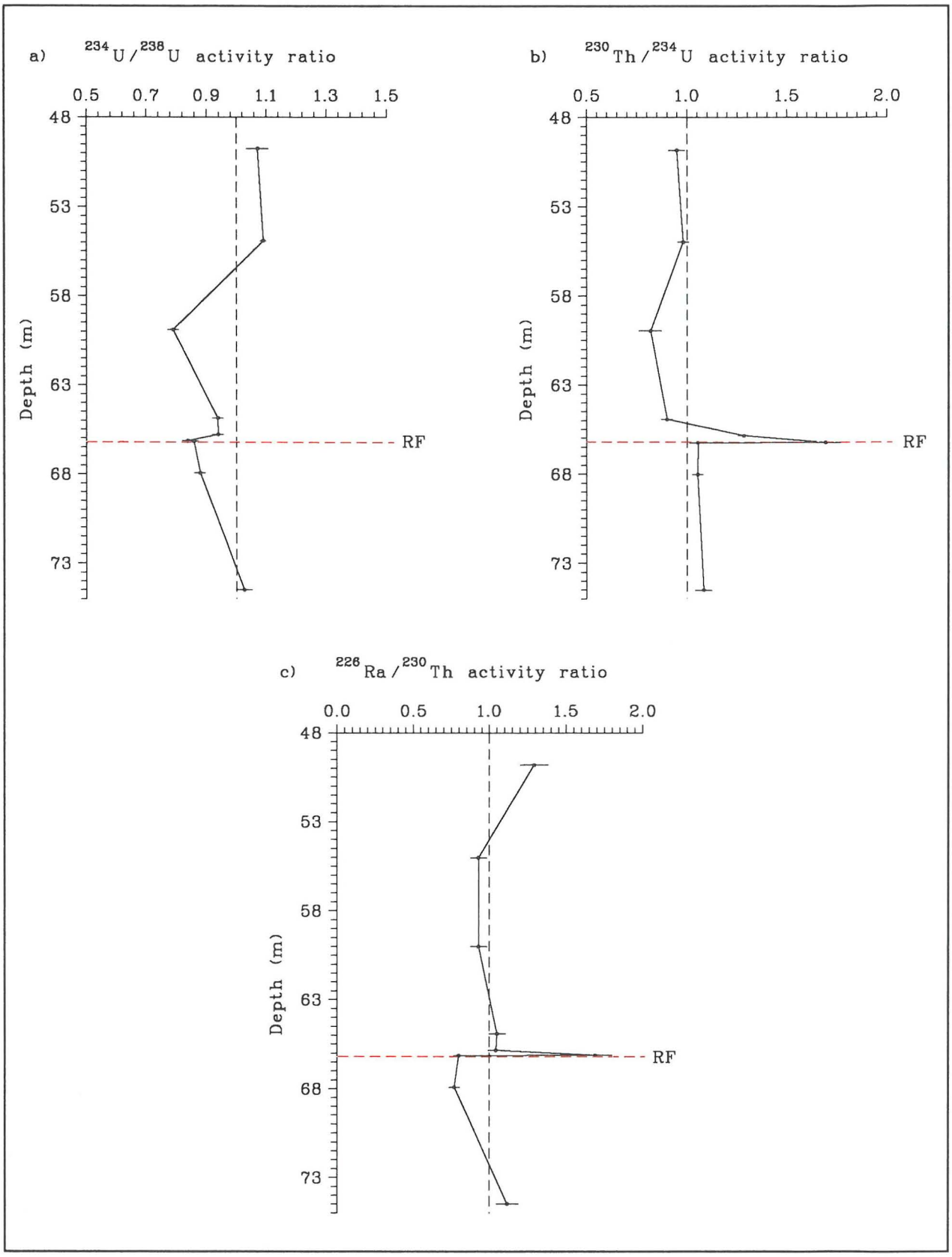

Figure 3.9. Activity ratio profiles across redox front 66.2 m for: a) $^{234}U/^{238}U$, b) $^{230}Th/^{234}U$ and c) $^{226}Ra/^{230}Th$.

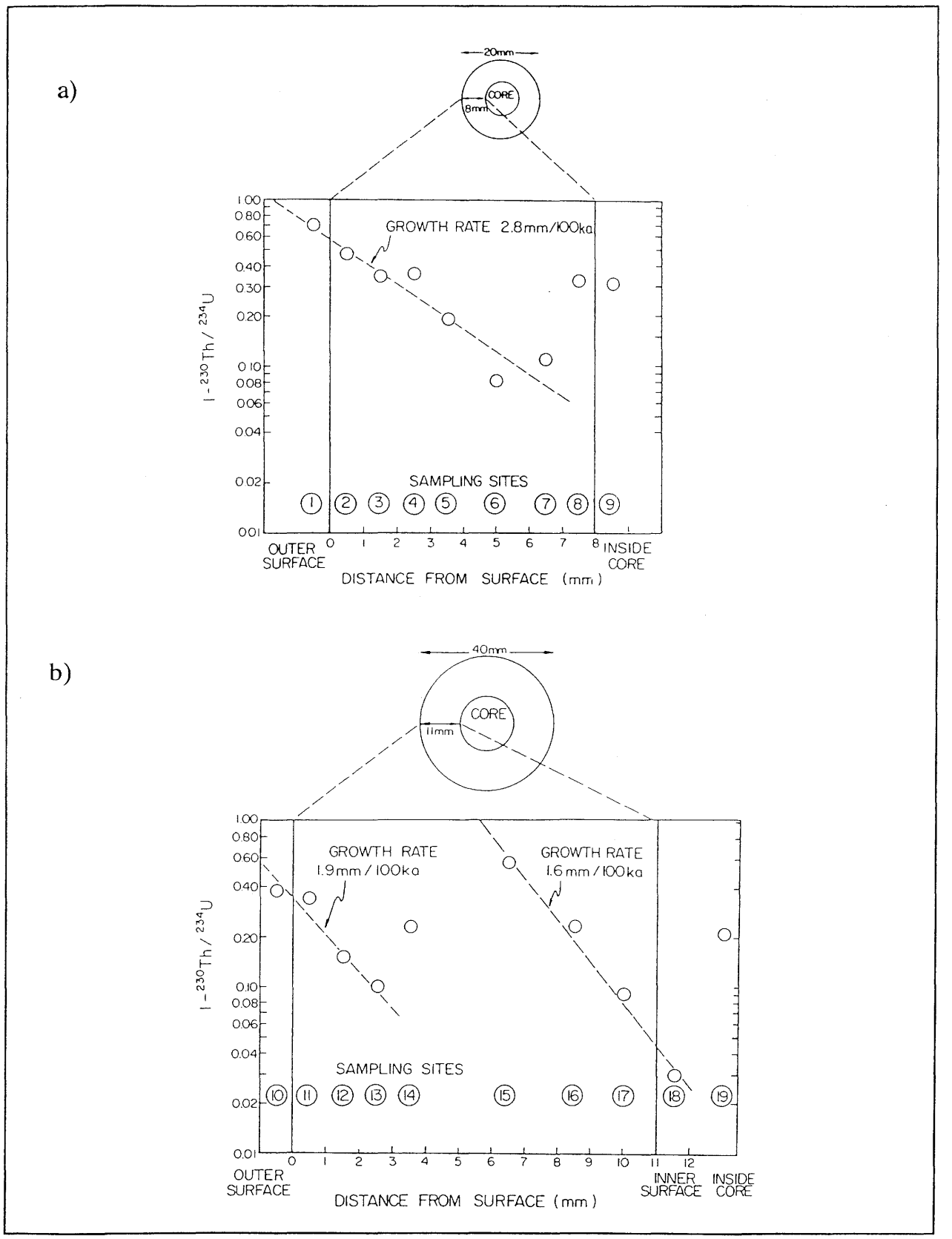

Figure 3.10. Plots of log (1 – $^{230}Th/^{234}U$) versus distance for: a) a small nodule, and b) a larger composite nodule.

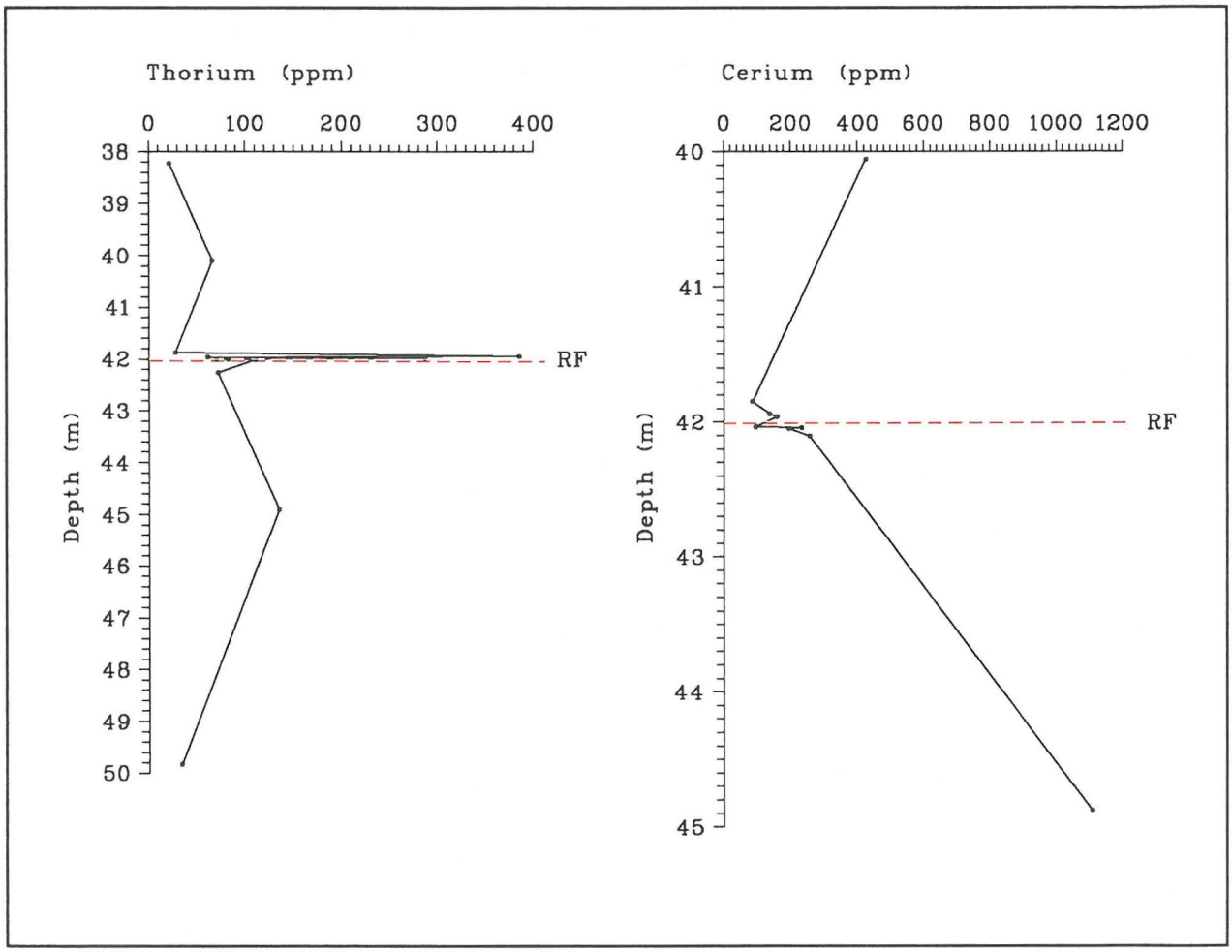

Figure 3.11. Thorium and cerium concentration profiles across the 42.0 m redox front in drillcore F1.

$^{230}Th/^{234}U$ disequilibrium has been established, then a downward rate of movement of the redox front may be in the order of 20 m in 10^6 a. However, if the decrease in the $^{226}Ra/^{230}Th$ activity ratio over a distance of 26 cm from the front is assumed to be only from excess ^{226}Ra decay after passage of the front through the rock, then a movement rate for the front of around 26 cm in 10^6 a is obtained.

In summary, the natural decay series studies from drillcore F1 confirmed the greater mobility of U and Ra than Th and Pa in groundwaters. Of the three redox fronts studied in detail, one was concluded to have been static (on a cm scale) for a time of at least $7x10^5$ a, whilst the other two were consistent with rates of movement ranging from 2–20 m in 10^6 a, which is in general agreement with the estimated regional erosion rates (see Chapter 2).

Pitchblende Nodules

Studies of uranium nodules have been carried out using uranium decay series measurements to determine their growth rates in relation to the migration of the redox fronts (MacKenzie *et al.*, this report series; Rep. 7). Assuming that the nodules have grown from the central core outwards, and that uranium precipitates without its thorium daughter, then the age of each layer can be determined by the growth equation. Even if some thorium is present at the time of precipitation, relative ages of the layers can be deduced provided that the relative amount of initial thorium has remained approximately constant.

Two nodules, one small and the other a larger compound variety, were analysed and averaged around 30 wt.% U as pitchblende (Table 3.3). There was a slight tendency for the uranium concentration to diminish from the outer rims to the inner cores, the lowest values being in the core material itself and the outermost surface material. Knowing the variation of the $^{234}U/^{238}U$ activity ratio in the mine groundwaters and in the leachable fraction of the mine rock samples, it is surprising to find the prevalence of equilibrium values of $^{234}U/^{238}U$ in the nodules (Fig. 3.10). Only the core samples from each nodule were out of equilibrium, both of which are characterised by a ^{234}U deficiency of about 8%. In contrast, the samples from the inner half of the large nodule appear to have an excess of ^{234}U, which may be due to its compound nature.

In addition, one older nodule and several younger nodules were analysed. The former mostly showed $^{234}U/^{238}U$ isotopic equilibrium and also $^{230}Th/^{234}U$ equilibrium, with the exception of the outermost analysed layer indicating, in this case, that the nodule is much

TABLE 3.3

Analytical results and calculated ages for two uranium nodules from the Osamu Utsumi mine.

Distance from rim (mm)	U concentration (%)	$^{234}U/^{238}U$	$^{230}Th/^{234}U$	Model age (ka)	Apparent age (ka)
Small Nodule (diameter 20 mm)					
0.0	6.2	0.99	0.30	38	0
0.5	45.2	1.00	0.53	81	43
1.5	41.4	1.00	0.65	113	75
2.5	31.9	0.99	0.64	111	73
3.5	34.7	1.00	0.81	182	144
5.0	20.2	0.98	0.92	276	238
6.5	37.7	1.00	0.89	235	197
7.5	31.0	1.01	0.68	123	85
8.0	15.5	0.93	0.69	127	89
Large Composite Nodule (diameter 40 mm)					
0.0	54.3	0.99	0.63	106	0
0.5	35.8	0.99	0.66	116	10
1.5	25.1	0.96	0.85	206	100
2.5	32.4	1.02	0.90	253	147
3.5	35.9	0.99	0.77	159	53
6.5	27.1	1.06	0.52	79	0
8.5	30.0	1.05	0.77	160	81
10.0	49.3	1.04	0.91	261	182
11.0	23.7	1.02	0.97	398	319
13.0	7.4	0.91	0.79	169	90

older than those described above and is growing at a very slow rate. The latter nodules (four from the oxidised zone, two from the reduced zone and one from directly on the redox discontinuity) recorded fairly high uranium concentrations (up to 22%), with the highest concentrations associated with the reduced and redox boundary varieties, and the lowest concentration in the oxidised varieties (lowest value of 0.1%). Furthermore, the lowest $^{234}U/^{238}U$ activity ratios are generally associated with the reduced samples and the highest values with the oxidised varieties. A further distinguishing feature of the oxidised varieties is their very high ratio of ^{230}Th to ^{234}U (5–7) compared to the reduced samples (0.33–0.64).

In conclusion, the young uranium nodules (on a timescale of 10^5–10^6 a) exhibit growth rates of 1.8–2.6 cm in 10^6 a, whereas the others are old on this timescale and exhibit

equilibrium within the natural decay series. The time required for nodule formation in the reduced rock is estimated to be at least in the order of 10^5 a, while a time of about 10^4–10^5 a is required for the dissolution of micronodules isolated in the oxidised rock following the passage of the redox front.

3.1.4. Thorium, rare-earth (REE) and trace element distributions

Along the measured mine profile (Fig. 3.4), the thorium concentration distribution from 1340 m.a.s.l. upwards through the oxidised bedrock zone is fairly uniform to about 1390 m.a.s.l. (average value around 50 μg/g), before increasing to 89 μg/g at the surface. In common with the uranium, thorium also fluctuates around the redox fronts between 1255 and 1290 m.a.s.l. (range of 30–220 μg/g Th). From 1255 to 1200 m.a.s.l., the thorium values are reasonably uniform (20–60 μg/g).

The rare-earth distributions are also variable, in some cases related to zones of enrichment and depletion which reflect primary or early hydrothermal mineralogical/ compositional features of the phonolite layers/flows (Waber *et al.*, this report series; Rep. 2), and in other cases closely related to the low-temperature supergene redox fronts in close association with uranium and other trace elements (MacKenzie *et al.*, this report series; Rep. 7).

The thorium and REE contents of the reduced phonolites are associated with a broad variety of Th- and REE-bearing mineral phases which include monazite and cheralite (most abundant), bastnaesite, crandallite, florencite, gorceixite and goyazite. The textural relationships of monazite and cheralite indicate a pure hydrothermal origin, likewise for bastnaesite, most probably during an early mineralisation event. Less certain is the origin of REE-bearing phases of the crandallite group minerals (crandallite, florencite, gorceixite and goyazite), which tend to be more abundant in the oxidised and lateritic zones and therefore might be partly of supergene origin.

Supergene trace element distributions in the rocks across the redox fronts are unusual. For example, the REE data reveal a general loss of these elements from the oxidised rock as the redox front migrates through the phonolites of the Osamu Utsumi mine, with the degree of loss being greater for the LREEs (MacKenzie *et al.*, op. cit.). The non-redox-sensitive, refractory 3+ and 4+ oxidation state species behave in a systematic manner at the redox fronts, with preferential concentration in the reduced rock close to the fronts. However, Eu and particularly Ce, which is susceptible to oxidation to the 4+

oxidation state, sometimes show a pronounced concentration in the oxidised phonolite. Figure 3.11 illustrates the distribution of Th and Ce across the redox front at 42.0 m.

Trace elements, which are grouped along with U as being enriched in the oxidised phonolites relative to the reduced phonolites, i.e. Re, Mo, Ti, Rb, Bi, Tl, Sn and Ga, tend to be redistributed bimodally or asymmetrically around the redox fronts (e.g. Fig. 3.12). Both redox-sensitive elements such as U and Mo as well as elements which are not intrinsically involved in redox controlled processes, such as Cs, are concentrated in this area. In the case of the non-redox-sensitive elements, removal from solution in the vicinity of the redox fronts requires either that the solution phase concentrations of appropriate ions are high enough to lead to precipitation, or alternatively that the mechanism involved is scavenging or coprecipitation with some major mineral species.

The distribution of the REEs and selected stable trace elements thus indicates that the zone around the redox fronts generally contains enhanced concentrations of most elements associated with active dissolution at the front. These fronts therefore represent an initial zone of retardation which moves in response to the migration of the redox fronts.

3.1.5. Natural plutonium at the redox front

The natural plutonium concentration in a centimetre-sized nodule, similar to those described above, was measured by isotope dilution mass spectrometry at a detection limit of 2.8×10^{8} atoms. The measured quantity of ^{239}Pu in the nodule was twice the level of detection; neither of the anthropogenic plutonium isotopes ^{238}Pu and ^{240}Pu were detected, showing an absence of contamination in the sample. The Pu concentration in the sample was calculated to be $2.3 \pm 0.7 \times 10^{8}$ atoms per gram, with the uranium concentration 43 (± 2)% and the atom ratio of Pu $2.1 \pm 0.7 \times 10^{-13}$.

The presence of natural plutonium (formed via neutron capture by uranium) can be shown to be a function of the composition of the rock within a radius of about 50 cm of the sample, the spatial distribution of elements within that volume, and the length of time that the system has been open to loss and/or gain of uranium or plutonium. In a system that has been closed for about 10^{5} a, several half-lives of plutonium, a state of secular equilibrium is established between the parent uranium and the radioactive daughter plutonium. In such a system, the Pu/U ratio is independent of time. Calculations indicate that the Pu/U in the pitchblende nodule is consistent with a state of secular equilibrium in a matrix of reduced phonolite containing 3000 μg/g U. It would therefore

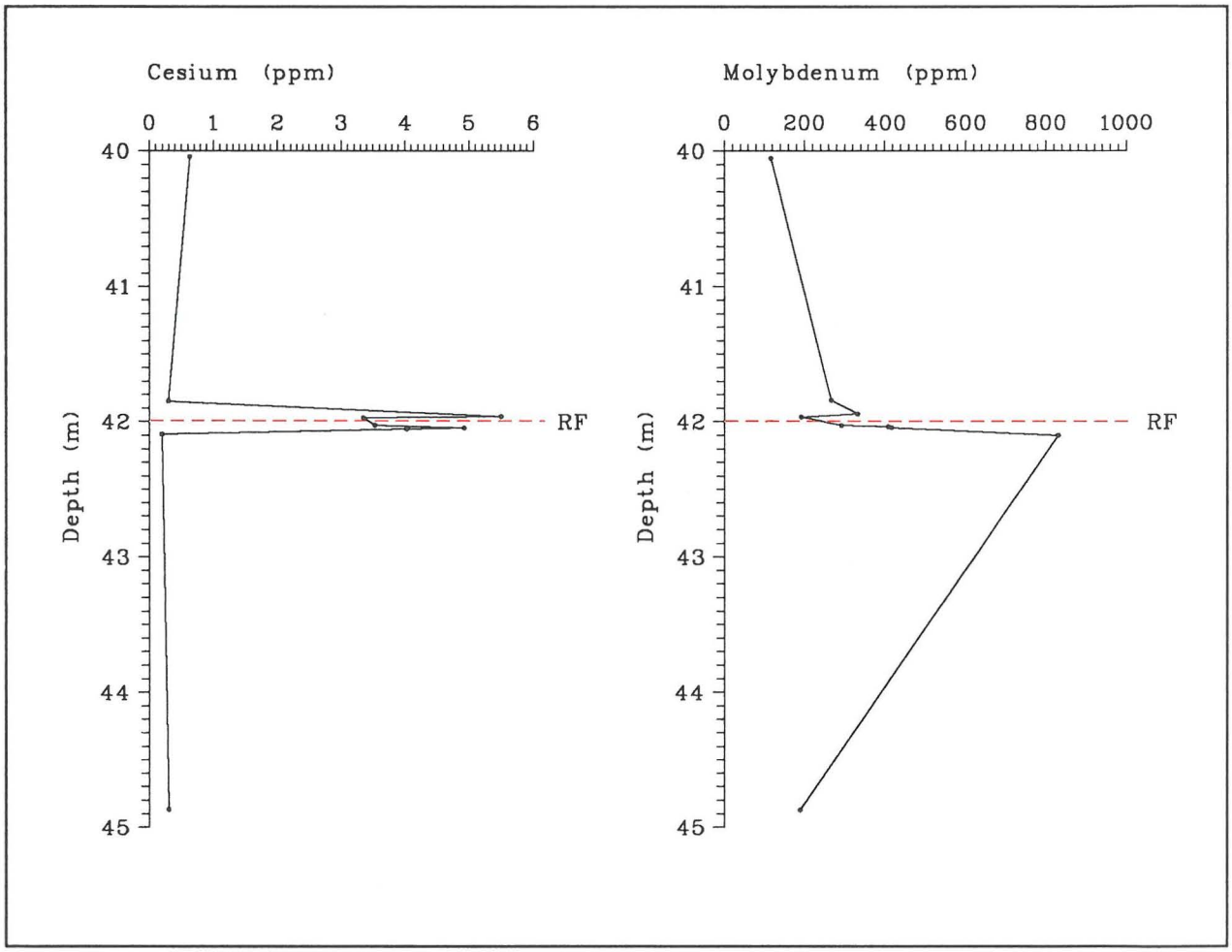

Figure 3.12. Cesium and molybdenum concentration profiles across the 42.0 m redox front in drillcore F1.

appear that the Pu/U ratio in the nodule suggests that the two elements have resided, unfractionated, in the most highly uraniferous rock in the deposit for the last 10^5 a. Even if alteration has occurred more recently, the processes did not significantly fractionate plutonium from uranium.

3.2. Hydrogeology

Prior to development of the open-cast mine, this area comprised a series of quite deeply incised, steep-sided valleys containing ephemeral streams. Groundwater flow at this time would have recharged on the interfluves and upper valley sides and discharged into the streams in the valley bottoms. Water recharging the interfluves would be oxidising and water discharging into the streams would be a mixture of reducing groundwaters from depth in the aquifer and shallow oxidising waters. The rock is highly fractured and such fractures would be expected to act as conduits carrying the bulk of groundwater.

Exploitation of the ore has lowered the local water table and gradually disturbed the old groundwater flow patterns. Additionally, the catchment area of the existing mine is larger than the original valley and intercepts groundwaters which originally flowed into other valley systems, thus extending the area discharging reducing groundwaters from the aquifer. Upward flow of reducing groundwater now occurs through rock which originally received downward-percolating oxidising waters. Figure 3.13a shows the relationship between the original topography and its influence on groundwater flow patterns prior to mining. Figure 3.13b shows the original topography and that after mining, and the influence of excavation on groundwater flow patterns. Flow close to the surface of the mine is affected by blasting damage and unloading of the overburden, which has enhanced permeabilities and generated horizontal flows. Additionally, the near-surface flow pattern and rates will be affected by the large number of exploration boreholes drilled into the mine floor as part of the ore reserve estimation programme.

Water levels measured in piezometers installed earlier by Urânio do Brasil show a steeply-dipping water table gradient towards the mine sump. Also, those piezometers on the edge of the mine show a slight vertically downward flow gradient, whilst those near the centre of the mine show vertically upward flows. Hydraulic conductivities measured in the piezometers range from $1x10^{-10}$–$5x10^{-7}$ ms^{-1}. Water levels responded rapidly to both seasonal rainfall and single rainfall events.

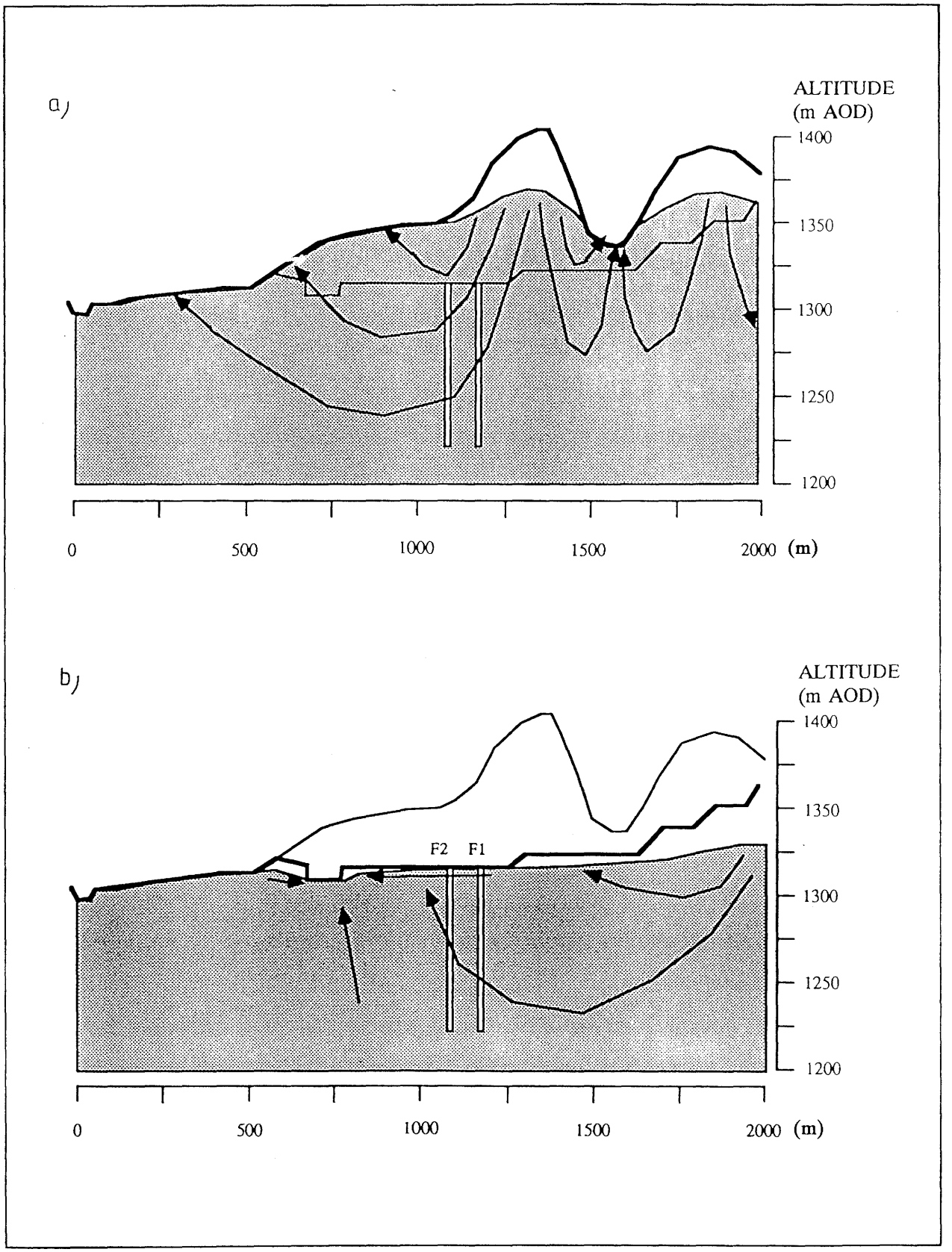

Figure 3.13. Simulated groundwater flows along the old valley system in the Osamu Utsumi mine: a) prior to excavations, b) subsequent to excavations. The thick line shows the original topography in (a) and the present topography in (b). Due to excavations, the same area of rock now receives the upward movement of predominantly reducing water.

(m AOD = *metres above ordnance datum*).

Present studies (Holmes *et al.*, this report series; Rep. 5) have produced information on the hydraulic conductivity of the rock and water levels or pressures, which give flow direction and flow rates. This has been made possible by supplementing earlier existing mine piezometric data with the present project data from hydraulic testing in boreholes F1-F4. The distribution of hydraulic conductivity below 30 m (boreholes F1-F3) based on the length of the sections measured was found to be relatively uniform (mostly around 10^{-5}–10^{-7} ms^{-1}; Fig. 3.14), which indicated that the bedrock is evenly fractured and can thus be generally regarded as a porous medium. The more highly conductive zones occur, for example, between 97–124 m in F1 ($2.5x10^{-6}$ ms^{-1}), and between 65–71 m in F3 ($1.2x10^{-6}$ ms^{-1}). Both of these zones represent reference location points selected for groundwater sampling and characterisation. Pressure heads indicated the groundwater flow to have an upward vertical component throughout the mine.

The upper 10–15 m of the rock contrasts strongly with deeper zones, having a high conductivity (10^{-4} ms^{-1}) and a marked lateral to downward flow component. Mixing between near-surface and deep groundwater components therefore occurs below this zone.

Three-dimensional computer groundwater flow models were produced for flow before mining excavations and for present conditions. Owing to the limited nature of the data, and in order to simplify the model boundary conditions, several assumptions were necessary (see Holmes *et al.*, this report series; Rep. 5).

The values obtained for head are presented in Figures 3.15 and 3.16 as contour plots on selected horizontal and vertical sections. In order to assist in the visualisation of the flow field, pathlines have been traced from a number of points at depth and plotted as projections onto the same horizontal and vertical sections. The pathlines show the route which a package of water would follow through the rock along the line of a stream running through the mine (profile A-A′).

Figure 3.15a shows a contour plot of the heads on the top surface for the pre-mine conditions which is, of course, the water table used for this calculation. Figure 3.15b shows the calculated heads contoured on the river section, and Figure 3.15c shows that pathlines selected to be in the plane of the river section behave in a simple and predictable fashion.

Figure 3.16 shows the effects of the excavation of the mine. Figure 3.16a is the contoured water table surface showing clearly the location of the mine. Calculated heads on the river section are shown in Figure 3.16b, and it can be seen that the effect of the mine on the river section is very marked. This is especially apparent in Figure 3.15c where pathlines from locations within the river section now run almost vertically up into the

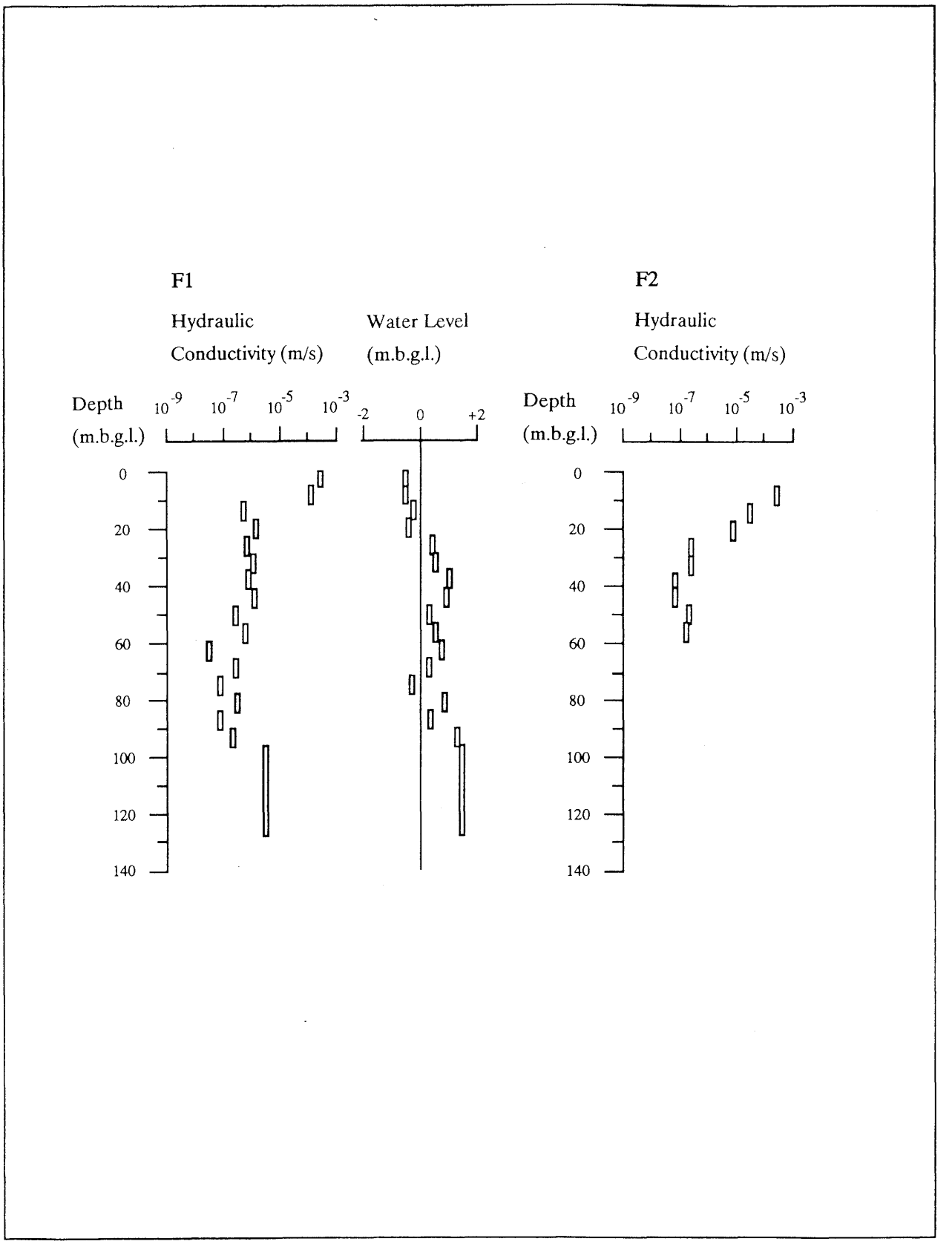

Figure 3.14. Hydraulic conductivity and head measurements in boreholes F1 and F2.

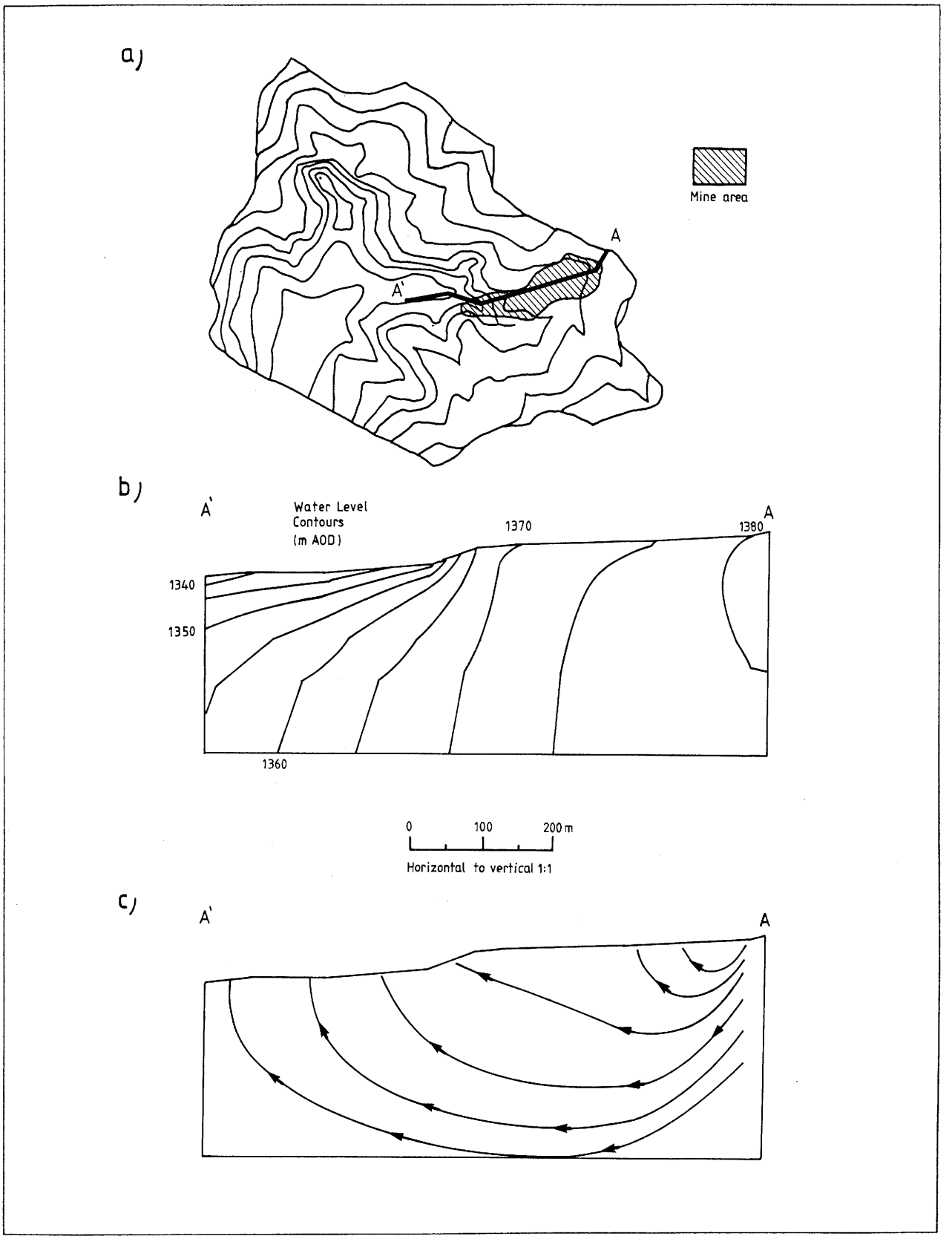

Figure 3.15. (a) Distribution of water levels (heads) generated by the hydrogeological model for the pre-excavation topography around the Osamu Utsumi mine, (b) vertical head distribution along the pre-excavation valley floor section (A-A'), and (c) the vertical distribution of flow-paths along the pre-excavation valley floor section.

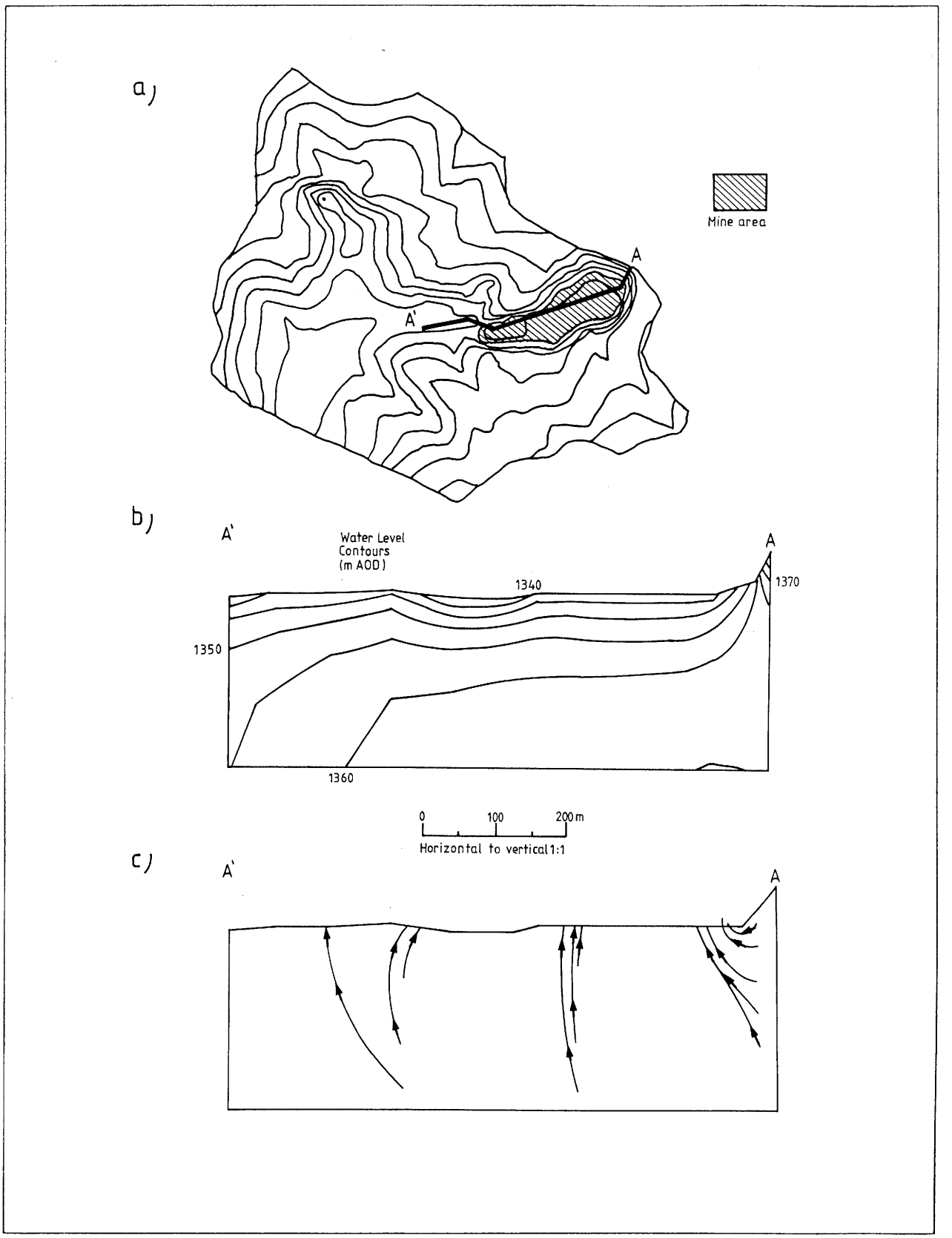

Figure 3.16. a) Distribution of water levels (heads) generated by the hydrogeological model for the post-excavation topography around the Osamu Utsumi mine, b) vertical head distribution along the post-excavation valley floor direction (A-A'), and c) vertical distribution of flow-paths along the post-excavation valley floor direction.

mine from the bottom of the model. Flow rates in the vicinity of the current mine surface are typically in the order of 3 to $5x10^{-10}$ $m^3/m^2/s$ directed upwards, though the dependence of these particular values upon the material properties chosen must be emphasised. These paths do not, however, represent the bulk of the flow into the mine, which comes instead from the sides of the valley. Flow rates just below the mine floor are now of the order of $3x10^{-9}$ $m^3/m^2/s$.

3.3. Chemical and isotopic character of the groundwater

The Osamu Utsumi mine groundwaters have been characterised in terms of major chemical, tritium and stable isotopic composition (Nordstrom *et al.*, this report series; Reps. 6 and 14). Although emphasis was placed on samples from the reference location points, other localities within and outside the mine confines were also sampled sporadically to provide a wider perspective for interpretation.

The main objectives of the hydrochemical, tritium and stable isotope studies were to a) classify the hydrochemical regime in the mine site, b) establish any physico-chemical changes in the groundwaters related to flow along the hydraulic gradient, c) establish the major water/rock interactions which produce the observed water chemistry, and d) assess the influence of seasonal precipitation on the groundwater chemistry. This information provides the background for the geochemical studies described in Chapters 5-6.

Groundwater sampling was carried out at seven reference locations namely four cased and packed-off borehole sections (F1-F3; F5) and three shallow cased boreholes (SW01-SW03) (Figs. 3.2 and 3.3). These sampling points were supplemented by artesian water welling up from an old shaft, and from an artesian piezometer station located at a higher level on one of the peripheral benches of the mine (Fig. 3.2).

Three analysis programmes were run in parallel; a) regular sampling at all locations and on-site analysis, b) monitoring boreholes F1-F3; F5, and c) sampling of (b) for the full hydrochemical analytical programme.

The selection of representative groundwater analyses given in Table 3.4 is highly unusual relative to most reported worldwide groundwater compositions, and suggests intense weathering by actively circulating fresh groundwaters in contact with a highly leached potassic-rich rock mass. The deuterium and ^{18}O isotopic analyses show that the groundwaters are meteoric in origin, lying on or near the meteoric water line. The waters are essentially of K-Fe-SO_4 character, with fluoride as a much more important anion than

TABLE 3.4
Selected groundwater compositions from the Osamu Utsumi mine.

Borehole	F1	F2	F3	F5	SW01	SW02	SW03	Piezometer station PM 22	SHAFT	SUPPLY DAM
Sample code no.	PC-GW-14	PC-GW-43	PC-GW-55	PC-GW-72	PC-GW-57	PC-GW-38	PC-GW-58	PC-GW-27	PC-GW-28	PC-SW-03
Sampling int (m)	96.5–125.7	45–60	50–77.6	275–300	3–12	3–12	3–12	0–20	0–40	---
Date collected	870106	880602	880916	881220	880921	880203	880922	871002	871007	870709
Temperature (^{O}C)	21.0	21.0	22.0	---	21.0	---	20.0	20.0	20.1	17.5
pH (field)	5.4	5.7	5.1	6.0	3.9	2.9	4.4	6.2	5.7	6.5
Cond.(mS/m)	6.0	0.7	<0.008	<0.008	3.3	---	4.6	6.3	6.4	6.0
Eh(mV)	---	323	338	---	694	---	657	---	---	---
Alkalinity (mg/L HCO3)	10	8.0	2.65	31.4	<0.60	<5.0	<0.60	30	20	9
Sum cations (meq/L)	0.47	0.511	11.6	1.42	4.57	6.27	0.715	0.84	6.77	0.16
Sum anions (meq/L)	0.50	0.503	11.7	1.46	4.83	7.82	0.773	0.93	6.66	0.18
Charge balance %	-7.4	1.65	-1.03	3.24	-5.53	-11.01	-7.85	-10.2	1.6	-9.3
Element	mg/L	mg/L	mg/L	mg/L	mg/L	mg/L	mg/L	mg/L	mg/L	mg/L
Ca	0.61	2.2	111	10.8	37	23.3	2.5	5.0	59.8	0.14
Mg	0.05	0.07	4.00	0.30	2.09	2.34	0.85	0.749	2.28	<0.10
Sr	0.10	0.064	2.1	0.26	0.86	1.41	0.25	0.154	1.61	0.01
Ba	0.14	0.11	0.051	0.110	0.051	0.028	0.095	0.043	0.059	0.014
Na	0.57	0.13	1.28	0.80	1.0	1.82	0.8	0.417	1.35	0.19
K	12.0	12	42.5	12.5	20	29.9	12	13.9	21.8	5.3
Li	---	<0.015	<0.010	<0.01	<0.010	<0.015	<0.010	<0.02	<0.02	<0.02
Fe(II)	1.53	1.05	88.7	---	<0.10	1.03	<0.10	2.08	44.5	0.012
Fe(tot)	1.62	1.11	88.9	8.68	0.011	8.53	<0.10	2.13	44.7	0.14
Al	0.155	0.23	4.420	0.6	10.380	35.2	0.790	0.048	7.68	<0.02
Mn	0.28	0.20	19	2.95	18	9.14	1.0	1.80	13.1	0.088
Zn	0.12	0.15	3.27	0.17	1.83	3.58	0.33	0.74	0.184	<0.02
Cd	<0.02	<0.005	<0.005	<0.005	<0.005	0.045	<0.005	<0.01	<0.02	<0.01
Cu	<0.02	<0.015	<0.005	<0.005	<0.005	<0.015	<0.005	<0.015	<0.015	<0.02
Cr	<0.05	<0.12	<0.02	<0.02	<0.02	<0.12	<0.02	<0.05	<0.05	<0.05
Co	---	<0.002	<0.020	<0.020	<0.020	0.043	<0.020	<0.035	<0.035	<0.035
Ni	<0.02	<0.003	<0.025	<0.025	<0.025	0.044	<0.025	<0.02	<0.02	<0.02
Mo	---	<0.050	<0.035	<0.035	<0.035	<0.050	<0.035	<0.03	<0.03	<0.03
Ag	<0.02	---	---	---	---	---	---	<0.05	<0.05	<0.05
Pb	<0.10	<0.050	<0.090	<0.09	<0.090	0.957	<0.090	<0.10	<0.10	<0.10
Zr	---	<0.045	<0.015	<0.0015	<0.015	0.064	<0.015	<0.01	<0.01	<0.01
SO4	15	12.8	540	30	209	458	33.1	10.4	278	0.98
F	0.47	2.00	7.05	6.16	8.50	8.98	0.47	4.15	10.30	0.13
Cl	---	<0.10	<0.20	<2.0	<0.20	1.1	1.00	<0.20	<0.20	<0.20
Br	---	<0.050	<0.010	<0.05	0.059	<0.050	0.010	---	---	---
NO3	---	<0.01	0.18	<0.10	1.74	4.05	1.93	0.04	<0.02	0.19
HPO4	---	<0.05	<0.10	<0.1	<0.10	0.18	<0.010	<0.02	<0.02	<0.05
B	<0.02	---	0.145	0.020	<0.015	<0.020	<0.015	<0.02	<0.02	<0.02
SiO2	34.5	32	36	37.3	32	54	21.4	44.6	38.6	8.0
S^{2-}	---	---	---	<0.001	<0.001	0.132	<0.001	---	---	---

chloride. Potassium, the major ion, is present at an order-of-magnitude greater concentration than any other cation, for example Na and Mg, which are more comparable in concentration to Sr and Ba. Rarely does any other cation achieve a concentration greater than 1 mg/L, whereas potassium is consistently about 10 mg/L.

The highest concentrations of iron, uranium, fluoride and sulphate are found in the surface and near-surface waters, which also exhibit the lowest pH. Oxidation of pyrite has produced these highly concentrated acid mine waters. Fluorite, together with pyrite, is also a common fracture mineral at the mine, and leaching due to contact with the acid mine waters has caused significant increases in the fluoride and calcium concentrations. The F3 and shaft waters contain the highest concentrations of iron, sulphate and fluoride, reflecting a significant contribution of acid mine waters even at these increased depths.

With increasing depth, the concentrations of iron, uranium, fluoride and sulphate all generally decrease and the pH and alkalinity increase. These concentration changes with depth suggest very active circulation of oxidising groundwaters in the top 10 metres and then perhaps moderately oxidising conditions combined with active groundwater circulation down to about 50 metres depth. This essentially conforms with the hydrogeological pattern.

The near-surface waters are relatively young, oxidising, and characterised by tritium values ranging from 1.1 to 3.3 TU, representing a 'tritium model age' of 30–40 years. This age range is only relative, however, as these waters are a result of mixing between recent recharge (around 4.5 TU) and older upwelling discharge groundwaters (>0.5 TU), and are also influenced by seasonal fluctuations in precipitation. This is supported by the hydrogeological model and also by the groundwater chemistry of the acid mine waters, both of which indicated groundwater mixing to around 50 m.

At greater depths (>50 m), the waters have no detectable dissolved oxygen and nearly all the dissolved iron is in the reduced Fe(II) state, indicating mildly reducing conditions. Some older groundwaters show signs of sulphate reduction, but only trace concentrations of sulphide are observed, which indicates that the rate of sulphate reduction is slow and any sulphide produced may be quickly removed by secondary sulphide (pyrite) precipitation.

The groundwaters that are the most indicative of the deeper aquifer (<150 m) are those collected from the F5 borehole. These waters have higher calcium, iron, aluminum, manganese, zinc and fluoride concentrations than those from shallower levels; the pH values and the alkalinities are also higher.

Geochemical processes involving water-rock-gas interactions in the Osamu Utsumi mine groundwaters have been modelled using groundwater compositions, mineralogical

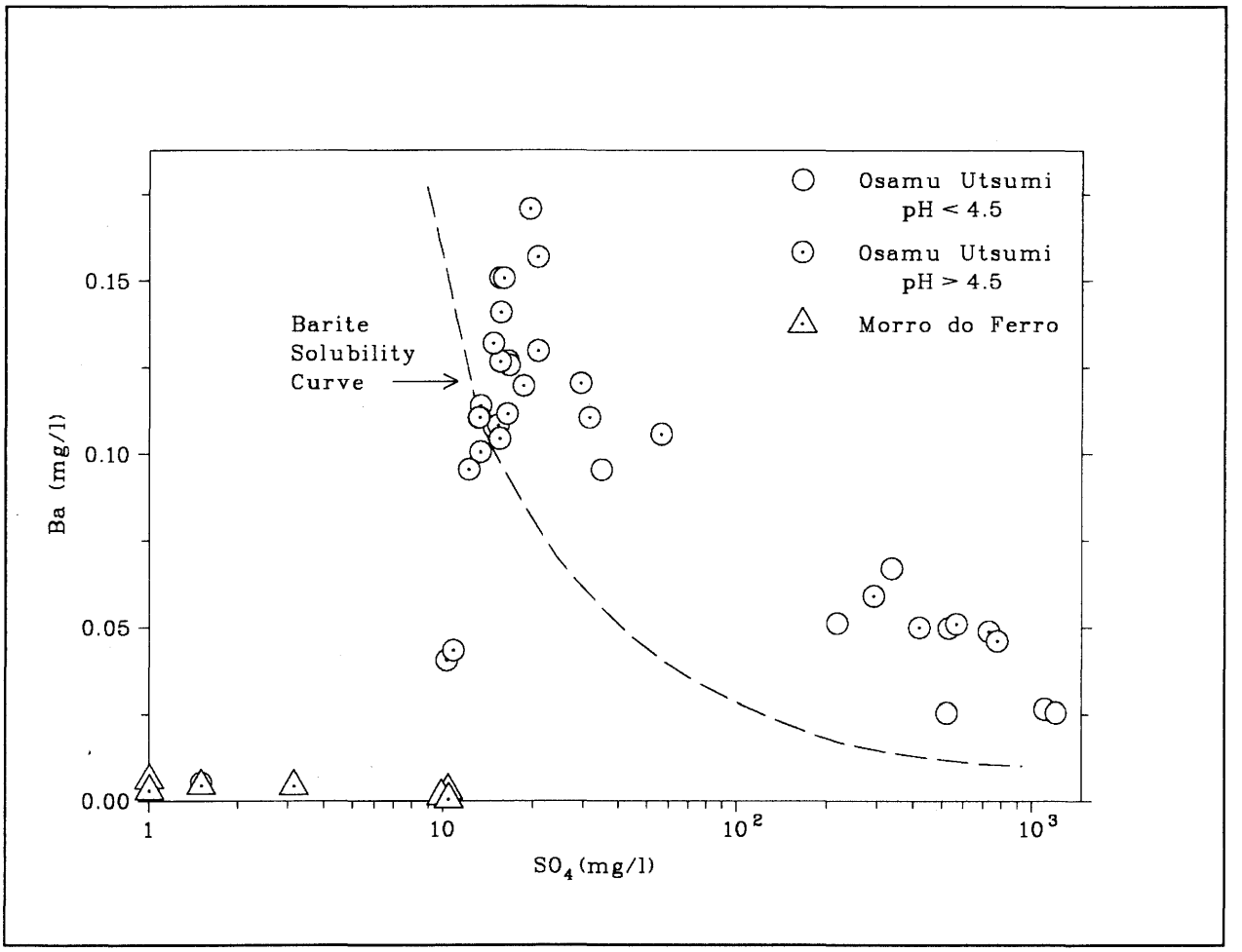

Figure 3.17. Common-ion effect of increased sulphate concentrations from pyrite oxidation on the solubility of barite. Symbols represent field data and the dashed line shows experimental measurements of barite solubility in the presence of sodium sulphate solutions.

data, ion plots and computations of speciation, non-thermodynamic mass balance and thermodynamic mass transfer. Modelling of some water-rock reactions indicated a very clear equilibrium solubility control, especially for barite, where field data for discharging or deeper groundwaters showed supersaturation when compared with the experimental data (Fig. 3.17).

Fluoride (resulting from the dissolution of fluorite, a common gangue mineral which is the only known source of fluoride ions) is usually about 2-3 times the molal concentration of calcium in these groundwaters, which indicates that most of the fluoride and calcium is coming from fluorite dissolution. This is demonstrated convincingly by plotting calcium against fluoride; the data points plot very close to the line representing fluorite dissolution. Furthermore, plots of fluorite saturation indices show that, whilst several water samples reach saturation equilibrium, most are unsaturated and indicate a tendency to dissolve fluorite.

Strontium isotope data show that the $^{87}Sr/^{86}Sr$ ratios of the groundwaters fall into two groups, with the deeper or more strongly leaching waters (acid mine waters) averaging about 0.7060 and the younger, more dilute waters averaging about 0.7075. These values do not match those of the calcites and fluorites, indicating that these are not the major sources of strontium. The sources are probably a mixture of several phases rich in strontium such as goyazite, K-feldspar, smectites, nepheline and some calcite and fluorite.

3.4. Natural decay series and REE character of the groundwaters

Studies of the uranium, thorium, natural decay series and REE character of the Osamu Utsumi groundwaters have been reported by Miekeley *et al.* (this report series; Rep. 8).

Total uranium and thorium

In groundwaters representative for the Osamu Utsumi mine, the total uranium concentrations range from 200–9000 μg/L in near-surface waters to 3-15 μg/L at depths from 45-125 m (Table 3.5). As the dominant water flow component is upwards, seasonal trends are not an important factor at depth, although small fluctuations (higher mean concentrations of U) have been noted for F1 and F2. On the other hand, the near-surface waters, characterised by a near subhorizontal flow gradient, show larger fluctuations. In

TABLE 3.5
Selected chemical data for subsurface and ground waters from the Osamu Utsumi uranium mine.

Borehole	Sample	Date (dd/mm/yy)	^{238}U (μg/L)	$^{234}U/^{238}U$ (activity ratio)	^{232}Th (μg/L)	$^{230}Th/^{234}U$ (activity ratio)	pH	E_h (mV)
	PC-GW-37	02/02/88	3200	1.22	360	0.18	3.10	806
SW01	PC-GW-46	07/06/88	4400	1.23	280	0.11	3.32	673
	PC-GW-57	21/09/88	270	1.23	4.1	0.026	3.92	666
SW02	PC-GW-38	03/02/88	10600	1.0	70	0.025	3.20	858
	PC-GW-39	03/02/88	7400	1.04	79	0.039	3.40	772
SW03	PC-GW-47	07/06/88	4500	1.02	36	0.016	3.57	751
	PC-GW-58	22/09/88	250	0.92	0.23	0.001	4.43	614
	UFWC11 C	24/05/88	4.9	2.3	0.030	0.004	5.44	379
F1	UFWC11-D	25/10/88	4.8	2.3	0.017	0.019	5.81	448
	PC-GW-63	29/11/88	5.1	2.4	0.120	0.11	5.37	261
	PC-GW-41	09/02/88	6.4	1.5	0.200	0.089	5.60	559
F2	PC-GW-31	21/12/87	6.2	1.7	0.036	0.003	5.80	198
	PC-GW-64	29/11/88	6.7	1.5	0.080	0.020	5.84	261
	PC-GW-36	01/02/88	25	1.2	0.06	0.004	5.45	420
F3	PC-GW-45	06/06/88	16	1.2	6.5		5.21	386
	PC-GW-65	30/11/88	4.5	1.3	0.34	0.20	5.10	370
F5	PC-GW-62	28/11/88	22	1.8	0.18	0.006	6.25	229
	PC-GW-72	20/12/88	11	1.8	0.13	0.004	6.30	155
PM22	PC-GW-19	15/07/87	0.19	2.3	0.087	0.5	–	–
	PC-GW-27	02/10/87	0.44	1.6	0.040	0.1	–	–
Sup.D	PC-SW-03	09/07/87	0.43	1.24	0.075	0.16	–	–

PM = Piezometric Station
Sup.D = Supply Dam

general the measured uranium concentrations are greater than might be expected when considering the solubility of U(IV) in natural waters of pH 4 to 7, i.e. generally below 0.05 μg/L. These higher concentrations suggest that uranium is transported predominantly in the oxidised hexavalent form (UO_2^{2+}). This interpretation is compatible with the Eh-pH conditions of the different boreholes which show that all the sampled groundwaters are marginally oxidising. The high concentrations in the near-surface waters are to be expected for acidic, highly oxidising waters in contact with weathered rock with a high residual U-content (which may be predominantly adsorbed or coprecipitated with ferric oxyhydroxides). Suspended ferric hydroxide particles in the Osamu Utsumi groundwaters are uranium-enriched by a factor of 10 000 to 100 000 when compared to the corresponding groundwaters. However, due to the low content of particulate matter (typically <0.5 mg/L), more than 90% of the uranium is in true solution (<1.5 nm). This dissolved component is in exchange equilibrium with the suspended ferric hydroxide particles (as indicated by the similar $^{234}U/^{238}U$ activity ratios of both phase; see Chapter 7 and Miekeley *et al.*, this report series; Rep. 9).

Oxidation of ferrous iron and the precipitation of ferrihydrites, accompanied or followed by sorption of uranium and other trace elements (and humic compounds), have to be considered as relevant processes which influence the migration behaviour of these elements (and their measured solution concentrations).

Concentrations of thorium in the prefiltered groundwaters (<450 nm) are typically between 0.01 and 0.1 μg/L. Complexation and/or association of thorium with suspended material, in particular the ferrihydride-organic species of colloidal size ranges 1.5 to 450 nm, are the generally accepted reasons for the observed higher concentrations (see Chapter 7 and Miekeley *et al.*, this report series; Rep. 9). In fact, suspended particulate material, mostly consisting of clay minerals in the near-surface waters and amorphous hydrous ferric oxides at depth, greatly influence or even dominate the hydrochemistry of thorium in these mine waters. A small fraction of 'dissolved' thorium (<1.5 nm range) is probably associated with low molecular weight fulvic acids. The observed thorium concentrations at Osamu Utsumi are in close agreement with those predicted by the geochemical models (Bruno *et al.*, this report series; Rep. 11).

Isotopic characteristics

The $^{234}U/^{238}U$ activity ratios (Table 3.5) in the superficial and near-surface waters (SW01 to SW03 and the supply dam) are low and typically range between 1.0 and 1.2.

These are believed to be the product of bulk dissolution of uranium (due to the severe leaching conditions) rather than preferential ^{234}U leaching. Towards greater depths (from F2 to F1) there is a progressive increase in the activity ratios (average of 1.54 for F2 and 2.26 for F1), which reflects an increasingly reducing groundwater environment. In addition, the high fluoride concentrations in the F2 waters (1.93 mg/L in F2 compared to 0.08 mg/L in F1) should be more conducive to pitchblende dissolution (see Chapter 5). This effect may explain the higher uranium concentrations and lower activity ratios characteristic of F2 compared to F1 groundwaters. This inverse relationship between uranium concentrations in water and isotopic ratios conforms to established models (Osmond *et al.*, 1983) and illustrates the two active processes, namely preferential leaching and recoil gain of ^{234}U versus bulk leaching of uranium.

In general, the low uranium concentrations and low to moderate $^{234}U/^{238}U$ activity ratios in the F1 and F2 groundwaters may be explained by: 1) the waters being in contact with weakly mineralised rocks, 2) high flow rates which prevent uranium mineral/water equilibration, and 3) scavenging of uranium by iron hydroxides. In contrast, borehole F3 shows a large variation of total and isotopic concentrations which are apparently related to fluctuations in redox conditions.

Based on hydrogeological considerations, the following model is presented for the distribution of uranium and its decay daughters in the Osamu Utsumi mine groundwaters:

* the deepest groundwaters (F1 and F5) are relatively reducing and may have achieved a steady-state of excess ^{234}U (balance between recoil, mobilisation, adsorption and decay),
* upward movement brings the groundwaters into a more oxidising environment where aggressive leaching occurs. This increases the total dissolved uranium but does not result in an increase in excess ^{234}U, i.e. the $^{234}U/^{238}U$ ratio falls,
* finally in the surface and near-surface waters (i.e. the supply dam, which can be considered as a composite sample derived from the mine drainage, and boreholes SW01 to SW03) the activity ratios are at, or very close to, secular equilibrium.

All the analysed groundwaters are in marked radioactive disequilibrium with respect to ^{234}U and ^{230}Th; the $^{230}Th/^{234}U$ activity ratios are typically between 0.01 and 0.1, reflecting the higher solubility of uranium and the greater tendency of thorium isotopes to sorb onto solid phases.

3.5. Rare-earth elements (REEs)

Rare-earth element concentrations in the groundwaters are, in common with uranium, very high (total REEs up to 29 000 μg/L) and represent the highest concentrations recorded in the published literature. The REEs are probably complexed by both sulphate and fluoride in solution, which also affects the REE distribution between the water and the suspended particles as previously mentioned for uranium and thorium (see Chapter 7).

The reason for the large disparity in REE concentrations between the near-surface and deeper groundwaters (for La compare 13 500 μg/L to 0.45 μg/L) is unclear. One explanation is that the lower complexation capacity of the deeper F1 and F2 groundwaters makes REE leaching from the bedrock less efficient, sorption/hydrolysis of the REEs stronger and, therefore, the REE concentrations in these deep groundwaters lower.

Work by Miekeley *et al.* (this report series; Rep. 8) has shown that a considerable fraction of the REEs is associated with colloidal particles in the 1.5 to 10 nm size range. This indicates that hydrolytic polymeric species of REEs could be important and/or that complexation/sorption of these elements by humic compounds and/or other colloidal phases (e.g. ferrihydrites) may partly determine the aqueous chemistry of these elements. In Morro do Ferro groundwaters (see Chapter 4), about 90% of the REEs were associated with humic compounds, mainly as humic acids.

In summary, REE concentrations in the Osamu Utsumi groundwaters are typically in the range of 0.1–15.0 μg/L for the LREEs (La, Ce, Nd) and 0.001–0.15 μg/L for the HREEs (Ho-Lu), but are much higher in the near-surface waters with high complexation capacities, as observed for thorium. The chondrite-normalised distribution patterns of the REEs in water samples (and in suspended particles) are similar to those observed in the bedrock, indicating congruent dissolution and sorption of these elements. A notable exception is cerium, which shows a very characteristic depletion in oxidising, shallow waters, probably related to its preferential oxidation and the much lower solubility of Ce(IV) species in natural waters.

3.6. Summary

Studies at the Osamu Utsumi mine, and to a much lesser extent within the caldera as a whole, have clarified the complex geological interrelationships between:

a) the primary magmatic/deuteric episode resulting in the emplacement of rocks with uranium, thorium, zirconium, molybdenum and REE concentrations typical of alkaline rocks,

b) the post-magmatic regional deuteric alteration of the caldera complex giving rise to argillation and zeolitisation of the rocks and, possibly, some mobilisation of uranium, thorium and REEs,

c) the localised hydrothermal events which have introduced, remobilised and concentrated uranium, thorium and the REEs (together, for example, with molybdenum and zirconium) mainly as stockwork mineralisations in and around the breccias, some of economic potential,

d) the development of deep weathering profiles and the formation of supergene uranium remobilisation deposits at and adjacent to migrating redox front systems with further argillation of the rocks and small-scale selective remobilisation of REEs and other trace elements in association with the redox fronts.

The uranium within the reduced bedrock is most commonly present as fine-grained aggregates of pitchblende disseminated throughout the rock matrix. Along the redox fronts, pitchblende forms larger, kidney-shaped accumulations (cm-size). Within the oxidised zone pitchblende is absent; autoradiography and leaching studies show that uranium mobilised by the generation of the redox fronts has become associated with Fe-oxyhydroxides intragranular to the K-feldspar, and pseudomorphed nepheline grains.

The variation of the $^{234}U/^{238}U$, $^{230}Th/^{234}U$ and $^{226}Ra/^{230}Th$ activity ratios in the rock demonstrates that dissolution, transport and precipitation processes have affected the uranium (within the last $3x10^5$ a) and radium (within the last 10^3 a), both in the vicinity of the redox fronts and in other parts of the bedrock. Detailed studies of the redox fronts confirmed that U and Ra are more mobile than Th and Pa in the groundwaters. Of the three fronts studied in detail, one was concluded to have been static (on a cm scale) for a period of at least $7x10^5$ a, whilst the natural decay series data for the other two fronts were consistent with rates of movement in the range of 2–20 m in 10^6 a, in good agreement with the estimated rates of regional erosion.

Stable and rare-earth element data show that the zones around the redox fronts are enhanced in most elements in conjunction with active dissolution at the fronts; the fronts thus represent a zone of retardation to the transport of many elements.

The site has been further influenced by the extensive excavations which have extended the groundwater discharge area, such that bedrock which originally received downward-percolating oxidising waters now receives upward-discharging waters of a more reducing character.

In general, the groundwaters are of unusual dilute composition and indicate intensive weathering from actively circulating fresh groundwaters in contact with the highly leached potassic-rich rock mass. As a result, the waters are essentially of K-Fe-SO_4 character. Oxidation of pyrite (dispersed throughout the reduced bedrock), due to the mixing of reducing discharge waters and near-surface oxidising waters within the upper 50 m of mine bedrock, has produced acid mine water at and near the surface. At greater depths the groundwaters are more reducing in character and some redox trends are indicated. Tritium and stable isotopic data support the present groundwater flow model.

Uranium concentrations in the groundwaters are generally high (up to 10 mg/L in the near-surface and 3-10 μg/L at depth) and thorium concentrations very low (<0.1 μg/L). Pronounced disequilibria were measured between ^{234}U and ^{238}U isotopic activities, caused by an excess of ^{234}U due to preferential leaching and/or recoil effects. An inverse relationship of uranium concentration and the $^{234}U/^{238}U$ activity ratio with depth is consistent with established redox and groundwater flow models. Due to the extremely low solubility of thorium and its strong tendency to sorb onto suspended particles (mainly hydrous ferrous oxides) the $^{230}Th/^{234}U$ activity ratios are very low (0.01).

The REE concentrations in the groundwaters are typically in the range of 0.1–15.0 μg/L for the LREEs (La, Ce, Nd) and 0.001–0.15 μg/L for the HREEs (Ho-Lu), but are much higher in the near-surface waters, as also observed for thorium. The chondrite-normalised distribution patterns of the REEs in water samples (and in suspended particles) are similar to those observed in the bedrock, indicating congruent dissolution and sorption of these elements. A notable exception is cerium which shows a very characteristic depletion in oxidising, shallow waters, probably related to its preferential oxidation properties.

CHAPTER 4. MORRO DO FERRO

4.1. Geology

The thorium/rare-earth deposit at Morro do Ferro is located five kilometres to the north of the Osamu Utsumi mine. The roundish hill has a diameter of about one kilometre and, with an altitude of 1541 m, represents one of the highest points within the Poços de Caldas plateau, rising some 140 m above the base. It is drained by two streams, one draining the north side and the other rising in the south and curving around the south-eastern periphery.

Aerial radiometric surveys carried out in the early 1950s recorded several radioactive anomalies within the Poços de Caldas caldera, one of which was Morro do Ferro. This was subsequently followed up in the 1950s and 60s by Tolbert (1955), Frayha (1962) and Wedow (1967), who employed ground surveys, drilling, trenching and gallery construction, geochemical analysis and limited mineralogical studies to evaluate the extent and economic potential of the ore body. The idea that some undiscovered uranium concentrations might exist somewhere deeper in Morro do Ferro persisted for more than a decade. By the mid-1960s it was verified that: 1) Morro do Ferro did not conceal any uranium mineralisation of interest, 2) no prospect existed for the use of thorium in the immediate future, and 3) the REE ores were very refractory to conventional extraction methods, making recovery costly.

Morro do Ferro is situated in a very similar geological environment to the Osamu Utsumi mine. The region is dominated by potassic rocks together with phonolites and nepheline syenites. All rocks are deeply weathered, the depth and intensity of alteration found at Morro do Ferro being much greater than in the surrounding area. The hill is completely altered down to a depth of at least 100 m; the deepest borehole (Fig. 4.2; borehole XIX) drilled from the top of Morro do Ferro (by Nuclebrás, now Urânio do Brasil, in a previous exploratory programme) encountered silt/clay material to 132 m; down to 426 m the core exhibits a strongly altered and brecciated potassic rock.

The current work at Morro do Ferro has entailed the drilling of four boreholes (MF10, MF11, MF12 and MF13) ranging in depth from 40–75 m. The location of these holes in relation to the mineralisation and the water table is illustrated in Figure 4.1. The holes were sited to form a profile within a magnetite breccia, contained on either side by massive magnetite dykes, which extends downwards from the Th/REE mineralisation located just below the hill summit. In comparison with the rest of the mountain, which

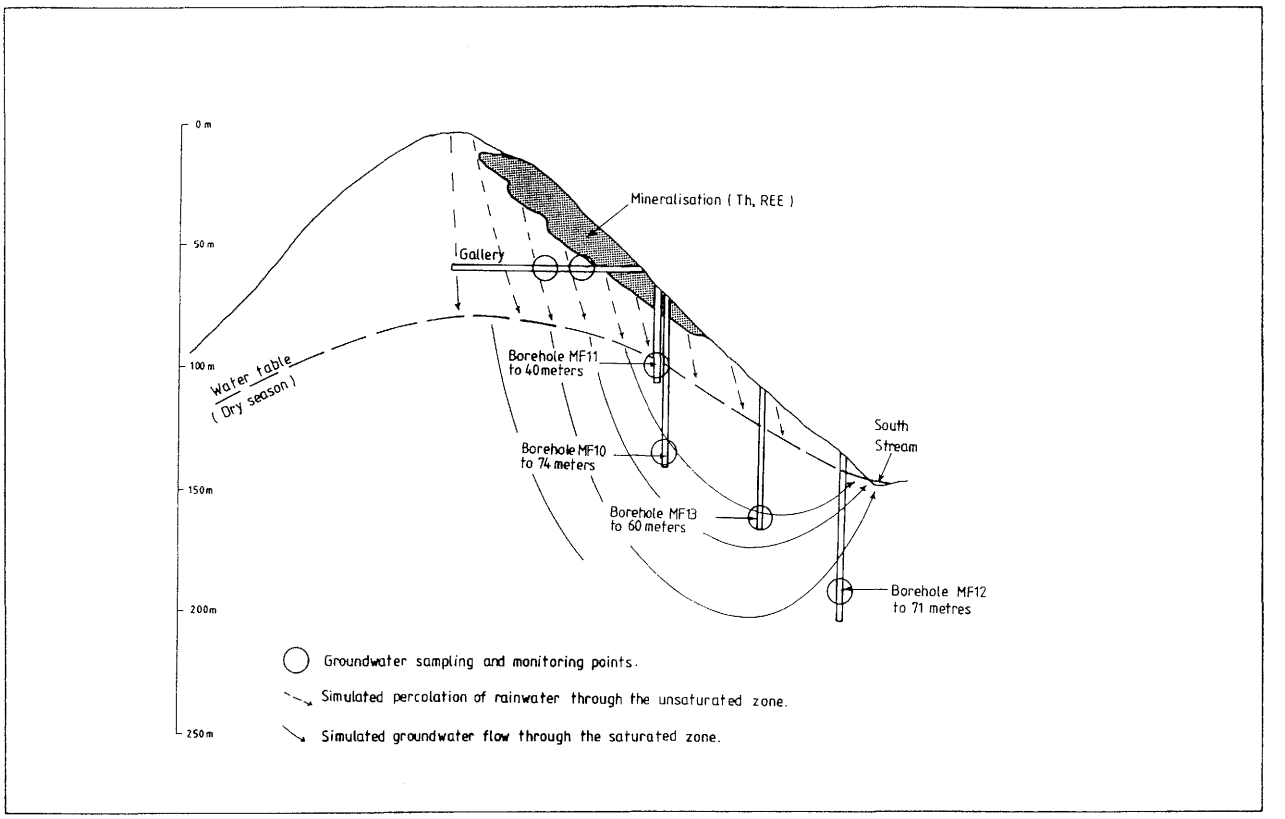

Figure 4.1. Location of boreholes MF10–13 at Morro do Ferro in relation to the mineralisation and the dry season water table.

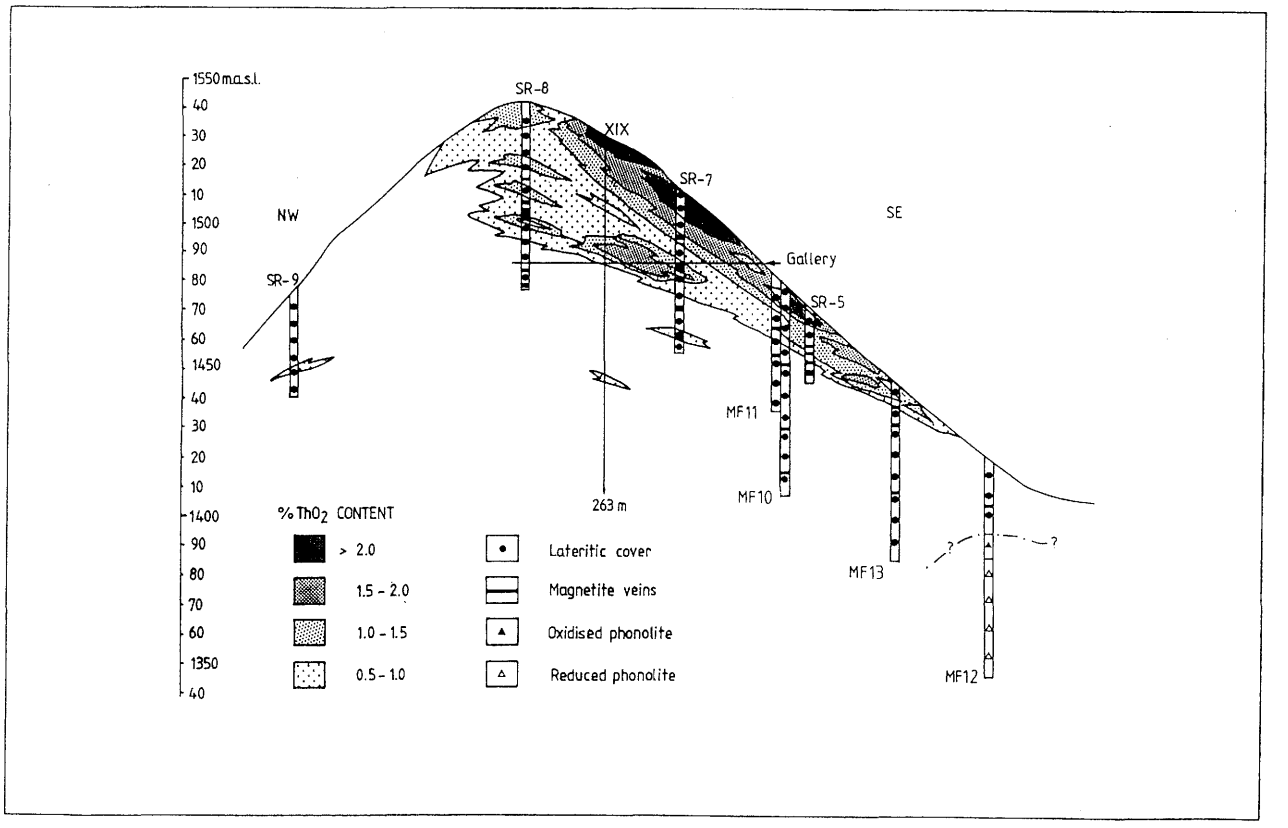

Figure 4.2. Profile across Morro do Ferro showing the distribution of thorium. Borehole XIX and those prefixed by SR were drilled during exploratory studies extending back to the 1950s. Construction of the gallery dates from the same period.

is weathered to a rich laterite/clay, this breccia is believed to represent the most hydraulically conductive zone, and the boreholes should therefore lie along the same groundwater flow path. This has obvious advantages for the studies of hydrochemical evolution and particle colloid transport.

Owing to the heavily weathered nature of the bedrock and the resulting rock friability during drilling, standard drilling techniques would only have served to wash out portions of the borehole. This difficulty was overcome by using a simple dry-pushing method using a short barrel (75 mm in diameter). This method was employed for MF10, to 60 m for MF11, and to 40 m for MF13, thereafter water-flush rotary coring was used to complete MF11, MF13 and most of MF12. For MF12, the upper 38.6 m were drilled using mud-flushing to ensure greater bedrock stability through the weathered horizon. MF10–MF12 have been logged and cased using PVC tubing, but only MF12 penetrated rock which was stable enough to allow adequate hydraulic testing. Both MF12 and MF10 were completed using mechanical packer systems which were installed at the bottom opening of a large-diameter steel casing. As the objective of MF11 was to provide access to the top of the saturated zone, completion using packers was not necessary. For MF13 the rock was too friable to install a packer and groundwater enters through the bottom 10 m of the perforated PVC casing.

In boreholes MF10, MF11 and MF13, all situated on the south-eastern slope of the hill, only totally altered lateritic material was recovered, interrupted by several small-sized magnetite veins. In borehole MF12, which was drilled at the bottom of the slope near the south stream, a lateritic alteration zone was encountered down to a depth of 27.5 m. There, the borehole encountered an oxidised, hydrothermally altered phonolitic rock. A redox front within the phonolitic rock was encountered at 35.7 m.

In addition to drillcore mapping and sampling, routine groundwater sampling was carried out at all four reference borehole locations. Supplementary sampling was also carried out periodically from the unsaturated zone (i.e. the old exploration adit; Fig. 4.1), the shallow piezometric well near MF12, and from the streams flanking the north and south sides of the mountain.

4.1.1. Mineralogy and petrology

Examination of the deeper core material from MF10, MF11 and MF13 suggests that the primary rock has been carbonatitic in type, composed of magnetite, jacobsite, apatite and carbonate. The upper laterite horizon is typically composed of silt/clay material

varying in colour from red-brown through brown to yellow-white. Down to about 30 m the laterite alteration zone is dominated by gibbsite, kaolinite and illite, with additional iron- and manganese oxyhydroxides, which occur either finely dispersed or concentrated in duricrust layers. At greater depth, the gibbsite content decreases drastically and kaolinite and illite form the major components. Iron and manganese oxyhydroxides tend to be concentrated in distinct layers. The magnetite veins consist of loosely arranged to massive nodular aggregates of magnetite and cryptomelane ranging in diameter from several millimetres up to decimetres. They are corroded and oxidised at the surface. Major magnetite veins that outcrop at the surface may reach a thickness of several metres.

In borehole MF12, the lateritic alteration zone consists mainly of gibbsite and kaolinite in the uppermost 10 m, changing with depth to kaolinite and illite. Intercalated thin layers rich in iron oxyhydroxides occur throughout the alteration zone. The phonolite is of subvolcanic origin and very similar in bulk chemistry to that encountered in the Osamu Utsumi mine. This phonolite was subsequently intruded by a tephri-phonolite less rich in K-feldspar but with abundant plagioclase. Both rocks underwent a strong hydrothermal alteration and potassium metasomatism, and display a disseminated pyrite impregnation. Fluorite and calcite often occur as fracture fillings. Whereas in the subvolcanic rock the hydrothermal alteration led mainly to the formation of illite and kaolinite, in the tephri-phonolite smectite and chlorite are important alteration products besides illite and kaolinite.

4.1.2. Distribution of uranium, thorium and the light rare-earths (LREEs)

The thorium-REE ore body of Morro do Ferro is about 150 m across at its widest point and 320 m in length, and is located directly below the surface, extending from the summit down the south slope of the hill. The highest thorium contents are reported from the drillcores in the uppermost 30 m, but mineralised zones may occur down to 100 m, although intercalated by barren zones (Fig. 4.2). Within the ore body, the ThO_2-content ranges from 0.1 to 2.9 wt.% and the total REE-content varies between 1.5 and 21 wt.%. Estimates of the ore reserves give about 30 000 tonnes of thorium with a cut-off grade of 1% ThO_2 and 50 000 tonnes of total REE with a cut-off grade of 4% REE (Frayha, 1962).

Scintillometric logging of the thorium/REE mineralisation (Waber, this report series; Rep. 3) observed in MF10 shows that the top 11 m are highly radioactive; a less active

zone lies between 15 m and 19 m and background activity levels characterise the remainder of the hole from 22 m to 74 m. The active horizon shows a close correlation with the red-brown clay layers rather than with the white variety. In these white clay layers the magnetite is always oxidised to limonite and hematite, while it seems to be less affected in the red-brown layers. No correlation can be seen between zones of high radioactivity and unaltered magnetite-dominated zones.

Samples taken from MF10 have been analysed for uranium, thorium and the LREEs in whole-rock samples, and for uranium and thorium in different grain-size fractions. Although uranium and thorium are depleted in the $<2\mu$ and 6.3–20μ fractions with respect to the whole-rock contents (which include those Th- and REE-bearing phases in the magnetite), both fractions still contain considerable amounts of uranium. Mineralogically there is an interesting difference between the $<2\mu$ and 6.3–20μ fractions. The main constituents of both comprise kaolinite, illite/sericite, gibbsite (boehmite), goethite, hematite and florencite. Additionally, Th-bearing minerals such as thorite, thorianite, cerianite, cheralite and thorbastnaesite are present in the 6.3–20μ fraction. Uranium is also probably associated with the same phases. In the $<2\mu$ fraction, in contrast, thorium and uranium appear to be associated with iron oxyhydroxides and the clay minerals, which are commonly coated with iron hydroxide.

The uranium, thorium and selected light rare-earth (LREE) whole-rock data for borehole MF10 (MacKenzie *et al.*, this report series; Rep. 7) are illustrated in Figure 4.3. Thorium concentrations decrease by a factor of 250 from the surface metre (57 072 μg/g) to 72.7 m below ground level (223 μg/g). The upper 20 m of MF10 show a rather erratic, although generally decreasing, thorium distribution, which is believed to correlate with the ratios of illite – sericite/kaolinite. In contrast, uranium (ranging from 19.8–76.3 μg/g, with an average of 34.5 $\pm$ 15.8 μg/g) shows no correlation with thorium.

The LREE data, in common with thorium, indicate highly variable concentrations from the surface to depth, with a sharp increase in the upper 5 metres. Excluding Ce, the remaining LREEs are highly correlated with one another (e.g. La and Sm; Fig. 4.3). Thorium is more closely correlated with Ce than the other LREEs, and both appear to be retained in relatively higher concentrations within several metres of the surface than U or the other LREEs (Fig. 4.3).

A comparison of normalised LREE concentrations between the saturated and unsaturated zones is presented in Figure 4.4. The most striking difference is the predominance of positive Ce anomalies in the unsaturated, upper 25 metres of the core, compared to negative Ce anomalies in the saturated zone. There is a possibility that these patterns represent a relict from the earlier migration of a redox front. For example, the

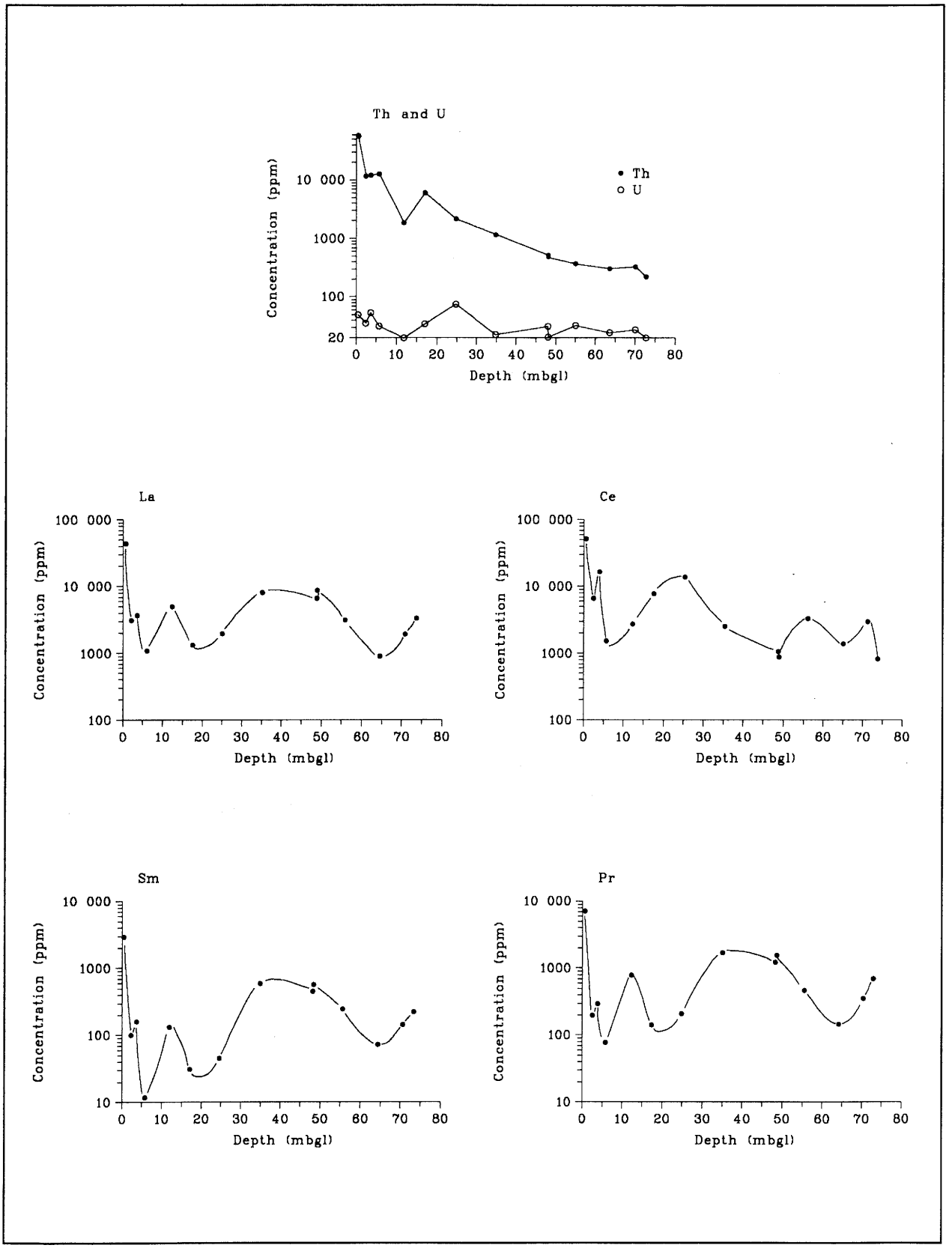

Figure 4.3. Distribution of La, Ce, Sm, Pr, U and Th along drillcore MF10.

oxidation of Ce(III) to less soluble Ce(IV) in samples taken near the current surface would tend to retard the vertical migration of this element, relative to the trivalent LREEs, resulting in an apparent Ce enrichment. The leached trivalent LREEs may subsequently become immobilised at depth, resulting in a negative Ce anomaly in the deeper core samples.

The MF12 core, in contrast, is not mineralised and the host rock is different, although uranium, thorium and the LREEs are still relatively enriched. Compositional ranges in μg/g are: U (25.3–87.1); Th (41.9–129.1); Ce (1040–1878); La (654–7353); Nd (258–4551); Pr (76–1414) and Sm (35–595). With the exception of one anomalous uranium value, the highest values correspond to the laterite horizon.

From the surface to the sharp contact between the laterite and the comparatively competent oxidised phonolite at 27.5 m, there is an order-of-magnitude decrease in the LREEs other than cerium; thorium, uranium and cerium decrease only marginally. Below the laterite cover the LREEs continue to show a decreasing trend with depth, whilst thorium, uranium and cerium show no distinct trends.

The normalised LREE profiles (Fig. 4.5) show a strong negative Ce anomaly within the laterite cover, which corresponds laterally with the laterite in the MF10 core. Otherwise, at greater depths, there is an irregular distribution of negative and positive anomalies.

4.1.3. Natural decay series

Isotopic activity concentrations and isotopic ratio data for borehole MF10 indicate that for the thorium series, at least through ^{228}Th, secular radioactive equilibrium is maintained (MacKenzie *et al.*, this report series; Rep. 7). This indicates that ^{228}Ra (half-life = 5.75 a), the parent of ^{228}Th and the likely candidate within the Th-series to have the potential for in-situ migration because of its relatively high solubility, is either retained where it is radiogenically produced, or is migrating from the mineralised zone very slowly relative to its decay rate. These results are consistent with the very slow current mobilisation rate that has been reported for ^{228}Ra based on the annual stream transport of ^{228}Ra away from the ore body in solution ($\leq$0.45 μm) and the estimate for the ^{228}Ra burden within the ore body, i.e. the flux/inventory ratio (Campos *et al.*, 1986).

The uranium series isotopic ratio data are shown in Figure 4.6 using an interpretative plot of ^{230}Th/^{238}U against ^{234}U/^{238}U (after Thiel *et al.*, 1983). With the exclusion of four points (two which cannot be explained in terms of a single process, e.g. 10–25 and 10–56,

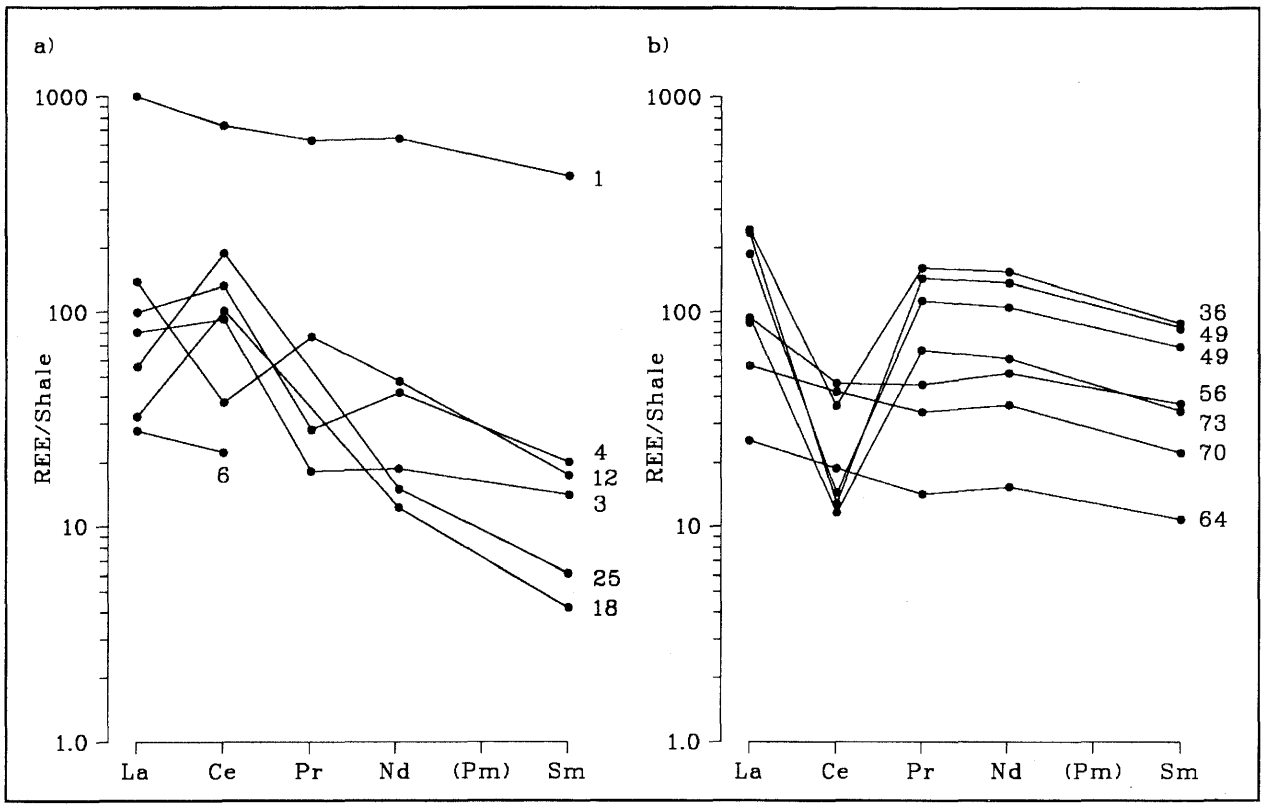

Figure 4.4. Normalised LREE profiles from drillcore MF10 for a) the unsaturated, mineralised zone and b) the saturated zone. (Numbers relate to sample depths in metres).

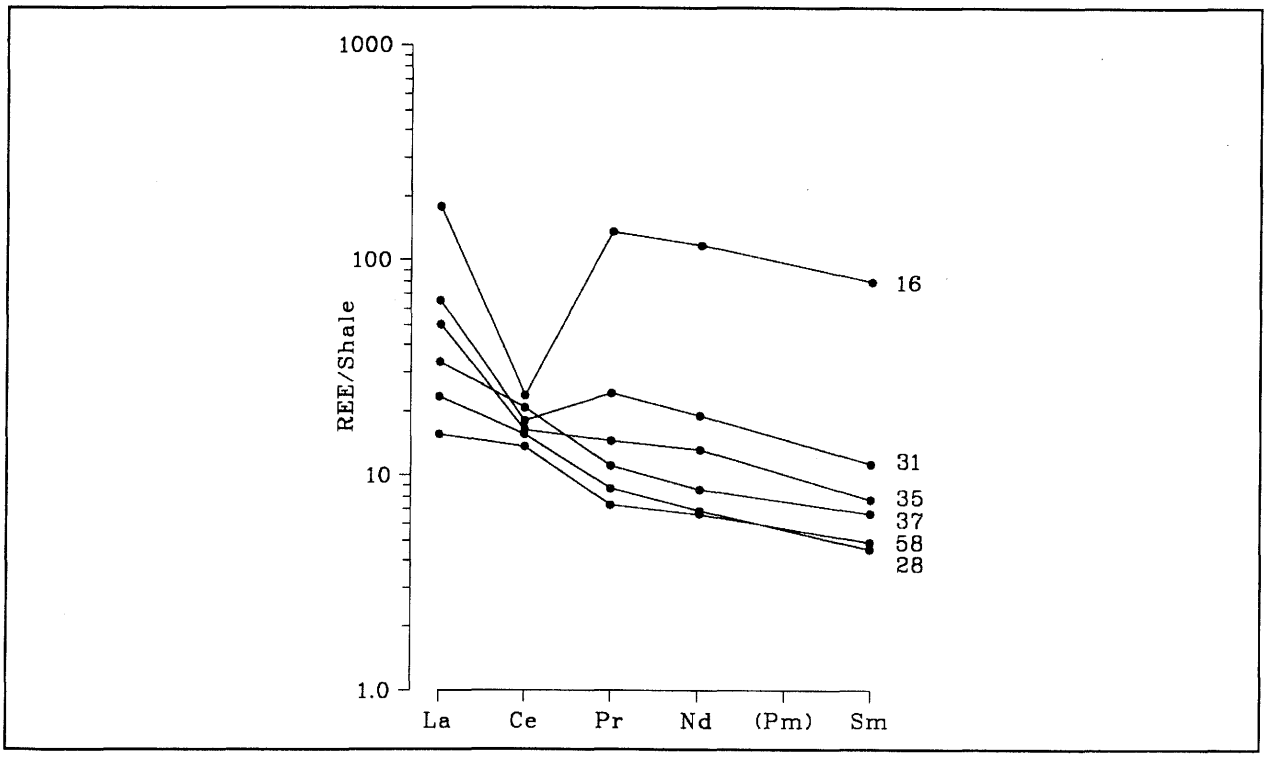

Figure 4.5. Normalised LREE profiles in the MF12 core. (Numbers relate to sample depths in metres).

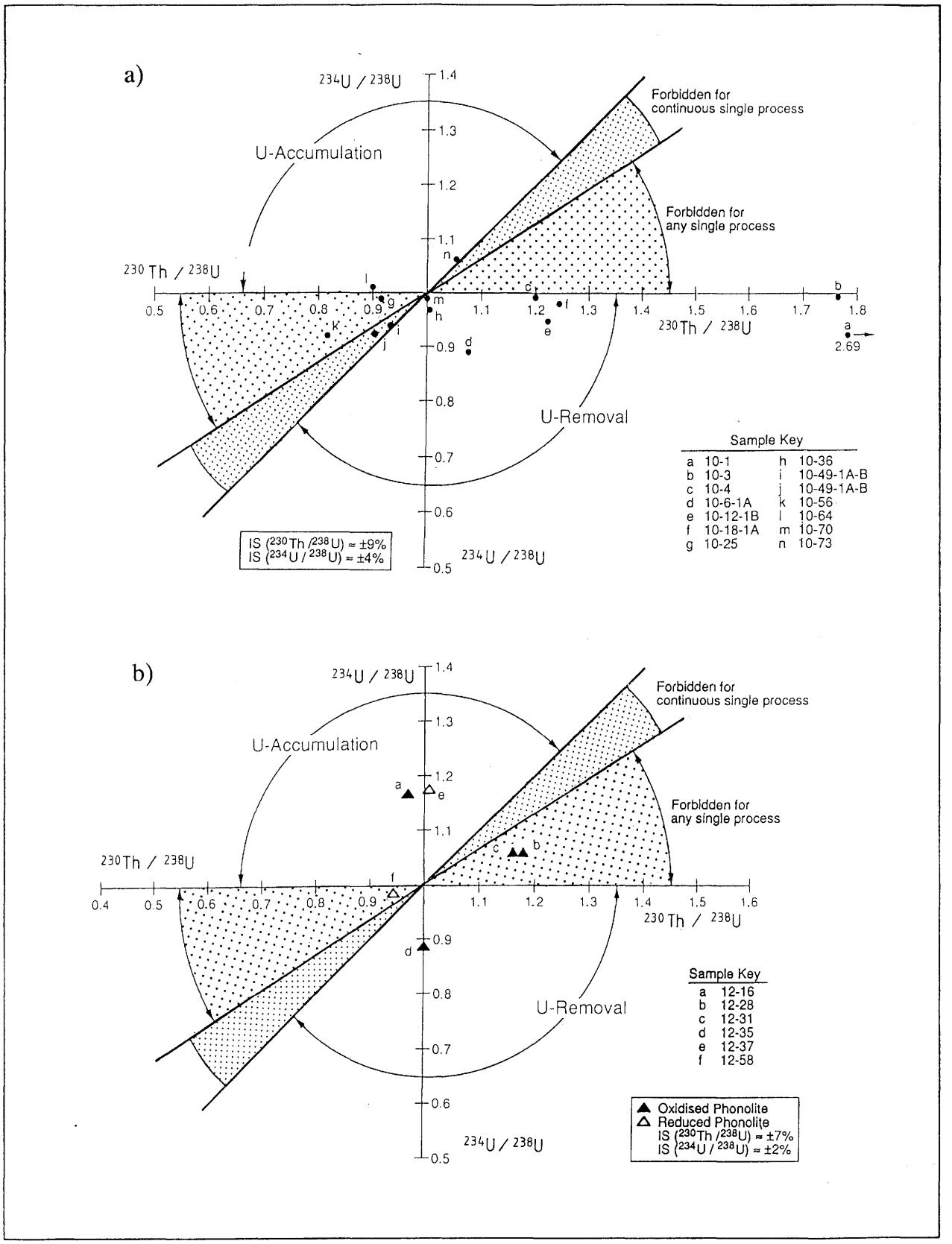

Figure 4.6. Thiel plots of uranium decay series analysis for: a) MF10, and b) MF12. (Sample depths are indicated in the key: plotted sample (a, b ...) borehole number (10, 12) and depth in metres).

and two of the deepest samples which lie in the zone of uranium accumulation, e.g. 10–64 and 10–73), the isotopic ratio data indicate uranium loss which can be interpreted as occurring from a single process.

As might be expected from infiltrating, oxidising rainwater which would oxidise uranium to the more soluble, hexavalent state, samples taken from near the surface, e.g. 10-3 and 10-4, have $^{234}U/^{238}U$ ratios of unity and $^{230}Th/^{234}U$ ratios of 1.8 and 1.21 respectively. This indicates that, for these samples, loss of both uranium isotopes by bulk leaching processes is masking, i.e. occurring at a greater rate than, any preferential removal of ^{234}U (although there is evidence that preferential removal of ^{234}U is also occurring both close to the surface and throughout the MF10 core up to about 64 m depth). Groundwater data from MF10 are indicative of present-day, preferential loss of ^{234}U, since $^{234}U/^{238}U$ ratios from five samples analysed range between 1.11 and 1.31 and average 1.29 ± 0.11 (±1SD).

Natural series radionuclide data from the downflow MF12 core indicate a more complex pattern than was observed in MF10. For example, samples 12-16 (laterite cover) and 12-37 (competent, reduced phonolite) lie clearly within the uranium accumulation zone which can be represented by a single process, while 12-28 (border between laterite and oxidised phonolite) and 12-31 (oxidised phonolite) lie within a zone of uranium accumulation which is forbidden for any single process (Fig. 4.6). The deepest sample analysed within this core, 12-58 (also a reduced phonolite), has isotopic ratios sufficiently close to 1.0 to imply attainment of secular equilibrium.

4.2. Hydrogeology

From previous work reported by IPT (1984), in which 9 piezometers were drilled to sample the upper part of the saturated zone, the water table appears to be a subdued reflection of the topography. The magnetite dykes, which run across the hill, appear to distort the water table to a limited extent. At the top of the hill the water table is at least 80 metres below the surface. In the valley bottoms the water table is at or near the surface, occurring as seepages or discrete springs.

Figure 4.7 shows diagrammatically the relationship of the water table to the topography. The difference in water levels between the wet and dry seasons appears to be at least 20 metres under the central part of the hill. This represents the water which is stored and slowly released as base flow to the stream. Rainwater enters the aquifer by percolating through the unsaturated zone until it meets the water table. Under the hill,

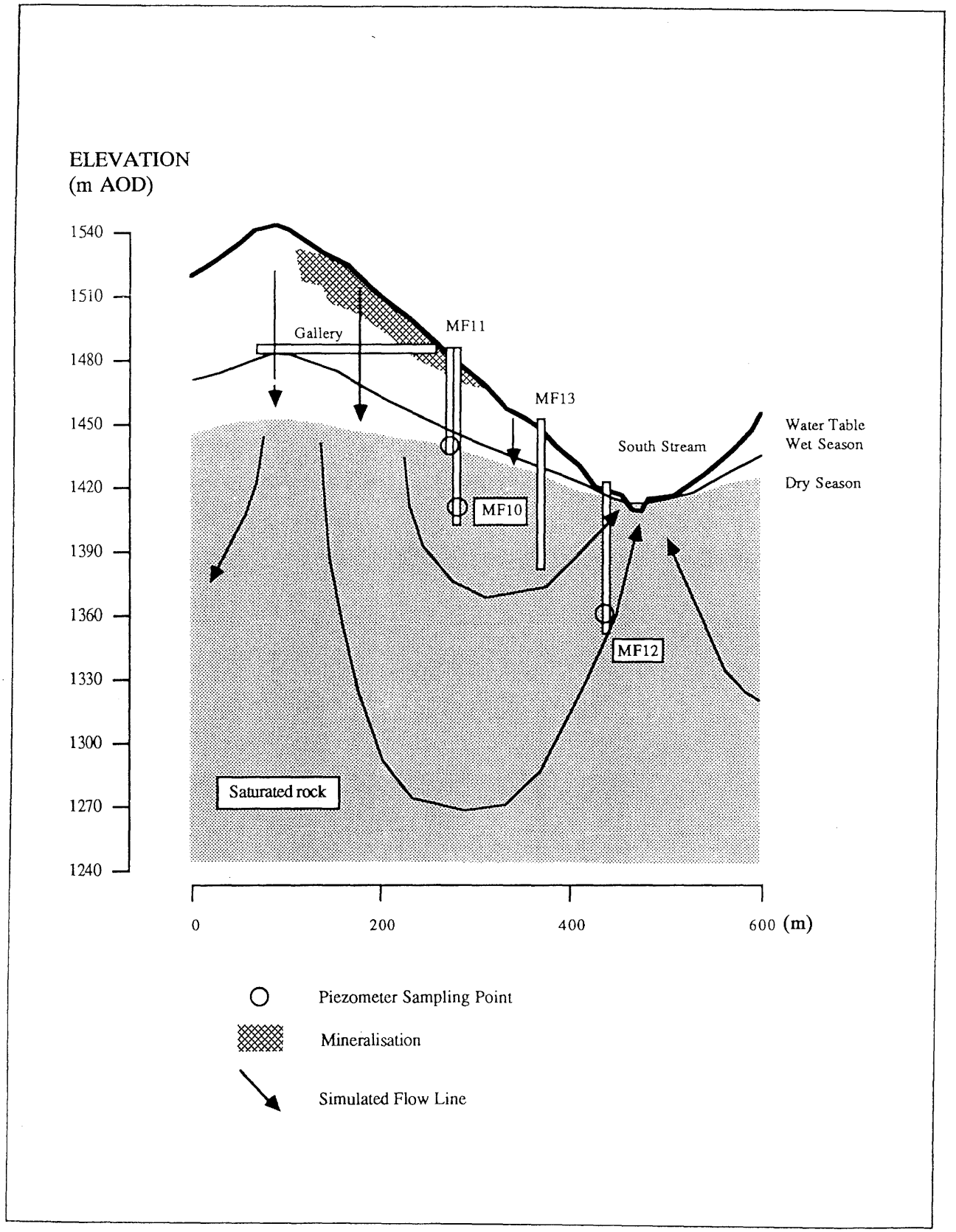

Figure 4.7. Seasonal relationship of the water table to the topography and main groundwater flow gradients at Morro do Ferro.

flow will continue downwards, maintained by a vertical component in the piezometric gradient. Near the stream the flow direction will change as water drains into the water course. This groundwater should have had the longest residence time in the rock mass and therefore have experienced the greatest chemical changes. The groundwater under the hill may have penetrated the rock mass to several 100 metres or more below the level of the stream.

During present studies, the bedrock instability in boreholes MF10, MF11 and MF13 meant that the double packer techniques used successfully for the hydraulic tests at the Osamu Utsumi mine could not be applied. However, two values for hydraulic conductivity were measured using slug tests during the construction of borehole MF10; one when the hole had penetrated the water table by about 6 m, and the second using a single packer to isolate the lower section of the borehole from 64 to 74 m. These resulted in values of 1.6×10^{-5} ms^{-1} and 1×10^{-6} ms^{-1} respectively. In the absence of head measurements, water level data collected during drilling indicated a significant downward vertical hydraulic gradient adjacent to the borehole (Holmes *et al.*, this report series; Rep. 5).

More success was achieved with MF12 due to the competent nature of the bedrock below approx. 28 m. Straddle packer tests indicated uniform permeabilities of 10^{-7} ms^{-1} down to 58 m; from 58 m to 64 m a marked decrease to 10^{-9} ms^{-1} was measured. No measurements were carried out at MF13.

Water levels have been monitored for a five month period, during which MF10 and MF11 showed a rise of some 2.5 m. The level in MF10 is consistently some 3 m below that in MF11, showing that a marked vertically downward gradient exists. The level in MF12 has risen by some 0.75 m over the same period, reflecting the closeness of the borehole to the discharge point in the stream bed.

A two-dimensional model of Morro do Ferro (Fig. 4.8) has been constructed, assuming homogeneous conductivity except for a region of enhanced permeability to a depth of 30 m close to the stream. This latter feature is suggested by the description of borehole MF12. The permeability of the bulk of the section has been taken to be 5×10^{-6} ms^{-1} with a porosity of 0.3. It may be noted that an earlier description of the area (IPT Report, 1984) assumed a porosity of 0.02, but it is unclear if this is a measured value or just a better informed guess.

Two separate steady-state calculations were performed; the first with the water table fixed at the dry season level, and the second with the water table fixed at a supposed wet season level. This latter value was obtained by raising the level of the water divide some

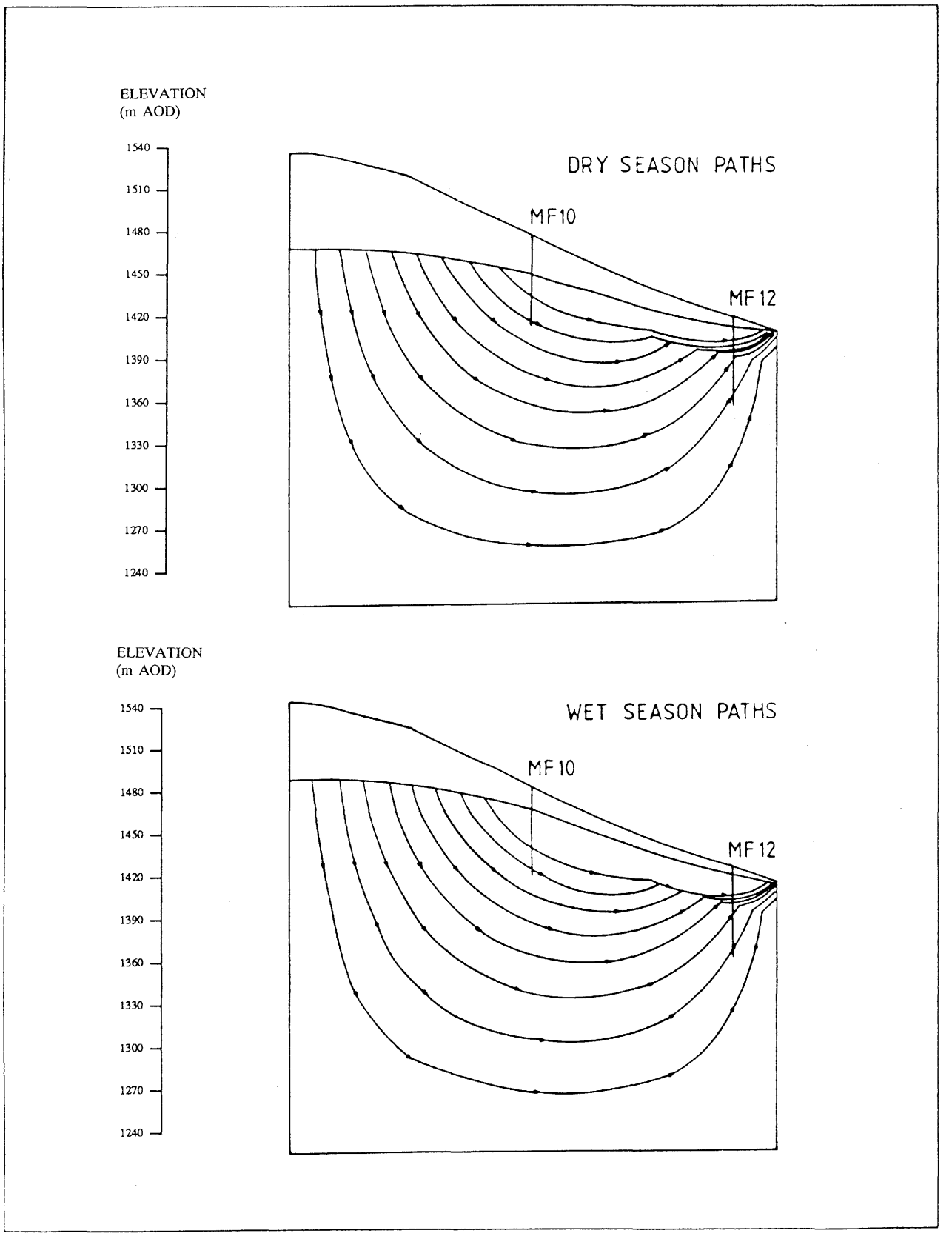

Figure 4.8. Hydrogeological modelling of Morro do Ferro during dry and wet seasons.

15 m to the bottom of the mine gallery, and raising the rest of the water table in proportion to its original height above the stream.

For each calculation, a series of pathlines was traced which allows an assessment to be made of the flow rates which can be expected in various parts of the section. In particular, flow rates in the vicinity of the bottom of borehole MF10 were found to be $1.6x10^{-7}m^3/m^2/s$ (dry season) and $1.3x10^{-7}m^3/m^2/s$ (wet season). The pore water velocities for mass transport calculations are obtained from these by dividing by the porosity. The effects on the pathlines of the high conductive zone near the stream can be clearly seen in the pathline plots, but it will also be seen that there is very little difference between the wet and dry season results (Fig. 4.8). This is also reflected in the flow rates given above.

4.3. Hydrochemistry

As at the Osamu Utsumi mine site, emphasis was placed on groundwater sampling from the reference location points (MF10, 11, 12 and 13; Fig. 4.1). Periodic sampling from the north and south streams flanking Morro do Ferro, and from piezometer hole PZ2 adjacent to MF12, was also carried out. (Nordstrom *et al.*, this report series; Rep. 6). The sampling and analytical protocols were similar to those for the Osamu Utsumi mine, and selected analytical results of groundwater samples from Morro do Ferro are presented in Table 4.1.

At this site the groundwater is much less perturbed than at the Osamu Utsumi mine. Iron and fluoride concentrations at about 70 m depth are comparable to those in the deep groundwaters at the mine, whereas uranium, bicarbonate and sulphate concentrations appear to be slightly lower and the pH slightly higher. These differences in water chemistry may reflect a less perturbed groundwater flow system, a lower abundance of oxidisable pyrite and/or more reducing conditions.

At Morro do Ferro both the MF10 and MF11 boreholes successfully tapped shallow recharging groundwaters with such a low dissolved solids content that most constituents were below analytical detection limits. These samples probably reflect the composition of rainwater, with small amounts of potassium, zinc, iron, manganese, fluoride and silica added from contact with the rock. This is supported by the tritium data for MF10 and MF11 (respectively averaging 2.2 TU and 8.9 TU) which, when compared with the local precipitation (4.5 TU), suggest only very short residence times. The groundwaters collected at MF12 show increased concentrations of nearly every constituent, as would

TABLE 4.1

Selected analytical results of groundwater samples from the Morro do Ferro study site.

Borehole	MF10	MF11	MF12	MF13	South Stream	North Stream
Sample code no.	PC-GW-52	PC-GW-82	PC-GW-56	PC-GW-73	PC-SW-04	PC-SW-05
Sampling int (m)	50-74	30-40	45-71	50-60	---	---
Date collected	880912	890404	880919	881220	870729	870810
Temperature (^{O}C)	21	22	24	23	---	---
pH (field)	6.13	5.31	6.13	5.45	6.3	4.9
D.O. (mg/L)	3.6	8.5	0.2	6.7	---	---
Eh(mV)	335	525	212	659	---	---
Alkalinity (mg/L HCO_3)	2.8	0.8	18.7	0.61	4	4
Sum cations (meq/L)	0.094	0.019	0.725	0.071	0.07	0.10
Sum anions (meq/L)	0.096	0.022	0.750	0.067	0.09	0.11
Charge balance %	-3.13	-15.8	-3.5	5.50	-32.4	-7.5
Element	mg/L	mg/L	mg/L	mg/L	mg/L	mg/L
Ca	0.13	<0.03	6.7	0.585	0.15	0.20
Mg	<0.07	0.029	0.50	<0.070	0.012	0.015
Sr	0.007	0.0015	0.22	0.002	0.002	0.006
Ba	0.006	0.003	0.003	0.003	0.003	0.005
Na	0.5	0.09	0.5	0.12	0.11	0.12
K	1.0	0.16	9.06	0.48	2.0	2.6
Li	<0.10	0.0003	<0.010	<0.01	<0.02	<0.02
Fe(II)	0.65	<0.10	0.66	<0.10	<0.10	<0.10
Fe(tot)	0.66	<0.010	0.68	0.010	<0.10	<0.10
Al	<0.050	0.002	0.42	0.16	<0.02	<0.02
Mn	0.309	0.05	1.2	0.041	<0.004	<0.02
Zn	0.119	0.05	0.80	0.030	<0.02	<0.02
Cd	<0.005	<0.0005	<0.005	<0.005	<0.02	<0.02
Cu	<0.005	0.004	<0.005	<0.005	<0.015	<0.015
Cr	<0.02	<0.020	<0.02	<0.02	<0.05	<0.05
Co	<0.020	<0.0005	<0.020	<0.020	<0.035	<0.035
Ni	<0.025	<0.025	<0.025	<0.025	<0.02	<0.02
Mo	<0.035	<0.0005	<0.035	<0.035	<0.03	<0.03
Pb	<0.090	0.002	<0.090	<0.09	<0.10	<0.10
Zr	<0.015	<0.015	<0.015	<0.0015	<0.01	---
V	<0.02	<0.2	<0.2	<0.0015	---	---
U	<0.001	0.0006	<0.001	0.001	---	---
SO_4	1.0	<2.0	10	1.0	0.50	1.5
F	0.1	0.1	4.4	0.64	<0.01	---
Cl	0.79	<2.0	0.13	<2.00	0.50	0.26
Br	0.009	<0.05	<0.005	<0.05	---	<0.01
NO_3	0.13	0.25	0.02	0.16	<0.02	0.18
HPO_4	<0.10	<0.1	<0.010	<0.1	<0.05	<0.05
B	<0.015	<0.015	<0.015	<0.015	<0.02	<0.02
SiO_2	1.2	1.08	30	2.58	9.30	12.0
S^{2-}	<0.001	<0.001	<0.002	<0.001	---	---

be expected for a discharging water with greater residence time, and are therefore more comparable to the Osamu Utsumi mine waters. This conclusion is also supported by the tritium concentrations (0.10 to 0.24 TU), suggesting an age of around 40–50 years if no mixing of old and young groundwaters occurs.

For geochemical modelling, the MF12 sample has been selected as a representative water for this area with a high residence time underground (i.e. with a chemical composition representative of a high degree of interaction with bedrock and probably in equilibrium with secondary minerals). The recharge waters are in general so dilute that pure water was used as an initial aqueous phase for the mass balance calculations.

Allowing for the very dilute nature of the Morro do Ferro groundwaters, as compared to the Osamu Utsumi mine, water-rock reaction modelling indicated that barite is undersaturated with respect to SO_4. This contrasts with the mine waters which are mostly supersaturated with respect to SO_4. However, in common with the mine waters, the fluorite dissolution plot demonstrates that all the calcium and fluoride concentrations can be accounted for by this process.

4.4. Summary

Morro do Ferro is a deeply weathered, topographically isolated hill, characterised by a resistant vein breccia of magnetite, and hosting a rich thorium/rare-earth mineralisation just below the surface extending from the summit down the south slope of the hill. Studies have indicated that this site may represent a carbonatite complex, intruded into phonolite rocks similar in texture and composition to those described from the Osamu Utsumi mine. Phonolite was intercepted in borehole MF12, located at the foot of the hill.

Weathering has produced an extensive laterite horizon which now contains the mineralisation. Alteration products such as gibbsite, kaolinite and illite dominate, together with subsidiary iron and manganese oxyhydroxides. In addition to distinct thorium- and REE-bearing mineral phases (e.g. cheralite and thorite), uranium and, to a lesser degree, thorium are associated with these oxyhydroxide phases which commonly exist as coatings on the clay minerals.

Rare-earth chemistry shows a not unexpected correlation with the Th/REE mineralogy; in particular thorium is best correlated with Ce. The correlation of uranium is more variable, reflecting its association with oxyhydroxide coatings on clay minerals, rather than with specific resistate radioactive minerals. Normalised LREE patterns

highlight a striking difference in the predominance of positive Ce anomalies in the unsaturated zone (upper 25 m), compared to negative Ce anomalies in the saturated zone. This may indicate a relict from the earlier migration of a redox front.

The natural decay series data show that, near the laterite surface, uranium is being lost by a combination of bulk leaching and preferential removal of ^{234}U, the latter also in evidence down to at least 64 m depth. In the phonolite rock at the foot of the hill, the oxidised section (including the overlying laterite horizon) shows uranium accumulation. The deepest sample from the reduced phonolite has an isotopic ratio close to secular equilibrium. Studies of ^{228}Ra, the parent of ^{228}Th, show that it is either retained where it is radiogenically produced, or is migrating very slowly relative to its decay rate.

The hydrogeology of Morro do Ferro is simple and supports many of the mineralogical, geochemical and natural series distribution observations reported. The water table is a subdued reflection of the topography. Oxidising rainwater percolates through the unsaturated zone to the water table, whereupon flow continues downwards, maintained by a vertical component in the piezometric gradient, and the groundwater becomes increasingly reducing in character. Discharge is mainly upwards to the stream in the valley bottom. This is reflected by the groundwater chemistry sampled at the base of the hill (i.e. longer residence times, greater dissolved ionic content), and is supported by the tritium and stable isotope data.

CHAPTER 5. GEOCHEMICAL MODEL TESTING AT POÇOS DE CALDAS

5.1. Introduction

Geochemical models are widely used in performance assessment studies for nuclear waste repositories. In the near-field, such models are used to evaluate the degradation of engineered barriers and waste matrices and to define the evolution of the resultant pore water. Given the near-field water chemistry, the solubility of radionuclides can be quantified, in many cases this parameter places an important constraint on releases. Additionally, definition of the aqueous speciation of radionuclides allows their transport properties to be estimated, or justifies the extrapolation of laboratory measurements to the near-field conditions.

In the far-field, where comprehensive and representative water sampling may be very difficult, models may be needed to define the water chemistry in "equilibrium" with the minerals present. As in the near-field, solubility and speciation of radionuclides in undisturbed groundwater may constrain release and transport rates. Additionally, a chemically disturbed zone may exist around the repository (e.g. due to high pH leachates from L/ILW or radiolytic oxidants from HLW) and may penetrate some way into the geosphere. Geochemical models are used to predict the movement of such fronts and their consequences for repository performance. This Chapter considers the application of geochemical models to static systems. Coupled models, which include both geochemical and transport processes, are discussed in Chapter 6.

5.2. Geochemical models and their validation

There are two different approaches to modelling geochemical systems. The more commonly used one assumes that chemical equilibrium is rapidly achieved and hence that the distribution of aqueous species and saturation indices for solids can be calculated from free energies of formation (or equilibrium constants) by solving a set of equilibrium distribution and mass balance equations. Another approach is to take explicit account of the kinetics of reaction, and hence to calculate distribution of aqueous species and solid phase dissolution/precipitation as a function of time from known rate constants.

The equilibrium approach has been successfully applied to a wide range of problems but is known to break down, to some extent at least, in low-temperature groundwater

systems. In particular, redox pairs which involve multiple electron transfers (e.g. sulphate/sulphide, nitrate/ammonia, carbonate/methane) may be very far from equilibrium. Even here, it may be possible to use the standard equilibrium models by "switching off" reactions known to be negligibly slow or by amalgamating equilibrium and kinetic approaches.

In the following discussion it is important to distinguish between application of codes to major elements and to the rather exotic trace elements of interest to performance assessors. In the former case, there are extensive thermodynamic databases which are well supported by many field and laboratory studies in a wide range of geochemical environments. Although even here care is required with the solid phases or redox couples assumed to be at equilibrium, enough information exists for such potential problems to be identified by a formal expert system approach. The use of thermodynamic models to interpret groundwater major element chemistry is well illustrated in the analysis of Nordstrom *et al.* (this report series; Rep. 14), which is consistent with mineralogical observations (see Chapter 3; section 3.3 and Chapter 4; section 4.3).

The situation is more problematic for the trace elements. In this case practical problems arise from the poor quality or absence of important thermodynamic data. For many important reactions, equilibrium constants are uncertain by many orders of magnitude and, in some special cases, alternative values differing by over 30 orders of magnitude have been used by different groups. Missing data are of particular concern, as they can potentially alter results by many orders of magnitude. In general, when evaluating solubility, it is considered that missing data on solid phases will tend only to give a conservative result (overpredicting solubility). Missing solution phase data could be non-conservative if the phase involved has a significant concentration under the conditions considered. Given that sorption is very dependent on solution phase speciation, it should be emphasised in the latter case that the major overall consequences in terms of repository performance assessment can be very large.

The alternative kinetic modelling approach can provide a useful representation of low-temperature systems but suffers greatly from the paucity of appropriate data. Rate constants are very difficult to measure and, being less fundamental than thermodynamic parameters, must be extrapolated from measured conditions with great care. Kinetic models have been successfully used in a few cases but require very great simplification of the natural system.

Both equilibrium and kinetic models of trace element geochemistry can be tested, to some extent, by comparison of predictions with results from laboratory experiments. An important constraint is the difficulty of simulating relevant systems in the laboratory and,

more fundamentally, the slow rates of some reactions which require impractically long measurement times.

A more rigorous test of geochemical models can be provided by natural analogues. In a system with geochemical similarity to that of interest in performance assessment, model predictions can be compared with field observations. For example, an ore body in a reducing groundwater system should provide a source of several relevant trace elements which should reach saturation. From the groundwater major element chemistry, the solubility and speciation of these elements can be predicted and the predictions compared to field measurement. It should be emphasised that, although a model can be disproved if prediction and observation disagree widely, the model cannot be validated in a rigorous sense. It is not possible to completely determine trace element speciation in solution or prove equilibrium with particular solid phases. Nevertheless, reasonable agreement in a number of tests greatly increases confidence in the applicability of the model.

All types of geochemical model inherently simplify nature, in particular considering "pure" solid phases. In reality, minerals are never completely pure and will involve a certain extent of substitution/solid solution which will alter their thermodynamic/kinetic properties. Additionally, microcrystalline or amorphous phases will be more reactive than the fully crystalline phases for which data usually exist. A match of predicted solubility of trace elements with observed concentrations to within about an order of magnitude or so should thus be considered to represent good agreement and such a level of uncertainty is generally taken into account in performance assessment.

5.3. Model testing at Poços de Caldas

The first requirement for testing models of trace element speciation is a rock/water system which is in equilibrium (or at least steady-state) with regard to the major element chemistry. A range of groundwater samples from the Osamu Utsumi mine and Morro do Ferro sites have been extensively interpreted using standard thermodynamic codes and their major element compositions have been shown to be compatible with the mineralogy along the identified groundwater flow-paths (see Chapter 3; section 3.3 and Chapter 4; section 4.3).

The second requirement for testing solubility predictions is a source of the element of interest which could reasonably be expected to dissolve in the groundwater. The most obvious sources here are uranium in the ore bodies at the Osamu Utsumi mine and

Th/rare-earths (REE) in the ores at Morro do Ferro. It should be emphasised that not only should high concentrations of the elements involved be present, but there should also be some evidence of their reaction with groundwater. At the Osamu Utsumi mine, there is clear evidence of mobilisation not only of uranium but also of a range of trace elements which are highly concentrated around the redox front (see Chapter 6). At Morro do Ferro, uranium, thorium and rare-earth elements show profiles in core samples indicating mobilisation (see Chapter 4; section 4.1.2). These elements are also found in colloidal phases which should be relatively reactive (see Chapter 7). The natural series radionuclide data from both sites provide additional evidence of mobilisation (see Chapter 4; section 4.1.3 and Chapter 6; section 6.4.1.)

The procedure for the model testing was:

1) Specification of three well-defined groundwaters from Morro do Ferro.

2) Blind prediction of elemental speciation, solubility and controlling solids for U, Th, Pb, V, Ni, Sn, Se and Ra.

3) Comparison of results with each other and, where possible, with observed concentrations at a modelling workshop.

4) Specification of waters from both Morro do Ferro and the Osamu Utsumi mine for a second modelling exercise.

5) Second phase of blind predictions for U, Th, Pb, Ni Sr, Mn, Al and Zn.

6) Final comparison with field measurements of concentrations, some simple determinations of rough speciation (separation of anionic, cationic and organic components) and observed mineralogy.

5.4. Results of model tests

Details of the geochemical modelling and the testing exercises are given by Bruno *et al.* (this report series; Rep. 11). The first modelling exercise showed reasonable agreement between the models and identified some particular problems with the different databases used. In the few cases where comparison of predicted solubility and observed concentrations were possible, the predicted values were similar to or less than observed values.

The second exercise was more extensive in terms of the participating groups, the range of waters considered and the extent of analysis of predictions. The predicted solubilities

TABLE 5.1

Summary of modelling results (all concentrations as log molar).

Element	Water	Observed	Predicted SKB	KTH	PSI	Harwell	Atkins
U	F1	-7.7	-4.3	-4.8	–	-4.4	-5.2
	F5	-7.5	-5.0	-6.0	-4.7	-5.2	-5.4
	MF12	-8	-5.9	-5.2	-4.4	-4.5	-5.0
Th	F1	-10	-9.3	-8.9	–	-7	-6.7
	F5	-9.8	-8.1	-9.4	-10.2	-8.7	-8.7
	MF12	-9.6	-9.4	-9.3	-9.6	(-6.0)*	-9.2
Pb	F1	-8.3	-3.9	-5.3	–	-4	–
	F5	-5.3	-3.6	-5.4	-4.7	-5.2	
	MF12	-5.4	-3.6	-5.4	-5.5	-5.1	
Ni	F1	-7.2	-8.3	-0.2	–	-3.4	–
	F5	-6.3	-12.0	-1.3	-3.2	-1.6	
	MF12	-8.3	-13.5	-1.3	-3.1	-1.6	
Sr	F1	-7.2	-1.8	-2.6	–	-3.0	-3.7
	F5	-7.2	-1.8	-3.0	–	-3.0	-3.3
	MF12	-5.4	-1.2	-2.4	–	-3.0	-3.7

*value includes phosphate complexes for which the data are rather uncertain.

of the safety-relevant trace elements in waters from an oxidising zone at the Osamu Utsumi mine (F1), a more reducing zone (F5), and a deep sample from Morro do Ferro (MF12) are summarised in Table 5.1 along with the measured concentrations. Without going into detail, it is clear from this table that, in most cases, the solubilities predicted by the various groups are in reasonable agreement and are "conservative", that is predicted solubilities are above measured concentrations.

5.4.1. Uranium

For uranium, the groundwater concentrations in all samples are fairly similar. All calculated solubilities are higher than these values and, as uranium is relatively plentiful in these systems, this would suggest that the models lack an important solid phase. The models generally predict pitchblende to be the solubility-limiting solid and this is certainly plentiful in the region around the F5 sample. The correlation of uranium concentration in the bulk rock around the redox front with iron and a range of other

elements indicates that uranium may be removed by coprecipitation with various iron minerals.

Field speciation analysis indicated that aqueous uranium was predominantly in an anionic form in F1 and F5 and distributed between anionic, cationic and neutral species in MF12. Although these data are derived from a novel technique and should be used with caution, if accepted at face value they would tend to contradict the models, especially for F1 and F5, which predict predominantly cationic complexes. This observation would allow for an alternative explanation for the observed overprediction of solubility if some of the complexation constants for the aqueous complexes involved were too large.

5.4.2. Thorium

For thorium, the predictions show rather good agreement and reasonable consistency with the measured concentrations. Thorianite is predicted to be the controlling mineral phase and this is found in the region, especially at Morro do Ferro.

5.4.3. Lead

Lead values again are reasonably consistent and agree fairly well with measured concentrations; the low concentrations in F1 could readily be explained by source term limitations.

5.4.4. Nickel

Nickel, however, is a clear case where very large differences occur between databases and where some databases appear to be non-conservative. The very low solubilities predicted by the SKB database clearly result from the inclusion of a Ni-ferrite solid phase. Such a phase seems very unlikely to form under low-temperature conditions and hence it should not be included in such simulations. A similar situation arose in the case of Zn. All other models predict very high solubilities which are not in line with the observed concentrations, despite reasonably high concentrations of nickel around the redox front and at Morro de Ferro. As in the case of uranium, it is very likely that nickel is removed by coprecipitation with iron minerals, a process which is not included in these models.

5.4.5. Strontium

Finally, for strontium, there is again reasonable agreement between the models, but predicted solubilities are much higher than observed concentrations. There are indications that a strontium phosphate (goyazite?) may be an important phase in this region but, unfortunately, no thermodynamic data have been found for this mineral. Alternatively, strontium may be limited by solid solution in calcium or barium minerals (Chapter 3; section 3.3 and Chapter 4; section 4.3) which, again, cannot be included in these models.

5.5. Summary and conclusions

In general, the predictions of the various modelling groups were reasonably comparable and consistent with field observations. Only a few specific cases can be identified where model predictions of solubility were highly non-conservative and these involved only Ni and Zn when a ferrite mineral is taken as the solubility limiting solid. It appears unlikely that such minerals are formed under low-temperature conditions and, unless there is evidence for their formation in a specific environment, it is strongly recommended that ferrite minerals be excluded from such solubility limit calculations.

For the waters which are most likely to be saturated (F5 and MF12), agreement between predicted and observed concentrations is best for Th, Pb and Al.

For all other elements, measured concentrations were below predicted solubility limits. For elements such as V this may reflect source term limits, but for U and Sr in particular, specific minerals containing these elements are present along with evidence of their mobilisation. For Sr, the discrepancy probably simply reflects the absence of key minerals (e.g. goyazite) from the databases used. For U, the discrepancy could simply be due to uncertainties in the databases used (which were generally selected to "conservatively" overpredict solubility) or could, as in the cases of Ni, Zn and Mn, reflect concentration limits set by coprecipitation with Fe-oxyhydroxides which are found at the redox front and could act as efficient scavenging agents for trace elements.

The role of coprecipitation or solid solution of radionuclides in Fe-oxyhydroxides has not been quantitatively included in performance assessment models due to lack of appropriate data. This study strongly suggests that neglecting this phenomenon is 'conservative', but may overestimate concentrations by many orders of magnitude. In order to realistically model trace element concentrations in a region of Fe-oxyhydroxide

formation (for example, in the vicinity of a corroding waste canister), it is recommended that coprecipitation /solid solution models be developed.

The extent of agreement between predictions of speciation was very variable, being very good for some elements (e.g. Sr, Ni, Zn, Al, Mn) and rather poor for others (e.g. U, Th). The discrepancies involved reflect both inherent differences in the complexity of the aqueous chemistry of these elements but also variability in the extent of their databases. Of key significance from a safety assessment viewpoint is the charge of the predominant aqueous complex(es). In general, free cations or cationic complexes would be expected to sorb more than neutral complexes which, in turn, sorb much more than anionic complexes. In this study, speciation predictions could be tested, to some extent, against field ion-exchange separation results and colloid fractionation studies. It should be emphasised that the former technique is not yet well established in this application, while information from the latter is rather indirect. Nevertheless, predicted speciation and ion-exchange/colloid fractionation results showed reasonable consistency for Al and Mn and, in some cases, U and Th. Given the great importance of sorption in the geosphere, it is recommended that techniques for in-situ speciation be further developed and applied to testing model predictions.

CHAPTER 6. REDOX FRONT PROCESSES

6.1. Introduction

In most concepts for deep disposal of radioactive waste the environment around the repository will, in its undisturbed form, be chemically reducing. Construction and operation of the repository will inevitably introduce air and hence a boundary between oxidising and reducing zones (a "redox front") will become established. In cases where the host-rock contains sulphide minerals in particular, the redox front formation and movement may be associated with significant alteration of rock properties and the production of acidic leachates which could cause further damage to repository structures.

For high-level radioactive waste, in particular spent fuel, further oxidants may be produced after repository closure due to radiolysis. Over long periods of time when flow occurs in distinct fissures, the redox front resulting from this source could potentially penetrate large distances into the host rock (e.g. KBS, 1983).

A number of simple models has been developed to predict the reactions occurring at such redox fronts and the rate at which they move. This Chapter summarises the predictions of such models and compares them with observations of the well-defined redox fronts in the Osamu Utsumi mine.

6.2. Components of a redox front model

The two fundamental components of a redox front model are a description of the principal geochemical processes and mineralogical transformations occurring in the region of the front, and a qualitative description of solute transport through the front. A model describing the near-field of a radioactive waste repository would require an additional model for oxidant production by radiolysis, but this is not addressed in the current study.

The supply of oxidants at the Osamu Utsumi mine is derived from infiltrating meteoric water which is saturated with atmospheric oxygen and picks up additional potential oxidants (e.g. SO_4, NO_3, CO_3, Fe(III)) during transport through upper layers of soil and weathered rock. The aspect ratio of redox front fingers (cf. Fig. 3.2) implies that, in these zones, solute transport occurs predominantly by advection in associated fractures with more limited advection or transport by diffusion in the surrounding rock (see Chapter

3; section 3.1.2). At the front, both natural series profiles, which indicate very low rates of movement, and trace element profiles, which are symmetric about the front, imply that transport here occurs predominantly by diffusion (MacKenzie *et al.*, this report series, Rep. 7).

The most evident chemical processes occurring at the front involve the oxidation of pyrite to form iron oxyhydroxides, which are responsible for the marked colour change observed. Additionally, on the reduced side of the front, pitchblende formation is noted, often associated with secondary pyrite (see Chapter 3; section 3.1.2). In the transition from oxidising to reducing zones (e.g. F2 to F5; Table 3.1), the groundwater pH stays relatively constant or increases slightly, sulphate increases and Eh decreases. Detailed analysis of water chemistry changes are, however, limited by perturbations caused by the presence of the mine (see Chapter 3; section 3.2 and 3.3).

Based on the information above, a number of modelling approaches can be considered. The simplest is a scoping mass balance which considers only the supply rate of oxidants and a simple chemical reaction to derive an estimate of the rate of front movement. A more sophisticated variant of this approach considers the preferential transport of oxidants along fissures to predict the evolution of the form of the front.

A better representation of the chemistry of the oxidation reactions can be obtained using chemical equilibrium models (see Chapter 5). Such models can incorporate a wide range of oxidation reactions and also associated weathering reactions caused, for example, by neutralisation of acid leachates produced by pyrite oxidation. These models can be loosely coupled to transport codes which allow the spacial development of the front to be simulated. The effects of sorption processes can also be included in this approach.

An alternative to the assumption of equilibrium is the direct representation of the kinetics of chemical reactions at the front. This approach can account for all the processes included in the equilibrium model and can also be directly coupled to a model of solute transport.

Finally, it should be mentioned that there are additional redox front "models" which do not attempt to evaluate the overall geochemistry but concentrate rather on particular aspects. Of special interest here are models of microbiological processes, natural series radionuclide profiles, and trace element redistribution (MacKenzie *et al.* and West *et al.*, this report series; Reps. 7 and 10).

6.3. Overview of the redox front models

Before presenting an overview of the results of various modelling studies, it is important to emphasise that these were initiated at different stages during the progress of the project, and therefore involve slightly different conceptual models of the Osamu Utsumi mine system and different databases of physical/geochemical parameters. The earliest work was the mass balance modelling, which was followed by the thermodynamic modelling, while the kinetic model represents the most recent work.

6.3.1. Mass balance models and studies of fissure flow

(cf. Neretnieks *et al.*, Chapter 3 in McKinley (Editor), this report series; Rep. 12)

In the simplest model, the rate of movement of the redox front was estimated from the supply of oxidants. The model makes the global assumption of:

i) A rainfall infiltration excess of 100 mm/year.

ii) Oxygen saturation (10 μg/g).

iii) 2% pyrite by weight in the reduced rock.

iv) Complete pyrite oxidation by dissolved oxygen, i.e.
$FeS_{2(s)} + 15/4\ O_{2(aq)} + 7/2\ H_2O \rightarrow Fe(OH)_{3(s)} + 4H^+ + 2SO_4^{2-}$

v) No other redox active components in the system.

This results in a predicted redox front movement rate of ≈ 25 m/10^6 a. This numerical value is not unreasonable, but the assumption of constant conditions over $> 10^6$ a, oxygen as the only oxidant and the production of very acidic waters at the redox front do not match field observations.

This first calculation assumes an ideal homogeneous, porous, anisotropic rock. In reality, the redox front shows marked fingering.

In order to analyse these redox fingers, a conceptual model was developed in which advective flow occurs only within fracture zones and, further, such fracture zones are themselves heterogeneous and contain channels in which the flow is focussed. Oxidants in the flowing water may, however, diffuse into the connected porosity of the surrounding rock.

Mathematical analysis, using data on channelling frequency from a Swedish granite, allowed the growth of such redox fingers to be simulated. This work gives some indication

of the scale at which processes operate and indications about the origin of observed structures, but the assumptions made are clearly very simplistic.

6.3.2. Thermodynamic models

Two independent attempts to simulate the redox front were carried out using the CHEQMATE and CHEMTARD coupled equilibration/transport codes. These improve considerably on the simple mass balance approach, for example, considering buffering reactions which bring the predicted groundwater pH much closer to that observed. Both models simulate the formation of sharp fronts and the formation of uranium minerals on the reducing side of the front.

The CHEQMATE calculations were carried out for pure advective flow (~0.7 m/a) and for a pure diffusive case (Cross *et al.*, Chapter 4; section 4.1 in McKinley (Editor), this report series; Rep. 12). The inflowing water was assumed to have pH 5.1, pe 13.6, 1.6×10^{-4} M total dissolved carbonate and 3.1×10^{-6} M dissolved oxygen. The reactive minerals in the original reduced rock are pyrite, K-feldspar, kaolinite and 'uranium'. A typical representation of development of the mineralogy around the hydrolysis/redox front is shown in Figure 6.1(a) for the advective flow case. Associated predicted pore water chemistry and uranium speciation in profiles though the redox front are shown in Figures 6.1(b) and (c).

To explain the sensitivity of the calculation to assumed flow conditions, simulations were also run assuming that solute transport occurs only by diffusion. Predicted mineralogy and pore water chemistry profiles are illustrated for this case in Figure 6.2. In general terms, the predictions in both cases are similar although, naturally, the rate of movement of the front is considerably slower for the 'diffusion only' cases.

The CHEMTARD modelling was predominantly aimed at elucidating uranium transport over the redox front (Read, Chapter 4; section 4.2 in McKinley (Editor), this report series; Rep. 12). The simulations run were based on a conceptual model including:

1) Percolation of oxygenated waters through the profile; rapid conversion of pyrite to iron oxyhydroxides.

ii) Slower dissolution of primary pitchblende ore; release of U(VI) species to solution.

iii) Fixation of U(VI) hydroxy and hydroxy-carbonate species by iron oxides.

iv) Diffusion and reduction across fracture-controlled redox interfaces; localised redistribution of uranium and formation of secondary pitchblende ore.

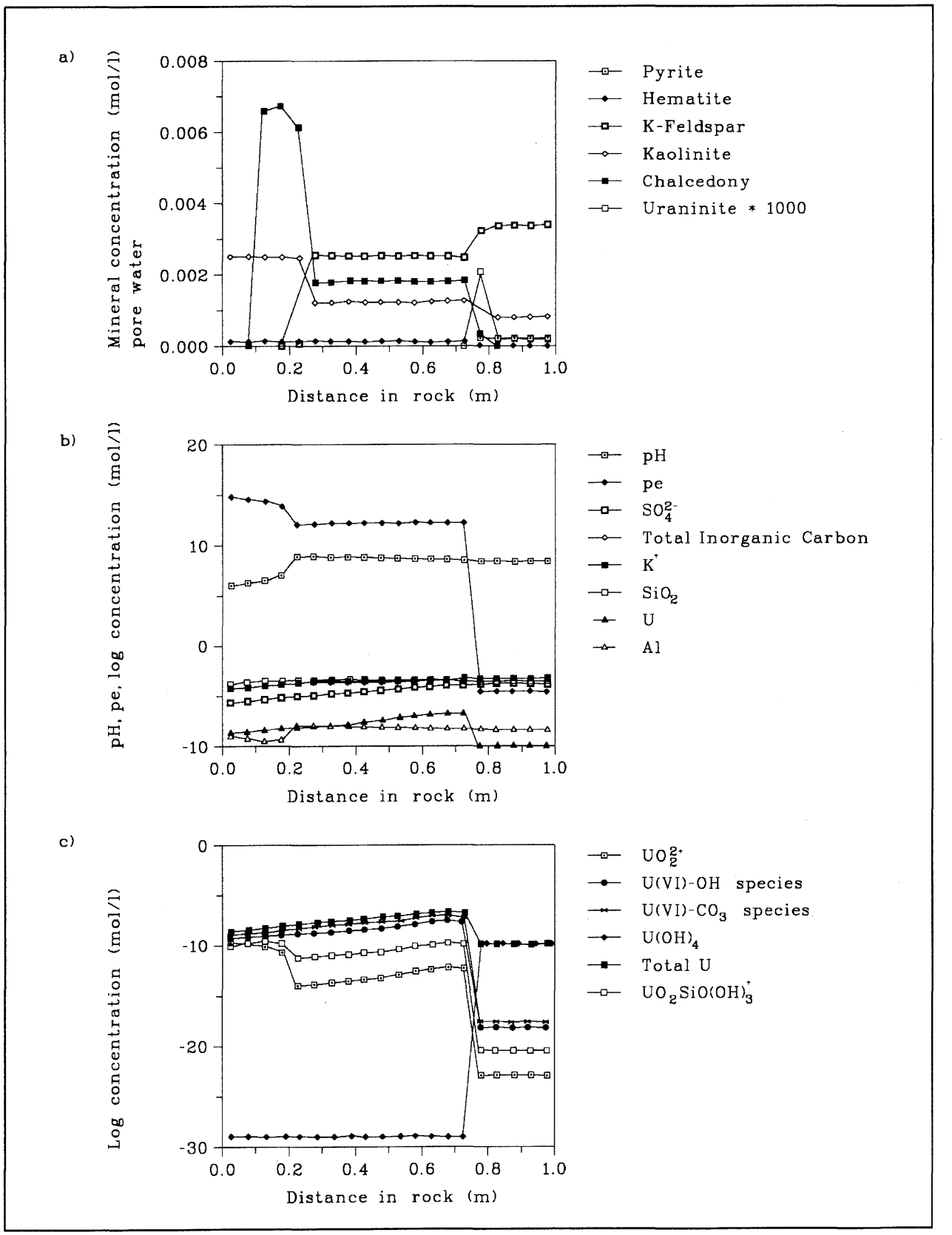

Figure 6.1.

a) Predicted mineral concentrations with depth at 38,000 a.

b) Predicted profiles of pH, pe and concentrations of various aqueous species at 38,000 a.

c) Predicted chemical speciation of uranium at 38,000 a.

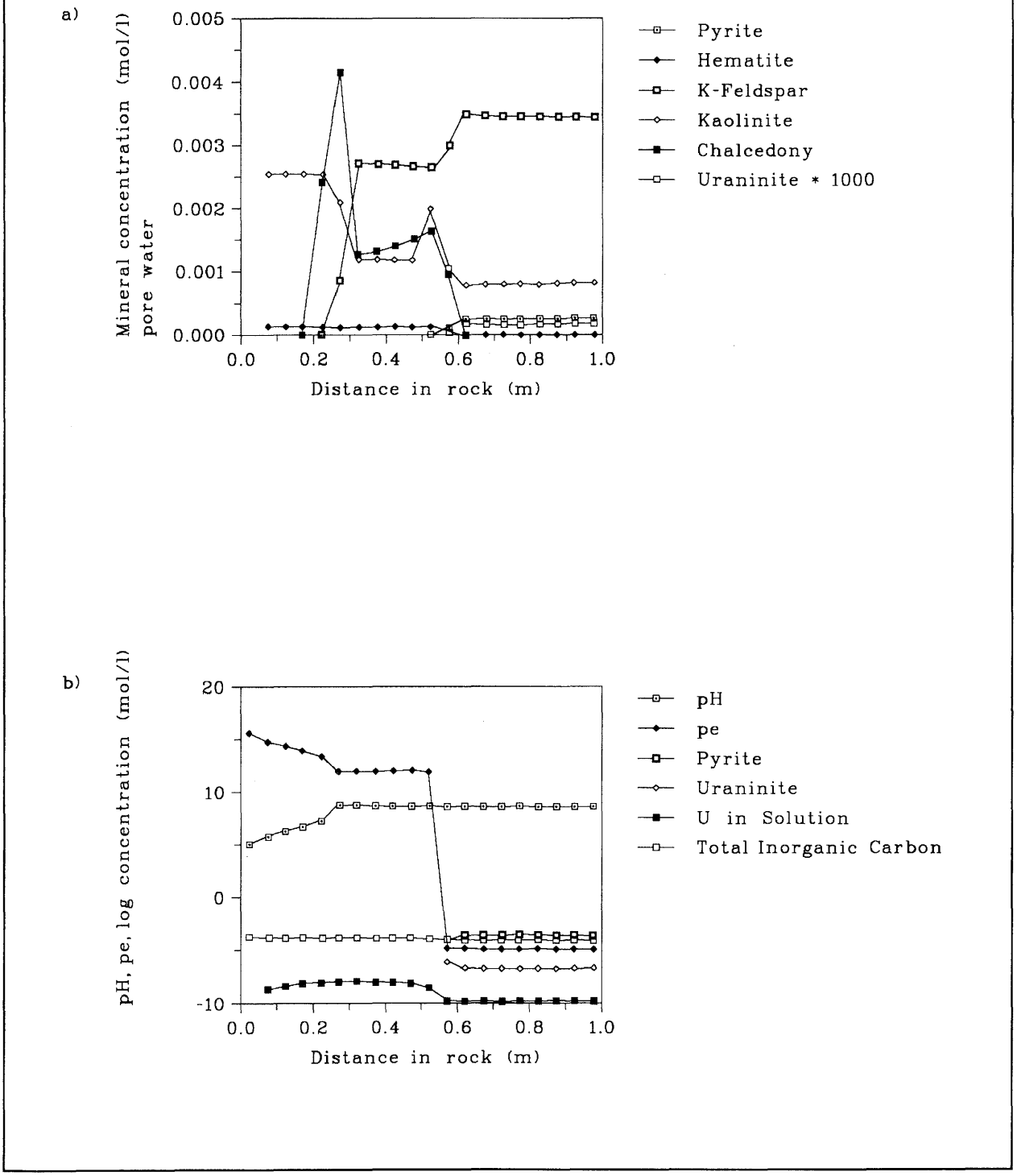

Figure 6.2.

a) Predicted mineral concentrations with depth at 1.25x10^6 a for the 'diffusion only' case.

b) Predicted profiles of pH, pe and concentrations of various species and minerals at 1.25x10^6 a (diffusion only).

Sorption on iron oxyhydroxides, which is not normally included in thermodynamic models, was represented by a triple-layer model. It should be emphasised that such an approach does not include coprecipitation processes and, in the model, uraninite was considered as the precipitating phase rather than pitchblende.

Typical results of such modelling (10^6 a simulation) are shown in Figure 6.3, which depicts a predicted profile of uranium concentration/speciation over the redox front. Figure 6.4 shows the location of uraninite precipitation at this time and indicates how the amount of precipitation (normalised to the pore water content) varies with the assumed diffusivity.

When examined in detail, however, both models deviate from reality both in their predictions of the alterations of water chemistry and, in particular, their inability to simulate the observed formation of secondary pyrite. Some of the problems involved are certainly associated with the databases used, e.g. predicting uraninite formation rather than the observed pitchblende, but there are indications that the simple equilibrium approach may give a poor representation of this system.

6.3.3. Kinetic modelling

(Lichtner, Chapter 5 in McKinley (Editor), this report series; Rep. 12)

The model applied here describes mineral reactions by pseudo-kinetic rate expressions when, as is commonly the case, accurate rate laws are not available, and is based on the quasi-stationary state approximation. This model gives a good simulation of the evolution of sharp fronts with associated uranium mineralisation and, interestingly, also predicts the formation of secondary pyrite. In its current form, however, the model does not evaluate rates of redox front movement.

In these simulations, K-feldspar, kaolinite, muscovite (in place of illite), fluorite and pyrite in the original rock body are considered. Gibbsite, ferrihydrite and uraninite are considered to form as secondary minerals. The results for a typical simulation are shown in Figure 6.5 which indicates the mineralogy profile. Figure 6.6 shows detail of the redox front with 'travel time' converted into distance by assuming a Darcy flow velocity of 1 m a^{-1}. Of particular note here is the simulation of the formation of secondary pyrite on the reducing side of the front. Under the predicted conditions, however, pitchblende would be unstable with respect to uraninite and would not be expected to form (as also indicated by the thermodynamic models). The profile of aqueous uranium speciation is shown in Figure 6.7.

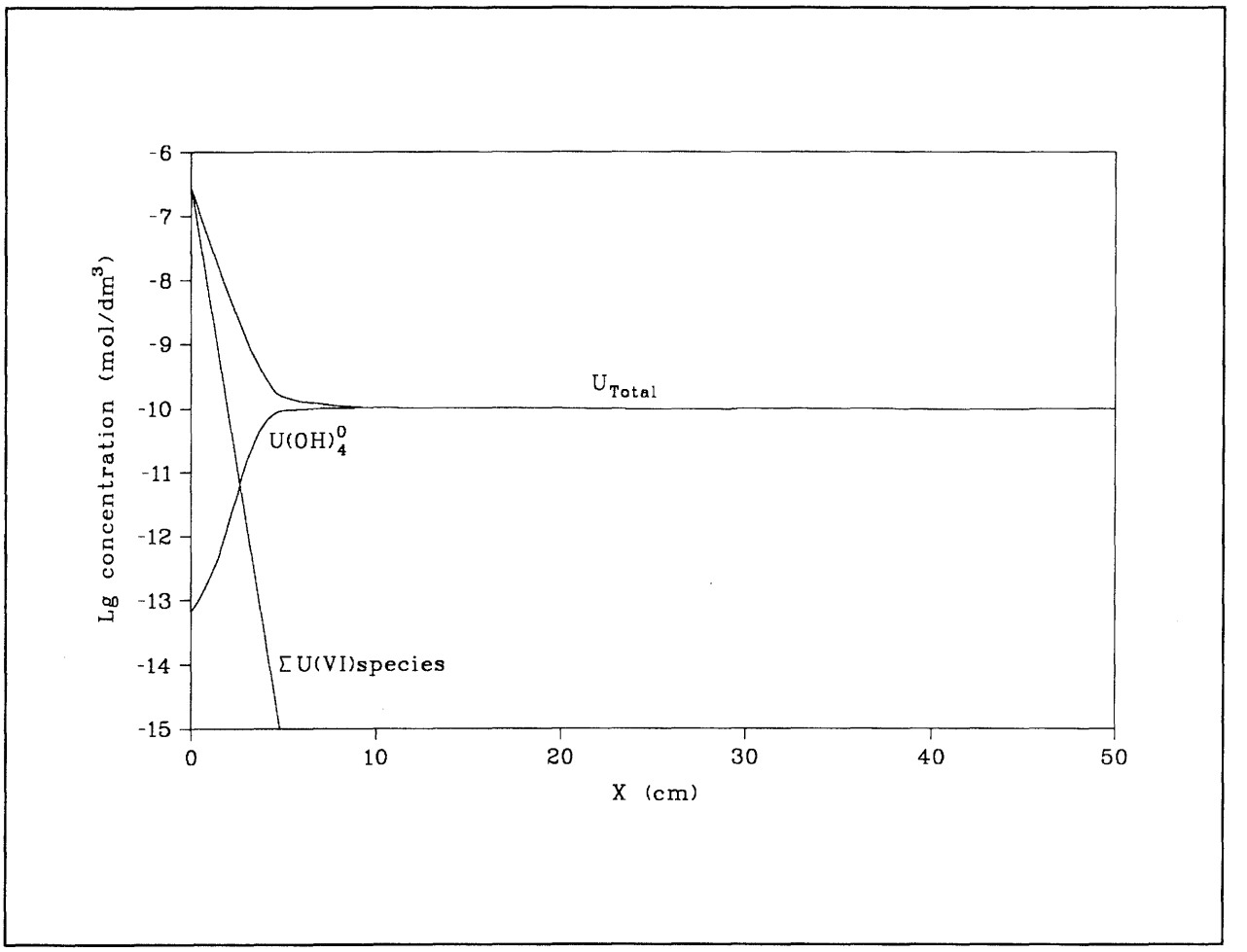

Figure 6.3. Change in uranium concentration across the redox front at t = 10^6 a.

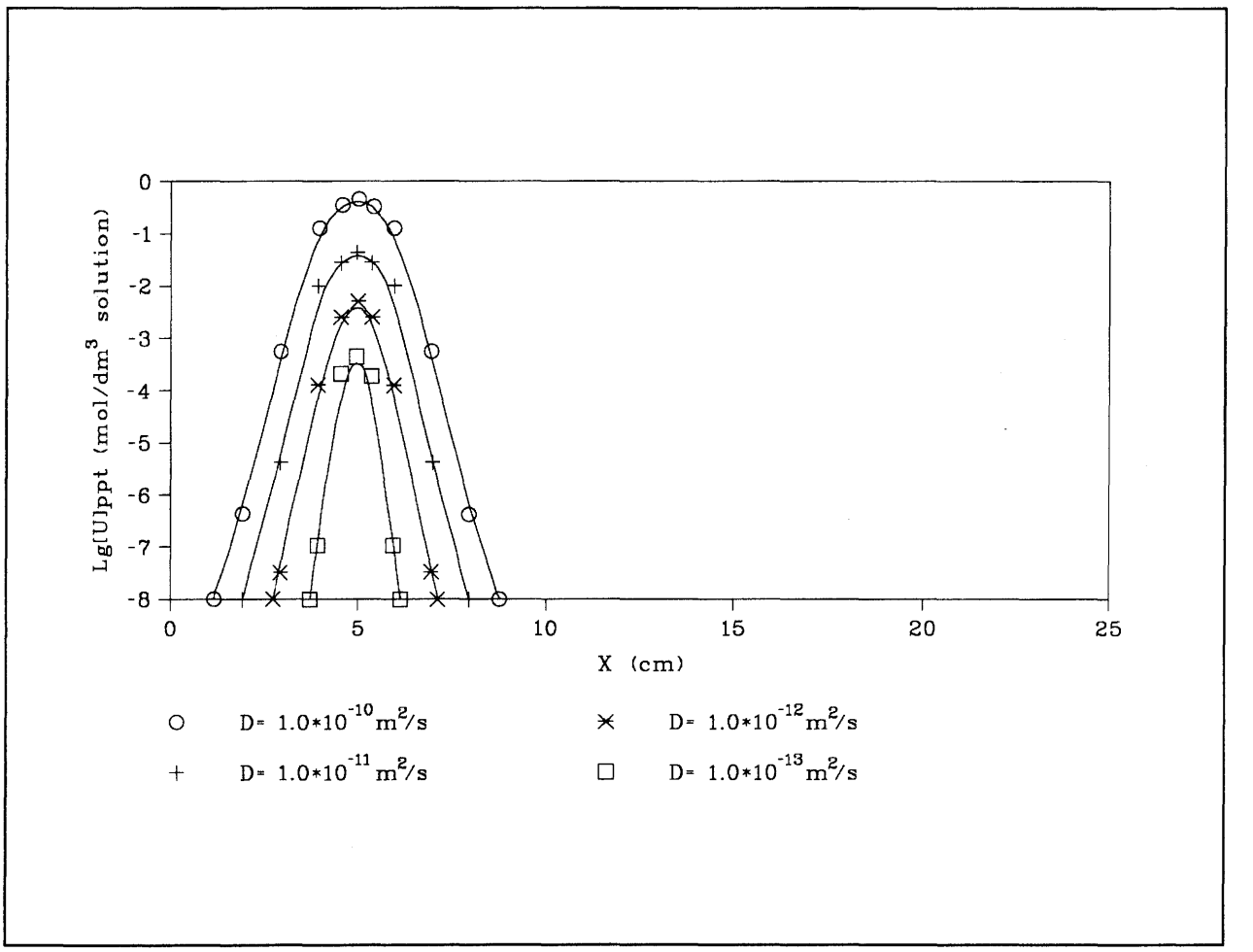

Figure 6.4. Precipitation of uranium at the redox front at $t = 10^6$ a.

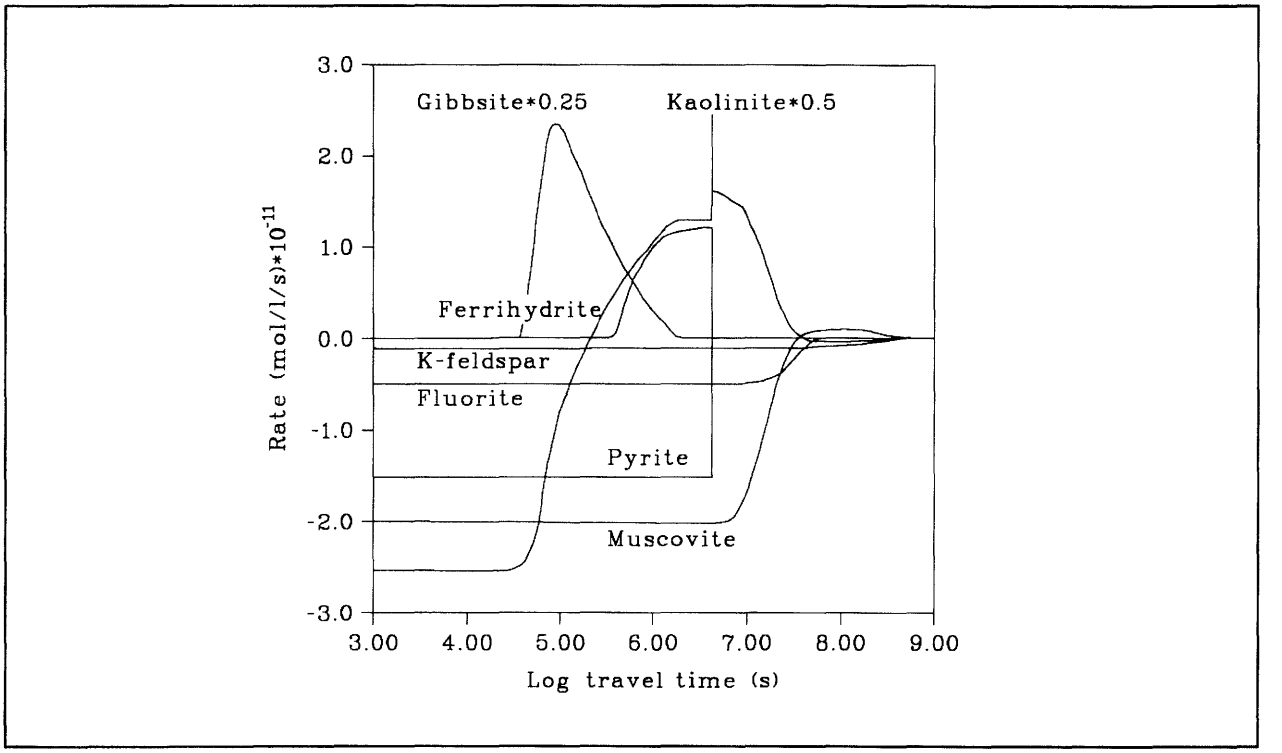

Figure 6.5. Weathering of hydrothermally altered phonolite rock including the oxidation of pyrite and uranium deposition. Reaction rates of the indicated minerals are plotted as a function of the logarithm of the travel time in seconds for a packet of fluid moving with constant velocity. A sharp change in redox state of the packet occurs where the ferrihydrite and pyrite rates rapidly approach zero.

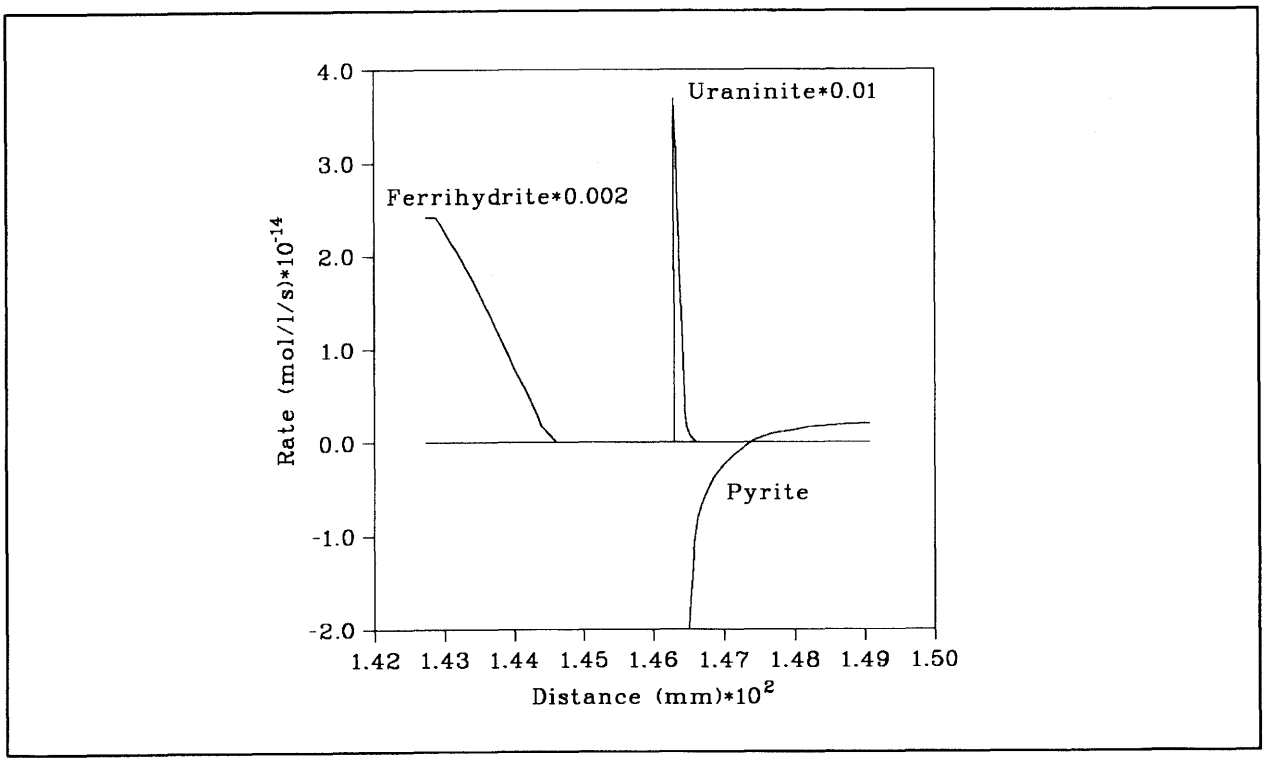

Figure 6.6. A close-up view of the redox front showing the reaction rates of pyrite, ferrihydrite and uraninite plotted as a function of distance. A Darcy flow velocity of 1 m^{-1} is assumed to convert travel time to distance. The placement of the uraninite zone and its narrow width is consistent with field observations at the Osamu Utsumi mine.

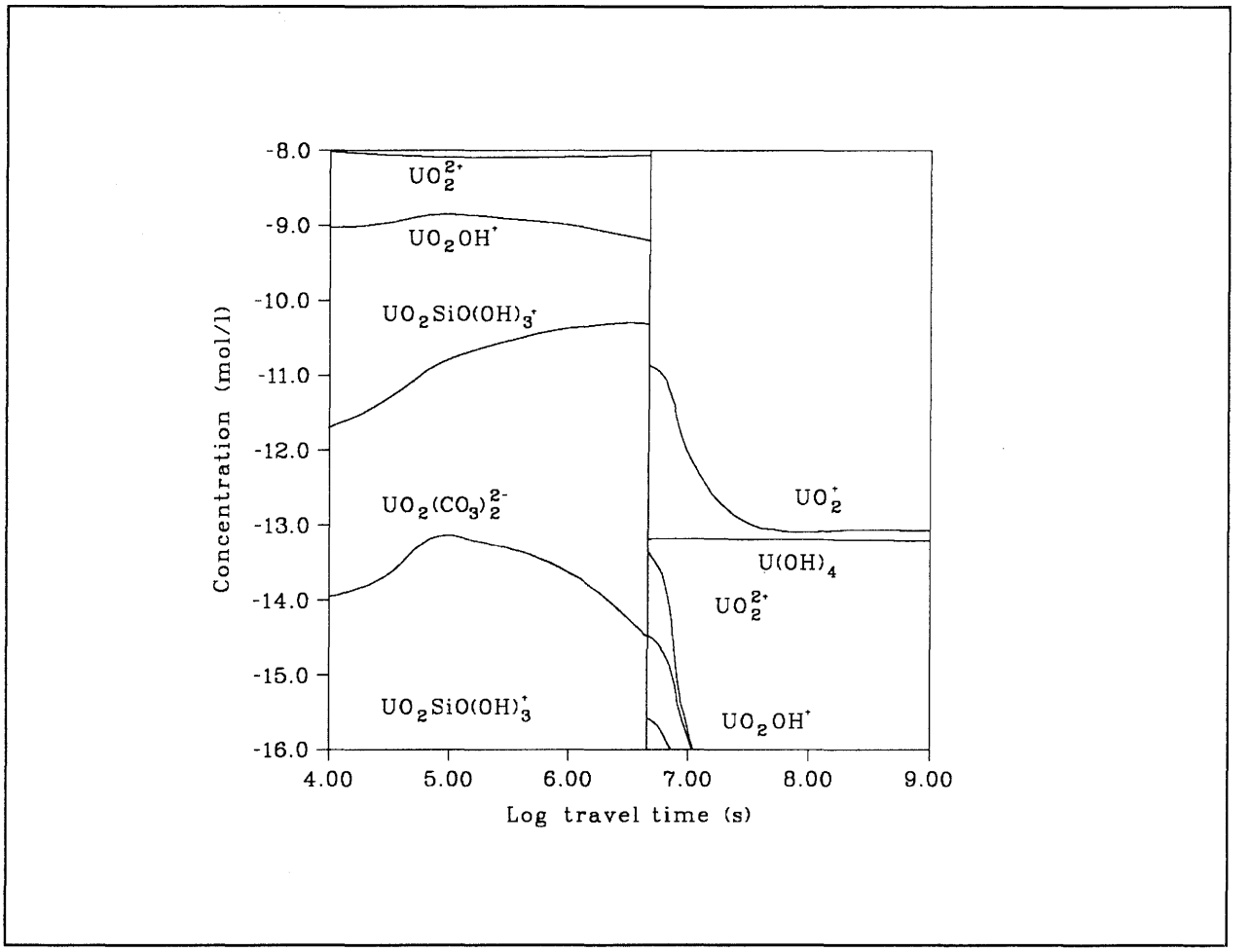

Figure 6.7. Log of the concentration of aqueous uranium species plotted as a function of the log of the fluid packet travel time.

This kinetic approach is particularly limited by the lack of appropriate rate data and hence, to some extent, involves a fair degree of curve fitting. The model does not reproduce the remnant uranium found in the oxidised zone although, in principle, sorption processes could also be incorporated in this approach.

6.4. Detailed observations of the redox front

The models discussed above were rather locally constrained by data on reasonable advective water flow rates, input water chemistry and the mineralogy of the unaltered rock. The results of the model simulations are now compared with some detailed observations of the redox front.

6.4.1. Natural series radionuclide profiles

(MacKenzie *et al.*, this report series; Rep. 7)

The analysis of profiles of natural series radionuclides through various redox fronts (Fig. 6.8; see also Chapter 3; section 3.1.3 and Figs. 3.7 to 3.9) places considerable constraints on models of the processes occurring. Some key observations are:

1) Uranium is enriched in all near-surface rocks, both oxidised and reduced, relative to "unaltered" deeper rocks. Uranium shows distinct maxima on both sides of redox fronts with that on the reducing side being sharper and larger than that on the oxidising side.

2) The shape of the uranium profiles suggest that advective flow occurs in plane fractures parallel to the redox fronts, with solute transport perpendicular to the fronts occurring predominantly by diffusion. Given the enhanced concentrations in both oxidised and reduced rock, a lateral supply of uranium is required (source areas being suggested in the studies of outcrop samples).

3) The natural series profiles indicate that some transport of ^{234}U occurs even in the "undisturbed" deep rock and unambiguously show evidence of uranium mobilisation within the last 10^6 a around all fronts examined. Together with ^{226}Ra data, this also implies that the rock matrix must be considered to be generally porous.

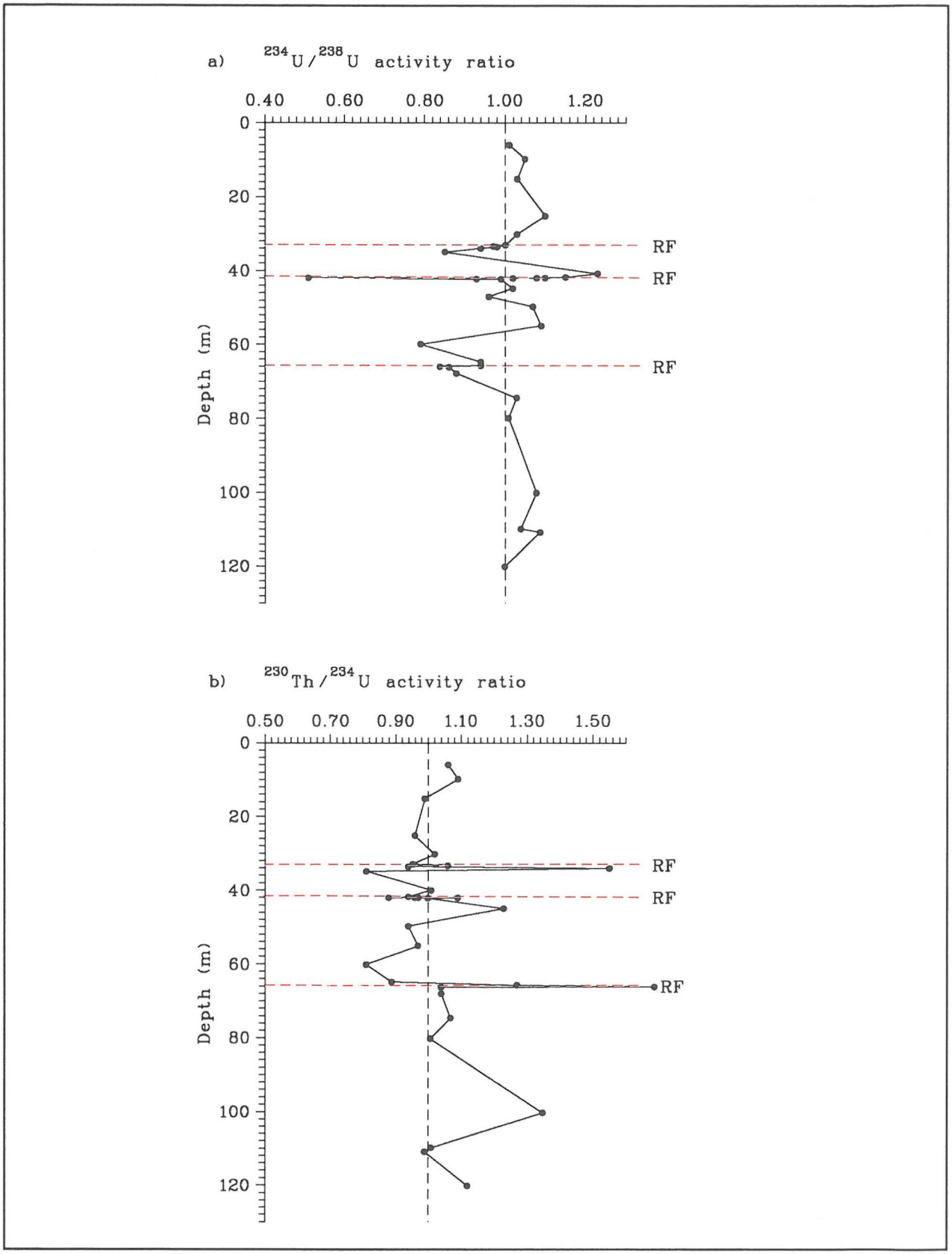

Figure 6.8. a) $^{234}U/^{238}U$ and b) $^{230}Th/^{234}U$ activity ratios as a function of depth for samples from the F1 drillcore. (RF = redox front: the redox front at 42 m is 'inverted" with reducing rock overlying oxidising).

4) Modelling of the isotope profiles indicated that the rate of movement of various fronts lies in the range of approx. <1 m–20 m/10^6 a. The evidence for very slow movement is most clear for an "inverted" redox front which shows very extreme isotope ratios ($^{234}U/^{238}U$ = 0.51) which require a very long period to be established (e.g. redox front at 42 m; Fig. 6.8 a).

5) Extreme isotope ratios also suggest that, in some areas, uranium is deposited as thin surface films or in a porous form. This is supported by leaching studies.

These observations confirm two of the model assumptions presented in the previous section, namely that;

1) The rock can be regarded as a porous matrix.

2) Advective flow occurs along major fractures, with solute transport at right angles to this flow occurring predominantly by diffusion.

However, they also illustrate some problems with these models:

1) The one-dimensional models do not consider the supply of solute from "the side". Such lateral supply appears to play a key role in this area.

2) Most models (except that of Read, Chapter 4; section 4.2 in McKinley (Editor), this report series; Rep. 12) do not simulate uranium concentration on the oxidised side of the front. The shape of the maximum on the oxidised side would not be simulated, even then, with the simple sorption model described.

3) All models could simulate sharp uranium maxima on the reducing side of the front but these do not indicate more widespread uranium mobilisation on the reduced side as illustrated by the uranium isotope ratios.

4) The models assume that all redox fronts develop in a similar manner; field observations, however, indicate that, while some general trends are present, there are significant differences in the development of uranium concentration profiles, isotope ratio profiles and the rate of front movement at different locations.

6.4.2. Mineralogy and trace element profiles

(Waber *et al.* and MacKenzie *et al.*, this report series; Reps. 2 and 7)

The mineralogical analyses show clearly that, although the iron oxidation front may be very sharp, remnant pitchblende nodules are found in oxidised zones showing that the model assumption of a homogeneous mineral distribution is inapplicable on a fine scale. The distribution of uranium and a range of trace elements about the redox front shows that bands of concentration occur on both the oxidising and reducing sides of the front. Such behaviour would not be predicted by any of the models considered in section 6.3, mainly because of their inability to consider coprecipitation/solid solution. As indicated in Chapter 5, iron oxyhydroxides appear to be a major scavenger for a range of trace elements on the oxidised side of the front. This was considered only in the CHEMTARD model and, even here, was treated purely as a surface sorption process where coprecipitation was suggested in Chapter 5 and is confirmed by mineral autoradiography.

The elements concentrated around the redox front include many of relevance to performance assessment. The profiles are most dramatic around the front predicted to be slowest moving on the basis of natural series measurement (at 42 m) and the symmetry observed in some cases provides additional support for solute transport in this region being dominated by diffusion (see Fig. 3.12).

Considering the various regions of oxidised and reduced rock in more general terms, distinctive patterns of enrichment and depletion emerge relative to the deeper "unaltered" rock below 25 m in borehole F1 (Table 6.1). The trace element patterns cannot be clearly explained by any of the models, although there are indications that these may reflect subtle changes in redox conditions (e.g. rare-earth element fractionation) or coprecipitation effects (common profile form of Cs, Pd, Pt, Au, etc.).

6.4.3. Microbiology

(West *et al.*, this report series; Rep. 10)

A range of microorganisms are found at depth in the Osamu Utsumi mine, including sulphur oxidisers and sulphate reducers which may be expected to be involved in redox processes occurring at the fronts. Simple scoping calculations indicate that observed populations are reasonably consistent with expected constraints set by the supply of nutrients and chemical energy from the oxidation of pyrite. The absence of sulphur

TABLE 6.1

Summary of enrichment (E) and depletion (D) patterns for average elemental concentrations in upper sections of the F1 drillcore relative to average concentrations in the section below 75 m.

Section																
0 – 33.4 m	E	E	E	E	D	E	E	E	D	D	D	E	D	D	D	D
33.4 – 42 m	E	D	E	E	E	D	E	D	D	E	E	D	E	D	D	D
42 – 66.2 m	E	E	D	E	E	D	D	E	E	D	E	D	D	E	D	D
66.2 – 75 m	E	E	E	D	E	E	D	D	E	E	D	D	D	D	E	D
	Ga			Al	Ge						B					As
	Sn			Se	Sb						Pb					
	Tl			Te												
	Bi															
	Rb			Be							Cs			Li		Mg
				Ba												Ca
																Sr
	Ti	Fe			Co			Cr			Sc				Zn	V
											Ni					Mn
											Cu					
	Mo			Ru	Nb						Pd		Y			Zr
					Rh											
					Ag											
					Cd											
	Re			W	Ta						Os					La
				Hg							Ir					Hf
											Pt					
											Au					
											Eu		Sn	Ce		Pr
											Gd		Tb			Nd
											Tm		Dy			
											Yb		Ho			
											Lu		Er			
	U			Th												

oxidising bacteria around the redox fronts led to postulation of a mechanism in which initial pyrite oxidation is incomplete, producing intermediate sulphur species such as polysulphide or colloidal sulphur which could then disproportionate on the reduced side of the front to form secondary pyrite and sulphate, possibly also providing the reductant needed to form the observed pitchblende nodules. This mechanism is supported by both the sulphur isotope analysis of the secondary pyrite and the shape of the pitchblende nodules but, unfortunately, cannot be analysed quantitatively due to lack of appropriate thermodynamic or kinetic data. Needless to say, microbial processes are not considered in any of the models described in 6.3 above.

6.5. Conclusions

Simple scoping calculations can explain the formation of redox fronts in very general terms but greatly simplify the processes known to be occurring at such fronts. Coupled transport/chemistry models can provide a better simulation of some aspects of the fronts but these are really interpretative models which do not display any convincing predictive abilities. They tend to be rather poor, in particular, in simulating trace element chemistry in either solution or solid phases.

Interpretative modelling of microbial activity, natural series profiles and trace element distributions gives strong indications of the reasons for the limitations of the chemical modelling. The role of microbial catalysis seems to be very significant in such systems, particularly affecting the redox chemistry of sulphur. Natural series measurements clearly indicate very slow redox front movement at particular sites and show that the profiles must be considered in at least two dimensions. Finally, the trace element distributions strongly suggest immobilisation of many elements as coprecipitates or solid solutions in major phases such as secondary iron minerals, a process not considered by current models.

It must, therefore, be concluded that the natural redox fronts are much more complex than the simulations were able to replicate, and that some of the simplifications introduced into the latter are not applicable.

In a repository performance assessment context, this study provides some support for the far-field conceptual model of advective flow of oxidants along major fracture zones with slow diffusive solute exchange with the surrounding rock. Pyrite is clearly identified as an important redox buffer. Current models do not, however, explain (much less predict) variations between different redox fronts and the trace element distributions around them. The concentration of a range of safety-relevant elements around very slowly moving redox fronts could be of considerable importance for performance assessment and is worthy of further study.

CHAPTER 7. PARTICLES, COLLOIDS AND RADIONUCLIDE TRANSPORT

7.1. Introduction

As discussed in Chapter 5, the standard radionuclide transport models used in safety assessments are based on the solution chemistry of the radioelements and other components of the rock and groundwater systems, and assume that all mass transport is in the form of dissolved species. The transport behaviour of each radionuclide is thus governed by its solubility, by sorption onto the rock, and by diffusion into dead-end pores in the rock.

Groundwater may, however, transport material in particulate form as well as in solution. Particle sizes can cover a wide spectrum, and they may be composed of eroded portions of the rock or chemical species precipitated from the groundwaters as their geochemical environment changes. In a repository environment, both the wastes and the engineered barriers can contribute an additional source to the natural particles as they are corroded, dissolve, and react with the groundwaters.

The importance of these particles is twofold; firstly they may play an important role in the solution chemistry of the groundwaters. Thermodynamic models, such as those used in performance assessments to predict radionuclide solubilities and speciation, usually only account for the rock mineralogy and soluble species in the groundwater. Since particulate material can be considered as an especially reactive (high surface/volume ratio) additional phase, it can have a substantial effect on these predictions and, if omitted, could give spurious results.

Secondly, radionuclides may be sorbed onto, or precipitate as particulate phases and in this form be advectively or diffusively transported in the groundwaters. The particulate species may be filtered out during transport or be either more or less sorbed onto the "free" radionuclide.

There is very little information on the behaviour of particulate material in deep groundwater systems. The aims of this component of the project were thus:

1. To characterise natural particles from a number of locations and attempt to classify any differences observed in concentrations, size distributions and compositions.

2. To test whether relevant trace elements are associated with particles and, if so, to test whether such associations are reversible, and whether they vary between different particle types.

3. To study the stability of particles, looking for indications of their formation or dissolution along geochemical gradients (e.g. at the redox front).

4. To examine evidence for the mobility of particles in deep groundwaters and, if possible, seek indications of mechanisms which could cause their retardation by sorption or filtration processes.

What are colloids?

Up to this point we have spoken only of *particles* in groundwaters. Much of the interest from the safety assessment viewpoint has been in the potential for transport of particles, rather than in their role in contributing to the solution behaviour of radionuclides. Naturally, this interest is focussed on the smallest sizes of particles, since it appears, intuitively, that these would be the most likely to be mobile over significant distances. These small particles are often loosely referred to in performance assessment circles as *colloids*.

Formally a colloidal system has two components: a continuous dispersing medium and a disperse (colloid) phase. The classical definition of this colloid phase is that it comprises particles (which may be macromolecules) between 1 μm and 1 nm in diameter. Particles smaller than 1 nm cannot exist as a discrete phase, and are thus considered part of the dispersing medium (i.e. are in "true solution").

Solids dispersed in groundwaters, which are of interest here, are, however, irregular in shape, and can be more usefully described as having an upper *hydrodynamic* size limit of 1 μm, which may, in fact, correspond to particle sizes up to 2 μm.

In reality, however, it is more convenient to apply an operational definition which relates to the filtration system and filter mesh sizes used to separate different sizes of particles from groundwaters in the laboratory. A simple particle classification is used in this report, where mobile particles with sizes between 0.45 μm and 1.5 nm are called *colloids*, those larger than 0.45 μm are called '*suspended particles*', and any species with an apparent size less than 1.5 nm is considered to be truly in solution. The generic term *particles* or *particulate material* is used to cover both colloids and suspended particles.

Modelling particle transport

A groundwater system containing mobile particulates contains three distinct phases; the groundwater, the particles and the surrounding rock. A model describing particulate

transport would need to include, as a minimum, a representation of the groundwater flow and a function describing the interaction of colloids with available rock surfaces. If the latter interaction is purely physical, due to filtration effects, the size distribution of the particles would need to be determined. Chemical interaction between particles and the rock would require a more complete description of both phases.

The situation becomes more complicated if different populations of particles coexist, each with their own characteristic chemistry and size distribution. Further, such particles are only metastable and, in general, further representation of their rate of formation and loss (by dissolution or aggregation) would be needed.

In systems of relevance in performance assessment, the main interest is the transport of particular trace elements which may be distributed between all three phases. Such distribution may be fast, concentration-independent and reversible, or it may be considerably more complicated.

To date, no model exists which directly considers all of the processes above for a realistic system. In performance assessment, the role of colloids is usually dismissed qualitatively by arguing that their natural concentrations/rates of production are negligible, that they are immobile or that their interaction with elements of interest consists only of fast, reversible sorption.

The importance of particulate material in the hydrochemical systems of Poços de Caldas

The dynamic hydrochemical system of the Osamu Utsumi mine, where abrupt changes in groundwater chemistry could be caused by the upward flux of reducing waters into an oxidising environment and by the presence of redox and hydrolysis fronts in the rock, was considered to be one in which particulate materials may be expected to play an important geochemical/radiochemical role. Such discontinuities in the geochemical regime parallel those predicted to occur at various locations (in particular the near-field) around a deep radioactive waste repository. This site is especially suited to test the effects of particulate material on the performance of thermodynamic speciation models, given the very considerable amount of supporting data available.

The opportunity to sample a recharge zone, points along a groundwater flow pathline, and a discharge zone was clearly evident at Morro do Ferro. This could be coupled with a well-defined trace element source in the recharge zone to provide a simple example of particulate transport and retardation through the ore body in the unsaturated zone,

down into the saturated zone, and downwards and laterally to the discharge zone in the valley bottom. (Fig. 4.1). Although no suitable quantitative models of particle transport through inhomogeneous dual porosity media exist, this site could be used to provide empirical evidence on the extent to which radionuclides (and other trace elements) associate with, and are transported by, particles.

Particulate material was isolated from groundwaters at both sites, and from shallow waters percolating through the unsaturated zone at Morro do Ferro, using a sequential ultrafiltration technique. This is described, along with the sampling and analytical techniques used, and all the data gathered, by Miekeley *et al.*; this report series; Rep. 9. In this summary, only selected data and their interpretation are reported.

7.2. Particulate material at the Osamu Utsumi mine

7.2.1. Suspended particles

Suspended particles (>0.45μm) fall into two distinct groups depending on the depths of the water samples. Near-surface waters (with a particle load of around 0.8 mg/L) contain predominantly clay minerals (illite, gibbsite and kaolinite) and microcline, while the 'cleaner' deep waters (with a particle load of between 0.05 and 0.5 mg/L) contain predominantly amorphous iron oxyhydroxides. Some of the particles have significant surface coatings of organic carbon, probably as humic compounds, and they contain significant quantities of uranium and thorium (in the general range of 100–1000 μg/g of colloid).

The $^{234}U/^{238}U$ ratios of these particles are similar to the groundwaters, being in the range of 1–2.6, indicating preferential leaching of ^{234}U into these waters and equilibrium between the waters and the particles. The $^{230}Th/^{234}U$ ratios in the particles are, however, very much higher (0.1–0.9) than those in the waters (0.002–0.09), indicating either that thorium is selectively taken up from the groundwater by the particles or that uranium has been lost from the source particulate.

The association ratios of elements in deep groundwaters (concentrations in suspended particles / concentrations in groundwaters; in mL/g) range from 10,000 to 100,000 for uranium, through 100,000 to 1 million for the rare-earth elements, to between one and ten million for thorium. The corresponding association ratios for shallow, low-pH, oxidising waters are one to two orders of magnitude lower than the deeper samples.

In the deep waters, more than 98% of the uranium is present in the <0.45μm fractions (i.e. in colloidal form or in solution). The <2% in suspended particles is primarily associated with amorphous iron oxyhydroxides, which are assumed to precipitate as reducing groundwaters pass upwards into a more oxidising region. The rare-earth elements behave in a very similar manner to uranium, being mainly concentrated in the colloid/solution phases. Thorium, on the other hand, is significantly concentrated in the suspended particles.

7.2.2. Colloidal material

The colloidal fraction in the groundwaters was separated into three size ranges (0.45μm–100,000 dalton; 100,000–10,000 dalton and 10,000–1000 dalton) by sequential filtration. Material passing through a 1000 dalton (1.5 nm) filter was taken to be in true solution. Operationally, this fixed the 'colloid' size range between 0.45μm and 1.5 nm. The colloid concentration in the waters was low and trace element concentrations in colloids and in solution were similar, and frequently at or below detection limits. The low concentrations of colloids (typically <500 μg/kg) is surprising, given the intense nature of the weathering and the dynamic hydrochemical system. (Nordstrom *et al.*, this report series; Rep. 6).

The main components of the colloid fraction are ferric oxyhydroxides and organic carbon. As with the suspended particles, these are thought to be ferrihydrite particles coated with humic materials. High resolution ESCA confirms the presence of oxidised carbon (C-O and O=C-O) typical of humics. Very high, but seasonally variable, concentrations of colloidal iron in near-surface waters are inferred from their colour. These cannot be separated into size fractions owing to their instability during filtration, but are predominantly colloidal rather than >0.45μm. These observations are supported by the thermodynamic modelling of the waters presented by Nordstrom *et al.* (this report series; Rep. 14) using in-situ determinations of ferric iron, which indicate ferrihydrite supersaturation. The silicate mineral component of the colloids is very small indeed.

About 3–10% of what is normally described as dissolved organic carbon (DOC) is present in the colloid fraction, normally in the 1K–10K dalton range (Fig. 7.1). The majority of the DOC is, however, truly in the solution phase, and may be low molecular weight fulvic acids or other organic species.

Between 5–30% of the uranium present in the colloid/solution phases is in the 1K–10K dalton fraction, clearly being associated with the colloidal iron and carbon. The $^{234}U/^{238}U$

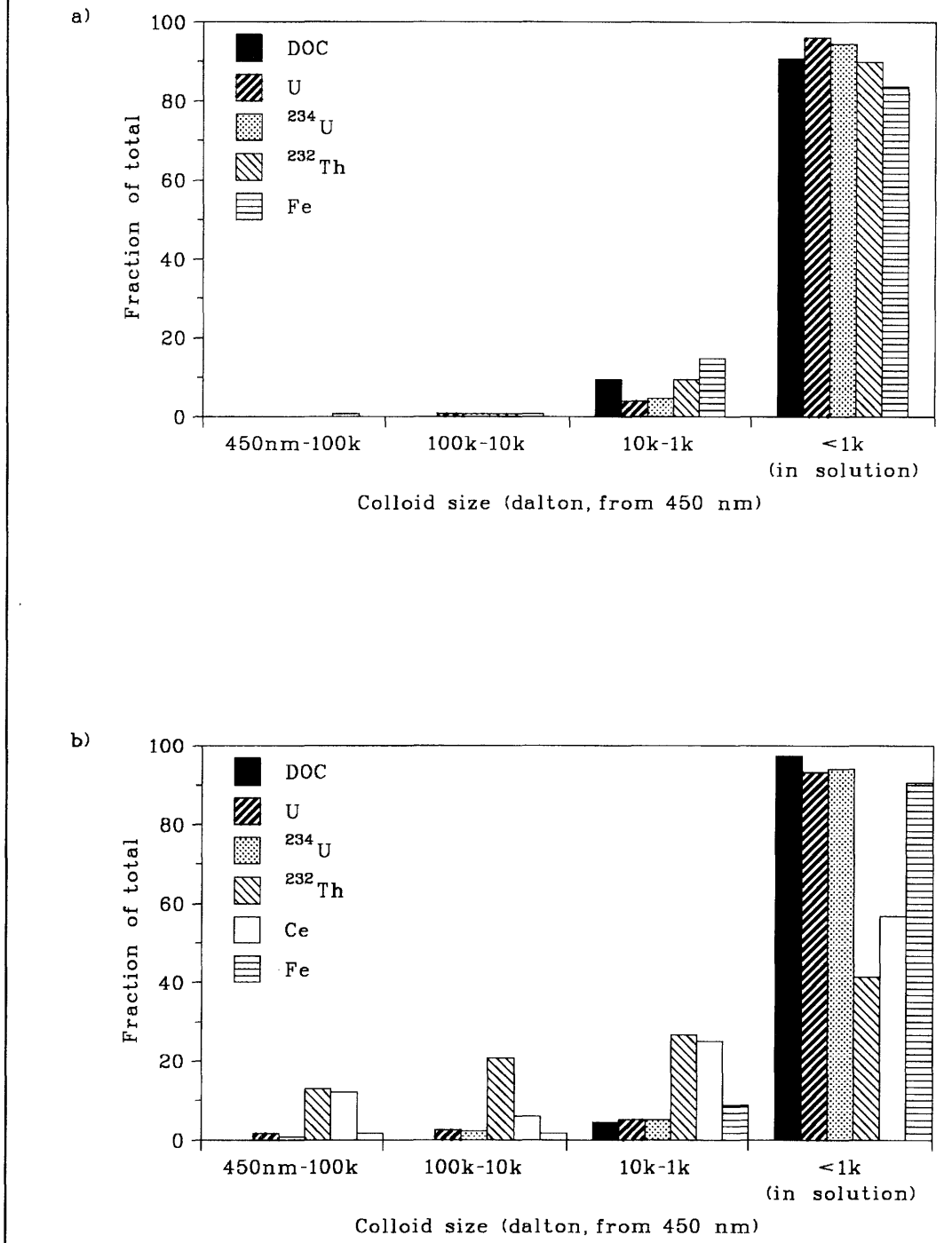

Figure 7.1. Distribution of organic carbon, iron and trace elements on colloids separated into various size ranges: a) colloids in shallow groundwaters from the Osamu Utsumi mine, and b) colloids in deep groundwaters from the Osamu Utsumi mine (from Miekeley et al., this report series; Rep. 9).

activity ratios of colloids and solution are very similar (as with the larger, suspended particles), indicating exchange equilibrium between phases. Most of the uranium is, however, clearly in true solution.

As with the suspended particles, thorium is preferentially partitioned into the colloids rather than into solution (>70% of the Th in the <0.45μm fractions being in the colloids), but is more evenly distributed across the size ranges than is uranium. There is no clear correlation of the thorium with organic carbon, so complexation with humics cannot be inferred as the principle thorium speciation mode. The high content of colloidal iron in these waters suggests that thorium and most of the other polyvalent trace elements (REEs, Ti, U, Mn, Zn, Cu, Pb, etc) are incorporated in these hydrous ferric oxides, which argues with the conclusions of the trace element modelling presented in Chapter 5. In the shallow waters the proportion of colloidal thorium is low, at around 10%, which may indicate the suppression of hydrolysis and sorption by the very high sulphate contents and low pH.

7.3. Particulate material in the Morro do Ferro groundwaters

The waters sampled at Morro do Ferro come from the unsaturated zone (waters percolating into the adit), just below the water table (borehole MF11), or deeper into the groundwater system and progressively further down gradient (boreholes MF10 and 13) to the upwelling zone (borehole MF12) below the discharge region.

7.3.1. Suspended particles

The suspended particles in these waters display very similar characteristics to those from the Osamu Utsumi mine, being chiefly amorphous materials in the deeper holes and clays in the shallow waters. Their concentrations are about an order of magnitude greater than in the mine waters, being normally between 0.1–3.1 mg/L. The uranium and thorium distributions follow similar patterns, although the association ratio for thorium in MF12 is lower by two orders of magnitude than in any of the other samples. This may be due to higher fluoride concentrations in this water, but the cause has not been definitively established.

One of the main objectives of the work at Morro do Ferro was to determine whether particles could be transported down gradient through the weathered rock system. In the

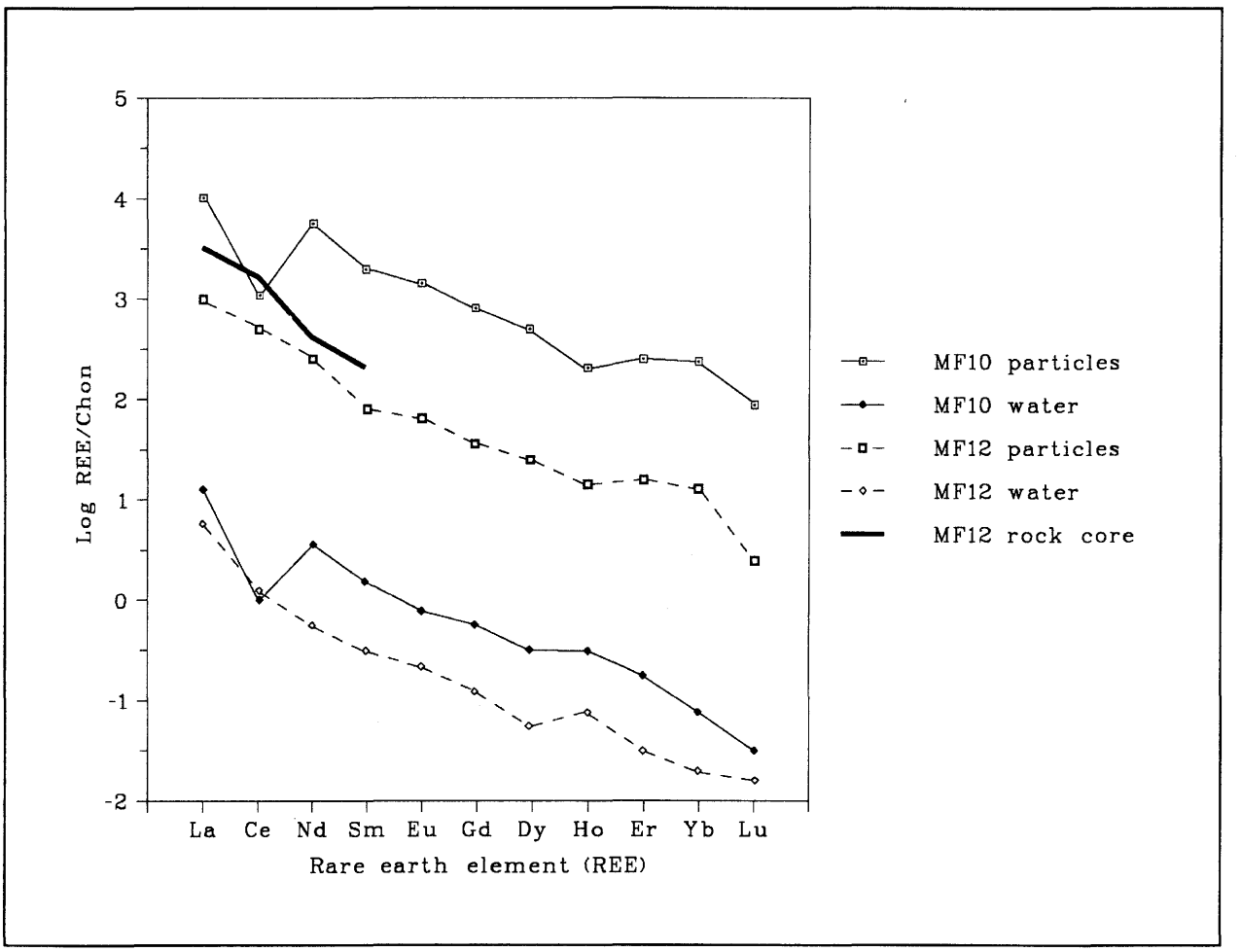

Figure 7.2. Chondrite-normalised REE patterns in typical rocks, groundwaters and corresponding suspended particles from Morro do Ferro.

mineralised zone (immediately above borehole MF11) the suspended particles (mainly clay minerals and gibbsite) have high thorium and REE contents (1000–4000 μg/g), whereas those from MF12 at the bottom of the hill are composed mainly of ferric oxyhydroxides with much lower concentrations (20–300 μg/g). These differences in the particles suggest that there has been little or no transport of the >0.45μm particles.

This conclusion is supported by the REE patterns of the suspended particles, which show a negative cerium anomaly in the chondrite-normalised plots of both particles and waters from the unsaturated zone, which is not seen in deeper waters and suspended particles or in the rocks themselves (Fig. 7.2). The similarity of the latter distributions suggests that the REE contents of the particles arise from congruent leaching of the rocks and sorption of the released REEs. The cerium depletion in the oxidising unsaturated zone samples may, perhaps, be explained by the extremely low solubility of $Ce(OH)_4$ compared to trivalent REEs. Whatever the cause, the cerium anomaly is not observed in material further down gradient, which indicates either (i) lack of transport of suspended particles if the sorption of REEs onto particles is irreversible or desorption is very slow, or (ii) rapid equilibrium between trace elements in solution and those sorbed on suspended particles.

The $^{234}U/^{238}U$ activity ratios of both the waters and suspended particles from Morro do Ferro are in a different range to those of the rocks (1.5–2.1 compared to 0.9–1.2), indicating that the suspended particles are not artefacts of the drilling process and indicating possible equilibrium between these particles and the groundwater.

7.3.2. Colloidal material

The colloidal material from Morro do Ferro groundwaters is also very similar in character to that from the Osamu Utsumi mine groundwaters, with a generally low colloid concentration (<1 μg/g), most of the organic carbon in solution, and 10–20% of the iron present in colloidal form. There is also an indication of exchange equilibrium of uranium between solution and colloids (although the activity ratio data are at the limits of reliability) and of a tendency to be associated with colloids increasing from U through the REEs to Th, as observed in the larger particles. Colloidal clay particles are found in the shallower waters.

Organic carbon is concentrated in the shallow percolating waters, where a large percentage is present as colloidal material and, indeed, dominates the total colloid content (Fig. 7.3). The size range of the colloidal organic carbon (COC) is typical of

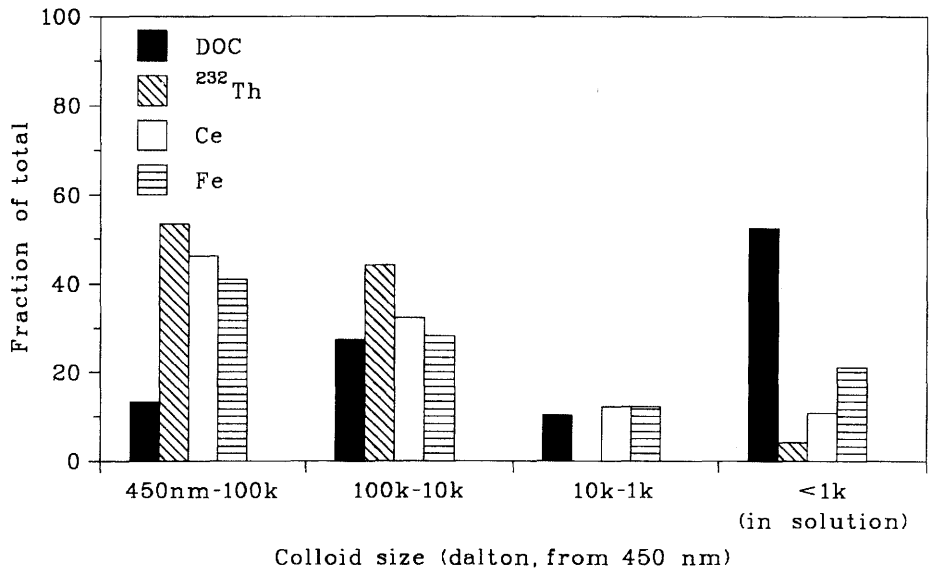

Figure 7.3. Colloids from organic-rich seeps into an adit in the unsaturated zone, Morro do Ferro (from Miekeley et al., this report series; Rep. 9).

humic acids. These colloids contain very high fractions of the total major and trace element contents of the waters, for example 97% of the Th, 80–90% of the REEs, and 80% of the iron. A systematic decrease of the colloidal fraction of an element with decreasing valency agrees with the concept of humic complexes with metals of higher ionic potential being more stable. The humics present are considered to be pedogenic, and are again associated with iron oxyhydroxides. It is interesting to note that the COC component of the total organic carbon load appears more effective in complexing metals than the true DOC component.

As with the suspended particles, the COC content of the deeper waters appears quite distinct from that in the shallow waters (Fig. 7.4). In MF10 and MF12 the COC content is very low, indicating very little colloid transport. Despite the strong association of trace elements with COC, this explains why the ore body leaves no 'signature' in groundwaters.

ESCA studies of the COC from deep groundwaters show it to be humic in nature, with about 8–12% carboxylic groups, 10% as C-O-groups, and about 80% as aromatic or aliphatic 'neutral' carbon. SEM colloid counts and size distributions from MF12 show a regular increase in population with decrease in colloid size, down to the measurement limit of about 40 nm. This may well continue to sizes below 10 nm. The actual colloid contents measured by this technique are about $2x10^{11}$ particles/litre from 10–440 nm. Chemical methods give a content of 265 μg/L in this range, comprising 50 μg/L of iron colloids, 5μg/L of clays, and about 210 μg/L of organic carbon.

A similar assessment of rare-earth element patterns in colloids to that described for suspended particles shows the same result; no cerium anomaly is observed in either the MF12 waters or the drainage stream waters. In addition, colloidal clays found in the unsaturated zone waters below the ore body are practically absent from deeper waters. Thus there is no evidence of significant colloid size particle transport down gradient.

7.4. Conclusions

Low concentrations (<1 mg/L) of colloids (450–1.5 nm), composed mainly of ferric oxyhydroxides and humic species, have been found in deeper waters at both sites. They concentrate minor amounts of uranium, but significant fractions of thorium and the REEs. The uranium in solution and in colloidal form is in isotopic exchange equilibrium.

Colloidal organic carbon is most common in near-surface waters, where it complexes strongly with polyvalent metals, especially thorium and the REEs.

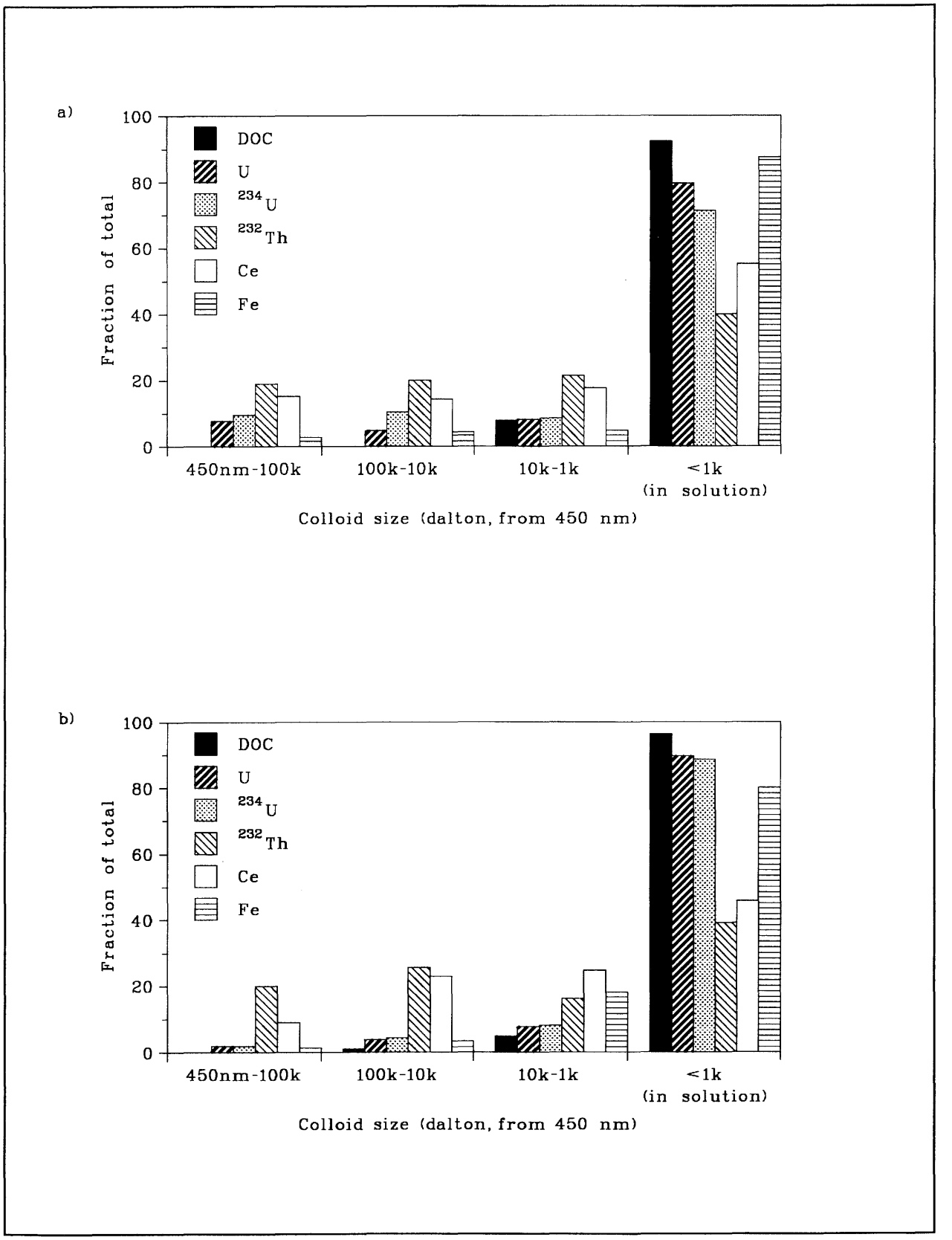

Figure 7.4. Colloids from a) deep, up-gradient (MF10) groundwaters and b) deep, down-gradient (MF12) groundwaters at Morro do Ferro (from Miekeley et al., this report series; Rep. 9).

Suspended particles (>450 nm) have uranium, thorium and REE concentrations orders of magnitude higher than the associated colloid/true solution fractions. However, the amount of these particles in the waters is very low, meaning that the bulk of uranium is in true solution. These larger particles would be the main carriers of thorium and the REEs if they were mobile. However, in practice, they seem to play no role in thorium and REE transport since both these particles and the smaller, colloidal particles are demonstrably immobile. There is no evidence for them having a radionuclide transport role. By providing additional reactive surfaces, these particles do, however, affect the solution chemistry and participate in a largely irreversible fashion in fixing trace elements after they have been released by weathering of the original host rock.

7.5. Implications for performance assessment

The results of this study suggest that radionuclide and other trace element transport by particulate material in deep groundwaters does not play a significant role in the geochemical processes of weathering, dissolution and erosion of these ore deposits. The reason for this must be assumed to be filtration of particulate material which, even in the highly porous and fractured rocks of the Poços de Caldas plateau, seems to be a highly efficient process. This suggests that 'colloid transport' would be of little relevance in performance assessment migration modelling of similar geological environments.

The importance of particulate material in controlling the concentrations of trace elements in solution has been discussed here, and in Chapter 5. They appear to act as efficient and largely irreversible sinks for many elements (especially as they are immobile), but need to be taken into account in equilibrium thermodynamic modelling of radionuclide speciation in any part of the disposal system.

In terms of both migration and geochemical 'intervention', particulate material seems to play a positive role in reducing the ability of radionuclides to migrate, rather than the 'migration-enhancing' role that has been suggested in some repository performance assessments.

CHAPTER 8. HYDROTHERMAL ALTERATION, METASOMATISM AND MINERALISATION MODELLING

Depending on the design of a high-level waste repository (thermal output of waste package, package emplacement, rock thermal conductivity, etc.), quite high temperatures may be attained in the near-field and sustained for hundreds or thousands of years. This may have the effect of promoting the circulation of warm (hydrothermal) fluids which, in certain scenarios, could be responsible for transporting radionuclides subsequent to an early container failure. Furthermore, enhanced rock alteration caused by the passage of hydrothermal fluids may affect radionuclide/rock interactions and resultant retardation of releases occurring long after the thermal period has passed.

Information on the volumes of fluid that can circulate during such hydrothermal periods, together with the scale and nature of the geochemical alteration and solute transport processes involved, is thus of interest in performance assessment. Natural hydrothermal systems which have been active over geologically short times lend themselves to this type of study, and the fourth analogue objective at Poços de Caldas concerned itself with this topic.

The chemical, isotopic, and mineralogical alterations which occurred during primary uranium ore deposition hosted by the breccia pipes at the Osamu Utsumi mine were studied and modelled and are reported in detail in Cathles and Shea (this report series; Rep. 13). The modelling was carried out by combining chemical and isotopic alteration models with finite difference models for the convective cooling of an idealised pipe and intrusive coupled system.

Both the hydrothermal alteration and primary mineralisation are related to the volume of hydrothermal fluid circulation. Modelling that can estimate the amount of fluid flow produced by such intrusive systems can, therefore, help to define the nature of primary mineralisation and alteration associated with them. The Poços de Caldas observations indicate how rock may be altered over relatively protracted periods of time (a few to tens of thousands of years) by high-temperature fluid circulation, and how that alteration is related to radionuclide (e.g. uranium) transport.

The models developed allow these observations to be applied to rock alteration in the near-field of radioactive waste repositories. The amount of hydrothermal circulation that could be driven by the heat from radioactive decay in the hypothetical repository was estimated using the same physical model employed to analyse the hydrothermal system

at Poços de Caldas. Assuming similar rock types and chemistry also allowed the application of the chemical transport models calibrated at Poços de Caldas to predict the near-field alteration and uranium transport during a 10,000 a period in the hypothetical repository.

8.1. General description of the natural system

8.1.1. Physical properties

The F4 drillcore at the Osamu Utsumi mine is located in a relatively permeable breccia pipe of approximately 0.5 km diameter that lies adjacent to a small nepheline syenite intrusive, which is an extension of a larger intrusion at depth. Taking into consideration the current studies of the geology and palaeomorphology of the caldera (Holmes *et al.* and Waber *et al.*, this report series; Reps. 2 and 5) and the ensuing erosion, it was assumed that the material studied came from a maximum burial depth of about 1.5 km.

Measurements in a number of boreholes in the mine area indicate that permeability typically decreases from approximately 10^{-4} ms^{-1} to about 10^{-7} to 10^{-6} ms^{-1} at depths of a few tens of metres. Groundwater modelling shows that the present pattern of groundwater movement is compatible with a "deep" permeability of 10^{-8} ms^{-1} (1 millidarcy).

It is sobering to realise how little of the system has been sampled from outcrop, mine workings and drilling (the "observation band"). Very little of the system that produced the primary mineralisation has, in fact, been sampled.

8.1.2. Geochemistry

The hydrothermal event caused marked elemental and isotopic changes in the rocks. The varied chemical data in the "observation band", especially when combined with the current physical and chemical modelling, strongly constrain the nature of the mineralising system.

The passage of hydrothermal fluids through the breccia pipe deposited approximately 40 μg/g of uranium, with local concentrations up to about 200 μg/g (see Waber *et al.*, this report series; Rep. 2). The most striking primary alteration was the nearly complete stripping of sodium and the concomitant, uncommonly high enrichment of potassium in

the hydrothermally altered nepheline syenites. Mass balance calculations indicated that titanium could be considered immobile during alteration and relatively uniform in concentration in the unaltered nepheline syenite. Assuming titanium immobility, approximately 70 g of unaltered predecessor corresponds to 100 g of altered product, with approximately 30 g introduced by hydrothermal solution. Elements added relative to titanium include Si, Al, Fe, H_2O, and Ca. Sodium concentrations dropped very rapidly with increasing alteration.

Furthermore, the hydrothermal fluids lowered the $\delta^{18}O$ of the rock a few permill and elevated the δD of the rock to approximately 30‰. The δD values appear to be in agreement with the equilibrium isotopic fractionation of nepheline syenite with meteoric water at moderate temperature (around 200°C). There is no indication of a similar equilibration in the $\delta^{18}O$ values.

8.1.3. Petrology

Alteration can also be viewed in mineralogical terms, and the chemical implications of the petrology must be consistent with changes inferred from chemical analysis.

Alteration in the Poços de Caldas breccia can be simply considered as the conversion of primary nepheline, sanidine and aegerine-augite to secondary kaolinite, illite and microcline (Schorscher and Shea, and Waber *et al.*, this report series; Reps. 1 and 2), with the inclusion of minor amounts of chlorite, pyrite, fluorite and hematite. Using both measured (product) and estimated (primary) mineral compositions, chemical changes required by the observed mineralogical changes were calculated. The petrographic observations are compatible with the observed chemical changes provided that the rock mass increased during hydrothermal alteration as noted above.

8.2. Hydrothermal modelling results

Available geological, geotechnical and geochemical information was used to develop a reasonably realistic base physical model for further simulation.

The intrusive body was modelled (Fig. 8.1) with a width of approximately 3 km from a depth of 5 to 3 km, and then tapering to 0 km at 1 km depth. Permeability at temperatures <300°C was taken to be 10^{-8} ms^{-1} (1 millidarcy) and was reduced

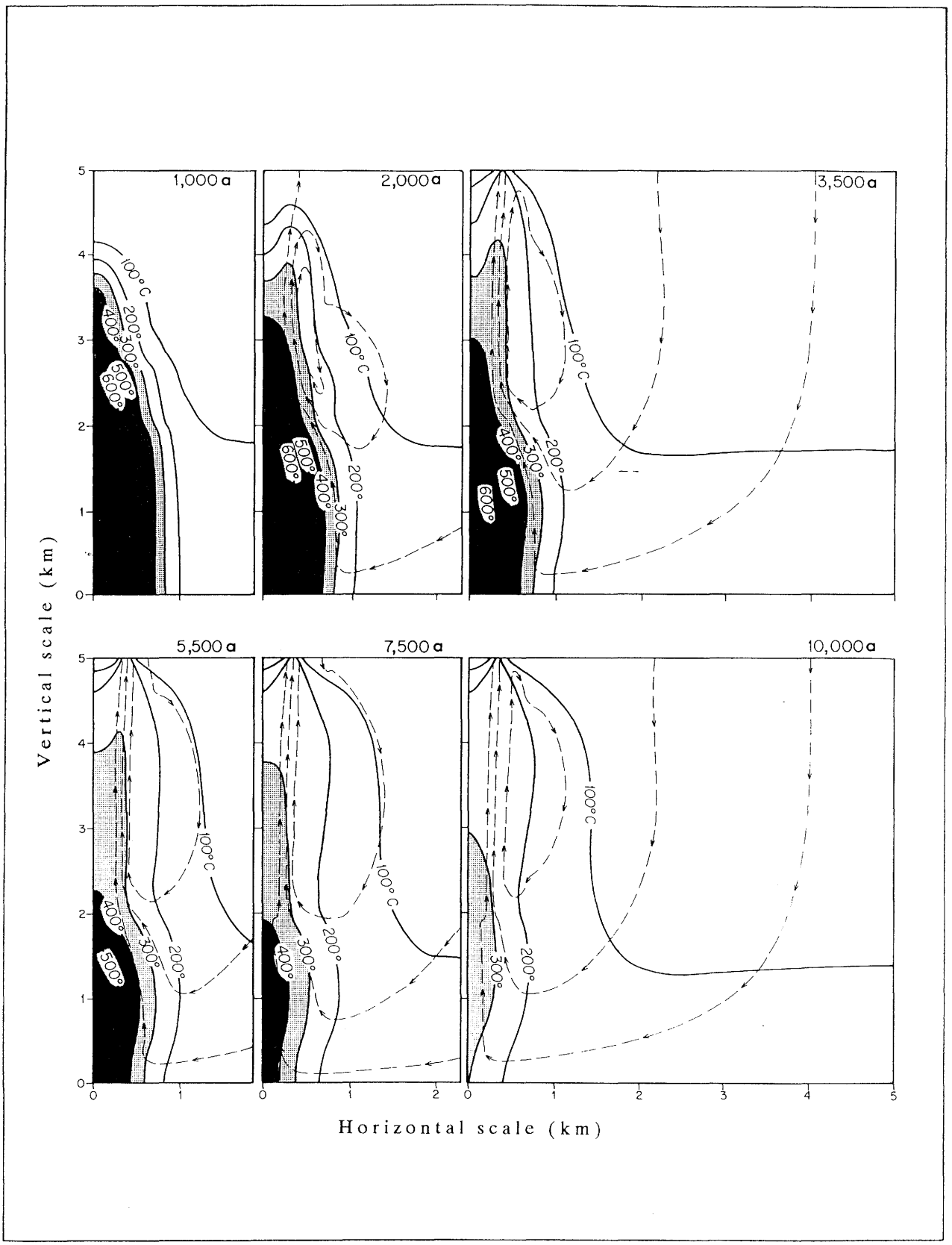

Figure 8.1. Cross-sections from 1000 to 10,000 a after intrusion showing the progressive cooling of the intrusion by groundwater convection. Temperatures around the initially 700°C intrusion are indicated by solid contours. Streamlines indicating the direction of fluid are shown with dashed lines and arrows. The general permeability is 1 millidarcy, except for the breccia pipe which has a permeability of 5 millidarcies and the intrusion whose permeability decreases exponentially with temperature for temperatures greater than 300°C.

exponentially at temperatures >300°C (Cathles, 1983). Its initial temperature was assumed to be 700°C.

The breccia body had a constant width of 0.5 km down to a depth of 3km. Its permeability was $5x10^{-8}$ ms^{-1} (5 millidarcies). Permeability in the host rock was set at $10^{-8} ms^{-1}$ (1 millidarcy).

The intrusion was modelled to cool for 1,000 a without any fluid convection in order to smooth the intrusive outline and increase computational stability. This also simulates deuteric alteration.

Free flow was allowed through the top surface; no flow was allowed to cross the vertical planes 5 km from the axis of the intrusive and the basal boundary at 5 km depth. Hydrostatic pressure was sufficient to prevent boiling in the convective calculations, and a normal hydrostatic pressure gradient was assumed to be maintained by the fluid throughout the system.

The coupled fluid convection and temperature equations were solved by a Douglas-Rachford alternating direction implicit finite difference scheme, updated from Cathles (1977).

8.2.1. Fluid circulation

The amount of fluid circulation through the breccia pipe depends mainly on the size and geometry of the intrusive driving the circulation, as well as the contrast in permeability between the breccia pipe and the surrounding host rock.

About 2,000 a of convection (3,000 a total elapsed time since intrusive emplacement) is required for the entire breccia pipe to heat up and for high-temperature fluids to reach the surface. Flow is strongly concentrated in the breccia pipe, and active convection occurs from 1,000 to 20,000 a. By 20,000 a, however, the intrusive is largely depleted of heat and the lower 2/3 of the breccia pipe has substantially cooled. By the time the intrusive has cooled, up to 2,000 kg/cm^2 of hydrothermal solution has passed through the high flow portions the pipe. (Fig. 8.2)

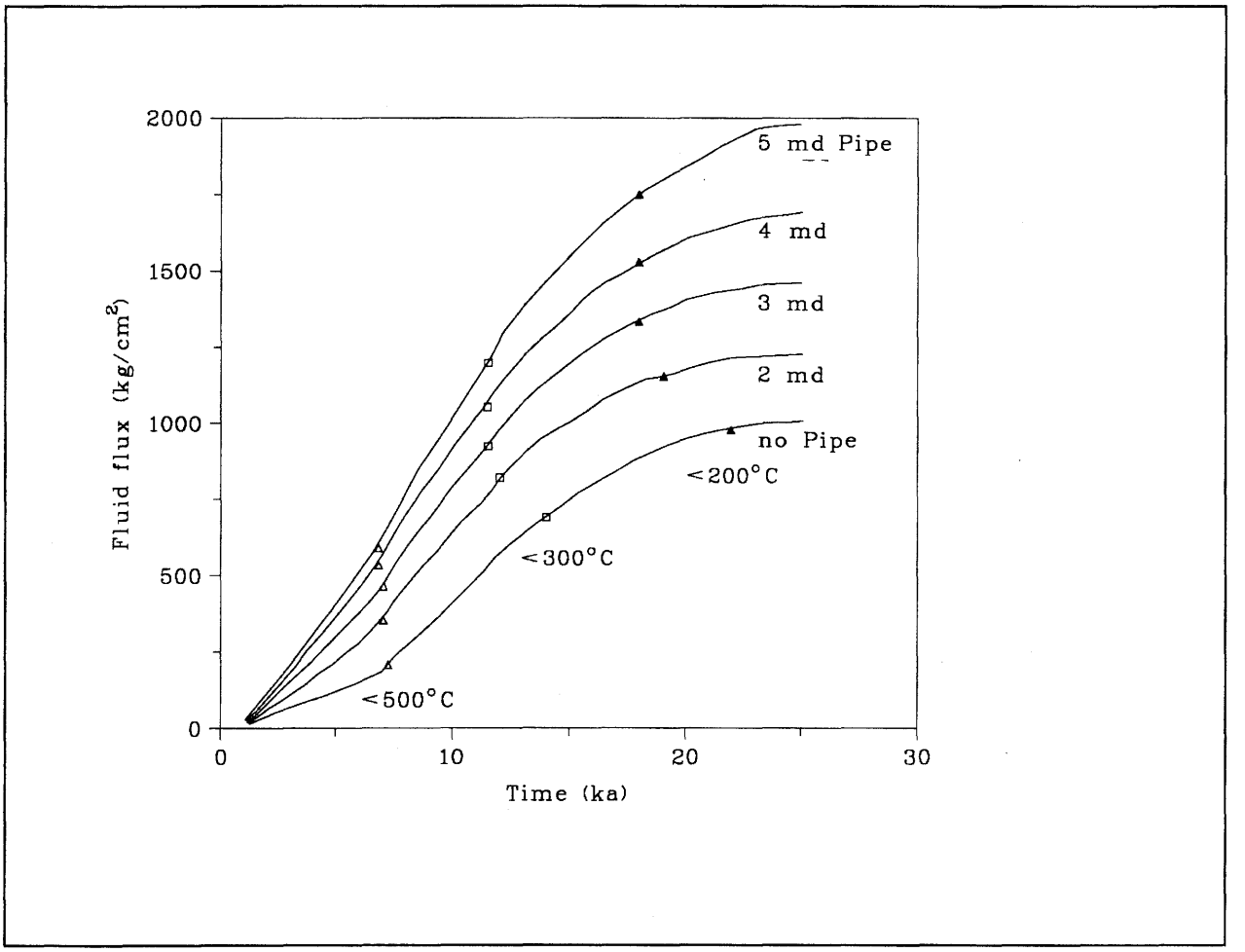

Figure 8.2. The maximum integrated fluid at any point in the breccia pipe as a function of time. Convection starts after 1000 a of conductive cooling. Points at which the maximum temperature of the intrusion falls below 500°, 300°, and 200°C are indicated on each curve.

8.2.2. Uranium transport

An obvious question to ask is whether the amount of hydrothermal circulation identified in the above base model is in reasonable agreement with the observed primary uranium concentration of approximately 40 μg/g at the Osamu Utsumi mine.

Estimates of the solubility of uranium in natural, near-neutral hydrothermal solutions differ by many orders of magnitude. Two representative sources were compared using the Poços de Caldas physical base model. The EQ3 database and experiments by Lemoine (Kertes and Guillaumont, 1985) suggest the solubility of uranium is 8.4 to 21×10^{-5} molal at 300°C, and strongly temperature-dependent. The most recently published experimental study (Parks and Pohl, 1988) found the solubility of uranium to be 3.3×10^{-10} molal, and both temperature-and pH-independent (near-neutral pH). Since there is general agreement that the main complex of uranium in natural waters is $U(OH)_4$, the difference apparently resides entirely in the dissolution log K of uranium minerals.

The use of the first solubility values can readily account for the observed uranium concentrations being supplied by between approximately 120 and 300 kg/cm^2 of hydrothermal solution if all uranium is assumed to be precipitated from a solution saturated at 300°C. This is less than the >1,000 kg/cm^2 of >300°C hydrothermal fluid suggested to have passed through the breccia pipe by the base model.

The second solubility value requires approximately 7.5×10^7 kg/cm^2 of hydrothermal fluid to pass through the pipe, which is almost 5 orders of magnitude more than that indicated by the base model. This is not considered geologically plausible.

8.2.3. Silica transport

Assuming a silica solubility of 3×10^{-3} molal, which is reasonable for nepheline syenite at 300°C, the 420 moles/cm^2 of silica addition observed in the Poços de Caldas breccia pipe would require about 140,000 kg of hydrothermal throughput per cm^2 cross-sectional area of the breccia pipe. This is around two orders of magnitude greater than indicated in the base model calculations.

8.2.4. Potassium, aluminium and sodium transport

Thermodynamic values for the specific mineral chemistries observed at Poços de Caldas were derived and refined from stoichiometrically pure mineral phase values by requiring the calculated solution composition, in equilibrium with the hypothetical buffer mineral assemblage, to be similar to natural rock buffered solutions observed in silica-saturated hydrothermal systems. Estimates were then made of the amount of fluid flux needed to pass through the breccia pipe in order to produce the observed metasomatic changes.

Two mineralogical issues required to be addressed in order to carry out these calculations. First, the non-end-member stoichiometry of some mineral phases was accommodated by combining the dissolution log K (or solubility product) data from their end-member minerals. Second, the extreme instability of aegerine-augite in the presence of hydrothermal water was dealt with by considering the outer layers of aegerine-augite to have immediately altered to a stoichiometric equivalent of riebeckite, and assuming that this effectively decreased the dissolution log K from 9.6 to -2.1, as used in the model calculations. Other thermodynamic parameters were adjusted slightly such that the log activity ratios of the principal dissolved elements were similar to the ratios encountered in hydrothermal systems in silica-saturated rocks.

With the above considerations and adjustments, the metasomatic alteration observed at the Poços de Caldas breccia, including the stripping of Na and addition of Si, Al, and K in a down-temperature flow regime, can be replicated by the model buffer mineral assemblage and changes in pore water composition brought about by the passage of approximately 10^5 kg/cm^2 of hydrothermal solution as temperature falls from 300°C to 200°C in the breccia pipe.

These chemical changes suggest that the observed alteration requires fluid fluxes considerably greater than indicated by the base model. However, the increased flux is not unreasonably large and can be easily produced by an intrusive body slightly larger (greater diameter) than assumed in the base case and extending to approximately 10 km (rather than 5 km) depth.

8.2.5. Oxygen and hydrogen isotopic transport

Oxygen isotopic alteration in natural rock/water systems is principally controlled by the temperature of hydrothermal interaction, whereas hydrogen isotopic alteration is

controlled by the δD of the meteoric water influx to the system and is relatively independent of temperature. Consequently, oxygen and hydrogen isotopic transport within the natural hydrothermal system can be predicted by superimposing alteration of the fluid upon the temperature evolution of the base model.

An isotopically light alteration prong related to the circulation of water up a steep thermal gradient and originating at the deep margin of the intrusive heat source is modelled to enter the breccia pipe by 10,000 a after intrusion. At the estimated level of the Osamu Utsumi mine, the modelled oxygen isotopic shift is small. Since only a slight negative oxygen isotopic shift is observed in the Poços de Caldas breccia pipe, the base model is compatible with the observed data.

The change in hydrogen isotopic values in the breccia pipe is much more rapid than that for oxygen. The meteoric hydrogen isotopic alteration front is estimated to sweep through the convective system almost 30 times faster than the meteoric oxygen isotopic front moving through the system in the first 5,500 a. Given a hydrogen fractionation of approximately -30‰ for the hydrothermal rock/water system at the Osamu Utsumi mine level, and an initial meteoric δD signature of approximately -20‰ , the observed rock should have a δD value of -50‰. The observed trend in variably altered samples from approximately -90 to -45‰ is predicted by the modelling. This is underscored by the excellent correlation between δD and K_2O, variations in which are directly attributable to the passage of hydrothermal fluid.

8.2.6. Petrological changes

The metasomatic fluxes to the rock can be combined with the stoichiometry of the model mineral buffer assemblage to determine the petrological changes that correspond to these fluxes. The petrological changes in the Poços de Caldas breccia pipe that were calculated in this fashion are generally similar to those observed.

In particular, the observed 60 wt.% destruction of high sanidine, 10 wt.% destruction of aegerine-augite and 60 and 23 wt.% deposition of maximum microcline and illite respectively, are well simulated for solutions with salinities around 10,000 μg/g Cl (aqueous solutions modelled with Ce^- salinities only). The precipitation of minor phases such as fluorite is also compatible with observations. However, the calculated destruction of kaolinite and precipitation of nepheline are the opposite to that observed.

8.3. Experimental verification

Some preliminary experiments were carried out to test the general validity of the calculated chemical model. These experiments involved the use of unaltered Poços de Caldas nepheline syenite in a flow-through temperature gradient apparatus. The sample was placed in a stainless steel tube that was pressurised to 238 bars to suppress boiling, centrally heated to 350°C to develop both increasing and decreasing thermal gradients relative to the flow direction, and water passed though at 5 microlitres/minute for 200 hours.

The altered nepheline syenite was examined by SEM/EDX. Bulk sample chips were almost completely depleted in Na, being comprised almost entirely of Al and Si on both sides of the thermal gradients. Sanidine was altered on the decreasing thermal gradient side and unaltered on the increasing thermal gradient side, indicating dissolution and replacement by maximum microcline by solutions flowing "down" a thermal gradient. Aegerine-augite, on the other hand, was altered on the increasing temperature gradient side and unaltered on the decreasing temperature gradient side, which appears to reflect alteration to a riebeckite-type phase.

These preliminary column experiment results appear to agree with many of the mineral alteration/precipitation observations at Poços de Caldas, and support the chemical model in most respects.

8.4. Hypothetical repository modelling results

The near-field hydrothermal circulation around a hypothetical nuclear waste repository, using parameters from a proposed U.S. repository, was modelled applying the methodology developed for the Poços de Caldas natural analogue. (Fig. 8.3)

If the bulk permeability is low (0.01 millidarcy), the repository heats up to a maximum temperature of 327°C after 2,500 a of burial, and then cools as the radiogenic heat output decreases. If the permeability is higher (10 millidarcies), more convection occurs through the repository and a maximum temperature of 245°C is reached 900 a after waste emplacement.

Regardless of the permeability chosen, the model repository circulated at most about 100 kg/cm^2 of hydrothermal solution that had interacted with rock hotter than 200°C (Fig. 8.4). Most of the convection in the 10 millidarcies case occurred after the repository

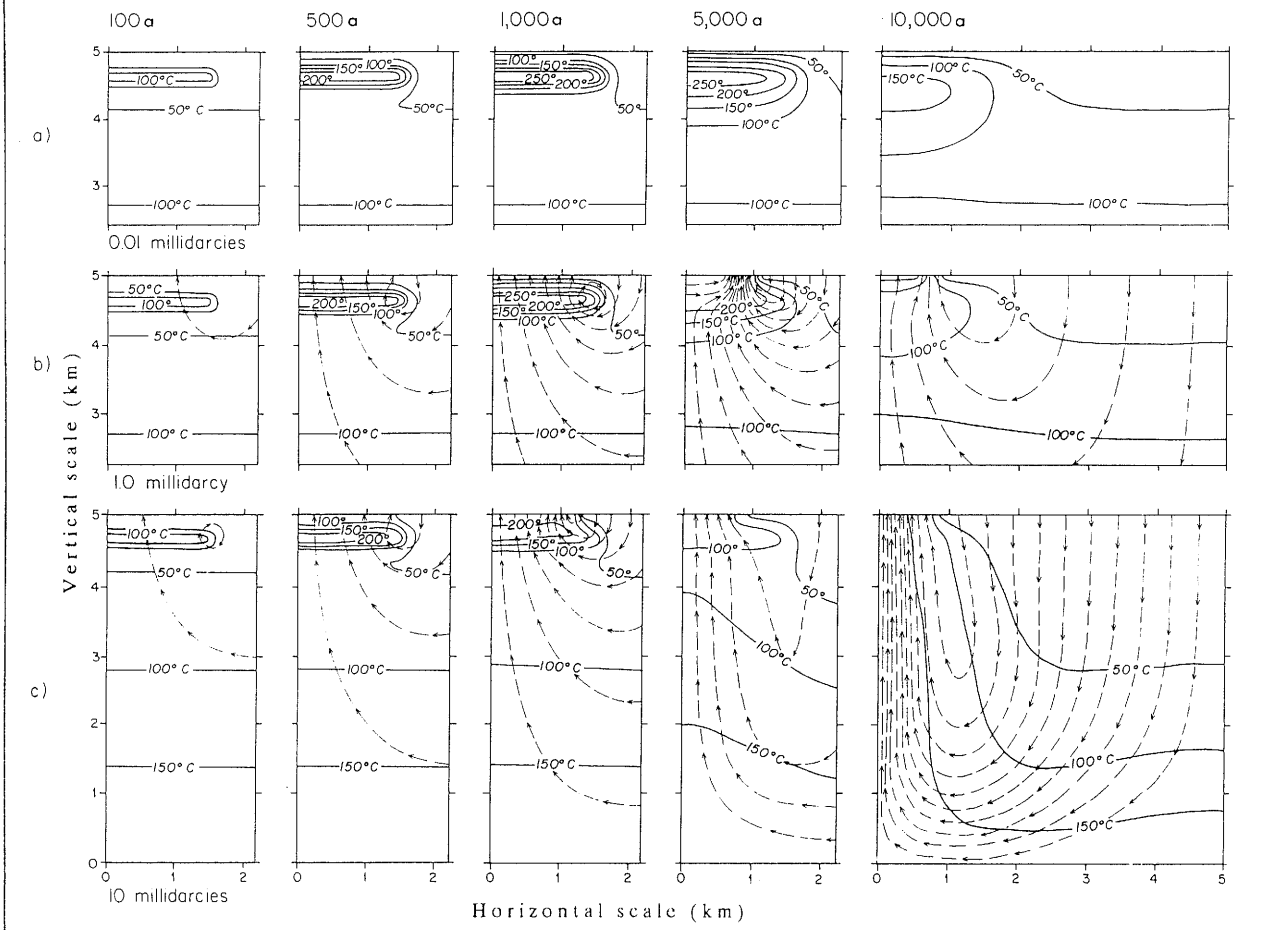

Figure 8.3. Calculated temperature and fluid convection around the 70,000 tonne U high-level nuclear waste repository. (a) Host rock is very low permeability (10^{-2} millidarcies); repository reaches temperatures limited only by conduction. (b) Host rock has permeability of 1 millidarcy, similar to the environment at Poços de Caldas; convection is induced to at least 5 km depth and temperature of repository is reduced. (c) Host rock has permeability of 10 millidarcies; extent of convection and rate of cooling of the repository are greater.

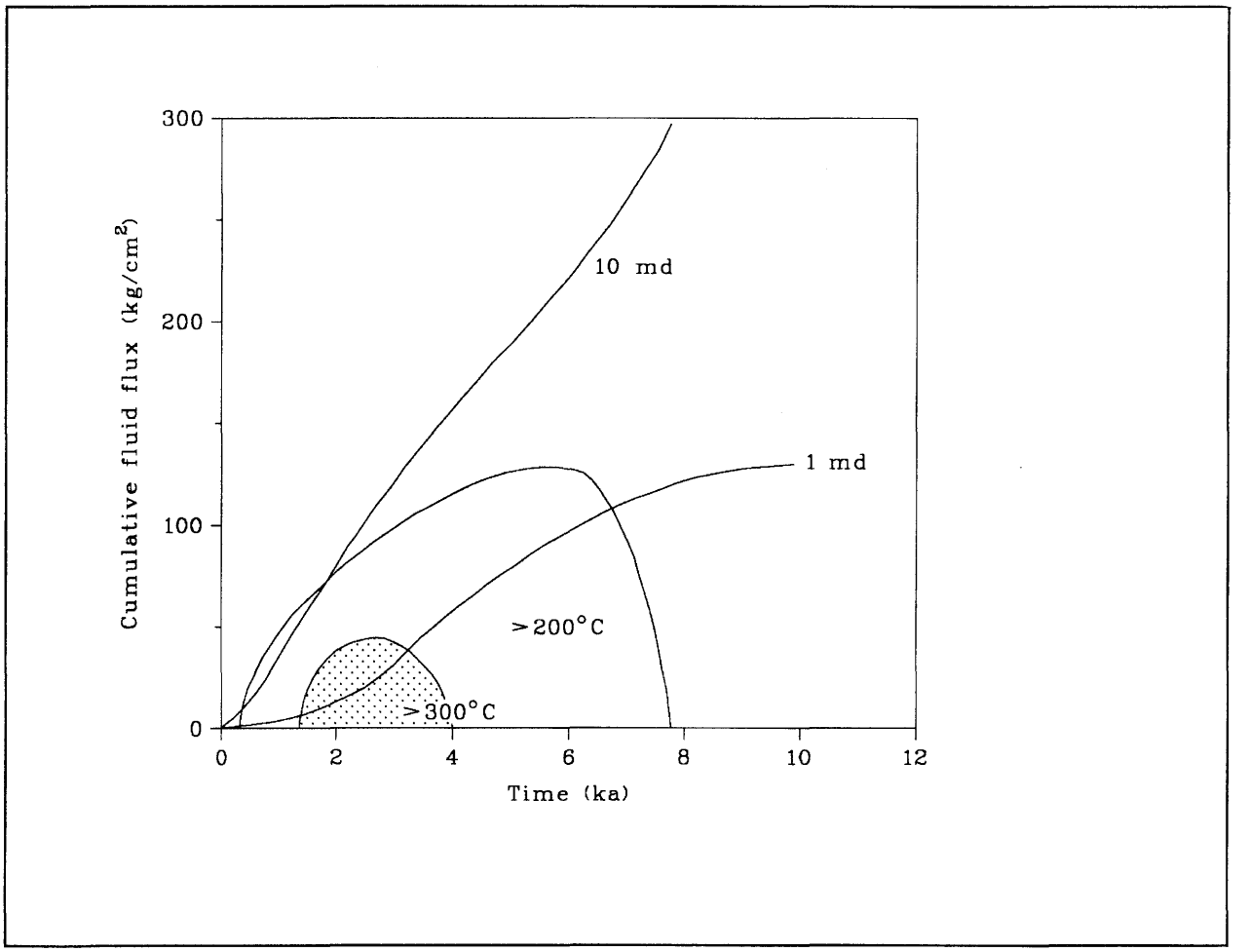

Figure 8.4. Cumulative fluid flux for the 10^{-8} ms^{-1} (1 millidarcy) and $10x10^{-8}$ ms^{-1} (10 millidarcy) cases. Points along curves at which the repository first exceeds 200° and 300°C, and the points at which the maximum temperature again drops below these values, are indicated and contoured. The time-cumulative flux domain where temperatures are greater than 300°C are stippled. This figure shows that less than 100 kg/cm² of fluids hotter than 200°C will circulate through the repository.

cooled below 200°C and was essentially Raleigh-Bernard convection driven by natural geothermal heat flux.

The derived values for fluid flow in and around the model repository, including depth of circulation, maximum temperatures reached, and probability of boiling, were strikingly similar to the Poços de Caldas analogue. The main difference is that the Poços de Caldas breccia pipe focussed much of the hydrothermal circulation and transmitted approximately 10^5 kg/cm^2 to the surface, whereas the model repository produced a more diffuse and much smaller circulation of around 10^2 kg/cm^2 (Fig. 8.4). Since chemical transport and alteration depend only upon the mass of fluid circulation when all other factors are equal, the three orders of magnitude difference between the two models indicates that alteration and uranium enrichment from the spent fuel around the model repository will be about 0.1% of that observed in the breccia pipe at the Osamu Utsumi mine.

8.5. Main conclusions

The intense alteration observed at the Osamu Utsumi mine required a cumulative fluid flux of approximately 10^5 kg/cm^2 through the breccia pipe. Fluids probably circulated to approximately 10 km depth through rock that had a permeability of at least 10^{-8} ms^{-1}. Uranium deposition occurred when the upwelling fluids, focussed in a few high permeability breccia pipes, boiled.

The temperatures, scale of the system, and mechanisms of alteration and precipitation were found to be remarkably similar between the natural analogue and the hypothetical repository. The main difference is that approximately three orders of magnitude less hydrothermal (T>200°C) fluid passes through the model repository even under a worse case bulk permeability scenario. Following this line of reasoning, the alteration and radionuclide transport associated with this model repository would be less than 0.1% of that observed at the Osamu Utsumi mine.

The mineralogy of the calculated alteration is extremely sensitive to the thermodynamic values chosen to characterise the reacting minerals. In fact, it may be that the only way to obtain mineral thermodynamic data accurate enough to predict natural rock/water alteration is by deriving the information through the inversion of petrological observations, as done in Cathles and Shea (this report series; Rep. 13). Thus, currently available thermodynamic databases can be used as starting estimates, but must be refined for each deposit (or repository) case.

Laboratory experiments could be carried out to determine solution compositions at different temperatures, pressures and salinities for representative mineral phases and rock compositions. These data could then be inverted to give thermodynamic data for the mineral phases known to be involved in the reactions. These results could then be used to model the alteration and mass transport associated with any given physical convective system, such as a hydrothermal deposit or hypothetical repository.

8.6. Implications for repository behaviour

When applied to a very simple model of a high-level nuclear waste repository, the same physical models used to characterise the Poços de Caldas natural analogue site illustrated that the heat from radioactive decay of the waste packages would produce a remarkably similar hydrothermal circulation system. Clearly, a detailed analysis of specific repository behaviour would have to account for specific waste thermal parameters (inventory, fuel burn-up, heat output, pre-disposal storage time, etc.), rock and engineered barrier properties (thermal conductivities, etc.), as well as the geometry of the repository.

The depth of fluid circulation induced in uniformly permeable host rock by the model repository was 5 to 10 km, the maximum temperature was approximately 300°C, the lifetime of the induced high-temperature phase was a few thousands of years, and boiling caused most of the alteration around the model repository. Although the model is very simple and omits heterogeneity in rock hydraulic properties, the physical analysis emphasises the importance of permeability on a regional (10 km) scale in controlling the potential amount of circulation through a repository.

The high-temperature chemical transport models that were successfully used to interpret the mineralisation and alteration at Poços de Caldas were also applied to the model repository. In the worst case, where waste is emplaced in a highly permeable host rock with no engineered barriers to restrict the mobilisation of uranium, the amount of hydrothermal alteration will be approximately 0.1% of that found in the Osamu Utsumi mine breccia pipe, and the average concentration of uranium precipitation around the repository would be 0.05 μg/g (rather than 50 μg/g), with hydrothermal alteration amounting to 0.03 wt.% (rather than 30 wt.%, etc). These results could be verified by appropriate laboratory experiments, and could be easily adjusted for different rock types and repository parameters.

CHAPTER 9. CONCLUSIONS AND PROSPECTS

As befits the conclusion of a summary report, this Chapter draws together only the broader findings of the project, rather than reiterating the detailed technical conclusions drawn in Chapters 5 to 8.

The Poços de Caldas project has provided valuable information and experience that can be applied to the waste disposal issue at a number of levels. Foremost among these are the findings related to the declared performance assessment-related objectives of the project, which have formed the core of this report. A second important outcome is that both the results and the methodology used in the investigation have implications for repository site investigations. Although not foreseen as a product of the project at the outset, some useful guidance has been gained in this area. Finally, comment is made on the experience obtained in the process of bringing together data and models to understand and, to some extent, predict the behaviour of a natural groundwater system. In this respect it is important to realise that analogues are the only real training ground where modellers can realistically test their models before moving on to site-specific safety assessments, so a review of how efficient this process has been may provide useful lessons for future performance assessments.

This Chapter is thus broken into three sections addressing these issues at a general level. Again, for more detailed technical conclusions concerning the four performance assessment related objectives of the project, reference should be made to the final sections of Chapters 5 to 8.

9.1. The processes addressed in safety assessments

Radionuclide transport models routinely address very simple rock-water systems. If these are to be used in safety assessments they must be shown to be robust, in that they either overpredict (reasonably), or correctly predict, migration rates. The extent to which the project will help to build or demonstrate robustness in future assessments is referred to frequently in the following discussion.

In common with other analogue studies, this project has illustrated the complexity of natural groundwater systems and, in particular, has highlighted the importance of amorphous phases in suspension or as coatings on rock as the principal reactive surfaces for many trace elements in solution. The manner in which these phases precipitate and

then evolve to more crystalline forms can control the solution chemistry of the waters, so it is important to know whether this can affect the robustness of simple models which do not incorporate these mechanisms. The results of the project do, indeed, suggest that the presence of amorphous phases in an active geochemical environment tends both to reduce the concentrations of trace elements in solution, and reduce their mobility. Some of the fixing processes appear irreversible over very long timescales (compared to the reversible sorption used in performance assessment models), all of which indicates that simple performance assessment models tend to be conservative and might, in some circumstances, be overly pessimistic.

In addition, trace element solubility and speciation modelling, as would be applied in a safety assessment, has generally been shown to be adequately robust in tending to overpredict or correctly predict groundwater concentrations. There are one or two very notable exceptions to this, for example Ni in particular databases, and the work has highlighted database errors that need to be rectified. Where the project has been able to compare the performance of different geochemical thermodynamic codes and databases, the results have been encouraging. Again, with a couple of rather dramatic exceptions, there has been a reassuring degree of comparability, which indicates that this approach to calculating solubility limits can be as robust as the simpler laboratory-measured limits in purer waters.

Many of the observations made in the course of the redox front study provide direct evidence of the operation of flow channelling in fractures and solute transport in the rock matrix as the key controls on the shape and movement of these fronts, although the processes involved may be more complex than currently addressed in transport models. A consistent picture of very slow front movement and solute transport over the front dominated by diffusion clearly emerges. The very significant role that the front plays in retarding a wide spectrum of trace elements, even many non-redox-sensitive elements, was not foreseen before the study and adds a further element of conservatism to transport models involving redox discontinuities.

Colloid transport has been something of an unknown entity in safety assessments to date; if it could occur it would dominate some radionuclide release calculations. The evidence from Morro do Ferro is that particulate material suspended in deep groundwaters is not mobile, even in the colloid size range; indeed it seems to play a positive role in radionuclide retention by acting as a preferential sink for trace element fixation, which is then filtered out during passage through the rock. This conclusion also seems to hold in general for the role of the organic carbon content of deeper groundwaters.

Microbially mediated chemical reactions have again featured as being very significant, even in relatively deep groundwaters. The models used to predict microbial populations and activity levels in repositories appear to be reasonably consistent with field observations, and the net effect of microbial activity seems to be positive, i.e. catalysing redox reactions which may immobilise radionuclides.

One aspect of the sites which has presented some problems in interpreting processes, but has also been the cause for many of the driving forces behind these processes, is the amount of heterogeneity in the physical and chemical properties of the rocks and waters. In this respect we believe the sites to be little different to any other site that will need to be studied for disposal purposes. Heterogeneity occurs on all scales, and it has not always been possible to characterise it adequately; an example is the variability in flow properties (permeability, porosity, fracturing) along the Morro do Ferro hydraulic gradient. In order to interpret sparse information, quite robust models had to be constructed in a similar fashion to that which might be needed when characterising a repository site.

Perhaps the most encouraging findings of the project have concerned the degree of immobility of many of the radionuclides and trace elements studied. The largely undispersed nature of the thorium and rare-earth element deposit at Morro do Ferro, together with the sluggish movement of the Osamu Utsumi redox front "element trap", suggest that large-scale, rapid transport of radionuclides has not occurred at either site.

The physical and chemical models used to study the high-temperature processes at the Osamu Utsumi mine were also applied to a hypothetical underground repository. The predicted hydrothermal circulation system proved to be remarkably similar to that observed at the mine, but the alteration as modelled was only 0.1% of that in the breccia pipes. This is because the maximum hydrothermal circulation in the hypothetical repository was 1000 times smaller than in the natural system at Poços de Caldas. Therefore, as in this worst case where no barriers to fluid circulation are effective, the high-temperature alteration and radionuclide transport associated with a repository should be much smaller than that which has occurred in natural systems.

9.2. Designing site investigations

A well-founded understanding of rock-fluid interactions at a repository site forms the basis on which predictive transport models are built, and the principal evidence supporting models of very long term hydrogeological fluxes and evolution of the site.

Consequently, obtaining high-quality, well-chosen and representative rock-groundwater pairs for analysis is a very important aspect of site investigation. This is also what forms the basis of most natural analogue studies.

Much effort was put into defining representative sample points and adequate temporal monitoring programmes in the project. One of the problems facing any investigation is to distill out a manageable, high-quality and comprehensive dataset from the mass of available material, and to ensure that no bias is reflected in this selection. Bias can be introduced through preconceptions of the operative geochemical processes, and can lead to missed opportunities to collect data relevant to real, as opposed to perceived, processes. Examples are the positioning of boreholes along assumed hydraulic gradients/flow streamlines that subsequently prove more complex, or inadequate sample spacing across discontinuities.

These problems were partially avoided by phasing the investigations and gradually building up the project in terms of detail and complexity of measurement, but there remained, nevertheless, gaps and inconsistencies that could not be filled. Perhaps one of the key lessons for site investigations is therefore that it takes time and patience to get at the answers and the process cannot be rushed, no matter how much effort is invested at the outset. In the end, three years was barely adequate for a major project of this kind, and a full site investigation will inevitably take still longer. It goes without saying that time and money is well spent in obtaining full, high-quality, on-site hydrochemical data. Early, incomplete analyses were confusing and ultimately of little use. In-situ speciation studies also began to prove their value towards the end of the project, and the importance of including microbiological characterisation work at the outset was fully justified.

Some lessons arise that can also be transferred most appropriately to future analogue studies. First, something which is probably almost universally true of any analogue site; although there are clear and obvious processes of interest to study, the site is inevitably more complex, ill-bounded, and of poorer quality in terms of multiple superimposed mechanisms and perturbations to the system than originally expected. This is also worth pondering by modellers looking for simple, robust models of the repository far-field. It should be borne in mind that no matter how obvious and interesting a process may appear, it is not always possible to constrain it adequately enough for fully quantitative interpretation; a site cannot be forced to yield all the data that one might want.

A final point concerns the question of how "site-specific" the results of this study are. "Transferability" of findings to other sites is obviously important. There is no obvious answer to this question. Many of the results concerning the hydrochemical trace element

modelling, together with mechanisms at the redox front, are non-site-specific or, at least, could be justifiably transferred elsewhere with judicious, but non-controversial, modifications. The "colloid" results reflect the physical nature of the rock mass in terms of weathering, clay content, porosity, etc. The lack of mobility detected is felt to be a robust finding, given the dynamic and open nature of the system compared to deep repository host rocks. It is, however, important that more observations of the kind made in this study be assembled from diverse environments before the "colloid problem" is finally solved.

9.3. The modelling experience

Opportunities for modellers from the hydrochemical, radiochemical and hydrogeological fraternities to converge on a set of large-scale problems that parallel repository site characterisation needs are rare. This is one of the most obvious values of analogue studies as a training ground for eventual assessors. Although not easy to summarise, much was learned during this project.

It was often clear that each discipline talks a slightly different language, and it is dangerous to assume that technical jargon is fully understood by, or means the same thing to, each group. There was no substitute for frequent meetings and workshops, increasingly so towards the end of the project as the modelling developed.

The modellers' requirements for data can be insatiable, and care needs to be taken to establish comprehensive, quality-controlled datasets. The measurement limits for each parameter need to be checked closely against the modellers' requirements (e.g. detection limits for trace elements in water).

Some of the modellers' data requirements are impractical or impossible to fulfill. This needs to be checked at the outset, so that alternative approaches can be adopted early in the project. This was not always possible, and it has to be accepted that obtaining some data from natural systems is not feasible and, despite the tantalising closeness of an answer, recourse to very simple models and interpretations was sometimes needed. In the event, these often proved very satisfactory from the performance assessment end-use viewpoint.

An issue that must often be faced when planning a data-gathering exercise such as a site investigation is that one group of modellers cannot see the need for some of the data required by another group. Ensuring that all needs are covered is a complex task.

Finally, it was very encouraging to see the relationship between data-gatherers, interpreters, and performance assessors develop during the project. Explaining the performance assessment objectives and the limited needs for robust performance assessment use to specialists in different research areas can be difficult, particularly as this can seem to limit the prospects for data analysis. Reaching a good understanding between the different modelling groups at the outset is very important.

The Poços de Caldas project has been an excellent proving ground for the multiplicity of techniques and approaches that will be needed in geochemical site characterisation.

CHAPTER 10. ACKNOWLEDGEMENTS

This summary report was prepared by the project Technical Committee. It contains the distilled scientific product of a host of researchers in 27 laboratories on four continents, all of which was made possible by the goodwill and enthusiasm of individuals and organisations in Brazil. Many of these people have contributed freely of their own time to see the project through successfully and, more or less, on schedule. It has been a pleasure to work with the project group, and to feel that both a structure and an approach were being built that would prove useful in the future. One of the greatest pleasures obtained from working in a successful large international project is watching new relationships develop between individuals, between laboratories, and between disciplines. The sum of what has been presented in this report series is only part of the overall value of the Poços de Caldas project.

It would not be possible to thank all those who ought to be included in these Acknowledgements without providing a formidable list. The Technical Committee would simply like to pass on their gratitude to everyone who has helped to make the project a success, particularly their colleagues in Brazil. We make specific mention of the unsung heroes and heroines who were involved only in the final stages of preparation of the report series, and hence are unknown to most of those involved in the project. Worthy of particular mention are Maj-Britt Danielsson (Sweden), Linda McKinley (Switzerland) and Tapsa Tammela (Sweden) who were, respectively, responsible for the typing, final editing and coordinating of the reports. Furthermore, the coordination provided by Aline Kriesten (Switzerland), drafting by Margareta Smellie (Sweden), and additional typing by Berit Lembke-Mattson (Sweden), have proved indispensable. Finally, we thank Professor Werner H.B. Fassbinder, Department of Natural Philosophy and Pure Mathematics, University of Poços de Caldas, for his silent, unobtrusive yet constructive support throughout the duration of the project, and also the Poços de Caldas Naval Cadets for providing us with many a headwind. For the future, let's go to see.

CHAPTER 11. REFERENCES

Alexander, W.R., Scott, R.D., MacKenzie, A.B. and McKinley, I.G., 1988. A natural analogue study of radionuclide migration in a water conducting fracture in crystalline rock. *Radiochim. Acta*, 44/45, 283-289.

Amaral, G., Bushee, J., Cordani, V.G., Kawashita, K., and Reynolds, J.H., 1967. Potassium-Argon Ages of Alkaline Rocks from Southern Brazil, *Geochim. Cosmochim. Acta*, 31(2), 117-42.

Campos, M.J., Penna Franca, E., Lobão, N., Trindade, H., and Sachett, I., 1986. Migration of Ra from the Th ore deposit of Morro do Ferro, Poços de Caldas, Brazil. *J. Environ. Radioactivity*, 3, 145-161.

Cathles, L.M., 1977. An analysis of the cooling of intrusives by ground water convection which includes boiling, *Econ. Geol.* 72, 804-826.

Cathles, L.M., 1983. An analysis of the hydrothermal system responsible for the sulfide deposition in the Hokuroku Basin of Japan, *Econ. Geol.* Monogram 5, 439-487.

Chapman, N.A., McKinley, I.G., and Smellie, J.A.T., 1984. The potential of natural analogues in assessing systems for deep disposal of high-level waste. *SKBF/KBS* Tec. Rep. (84-16), Stockholm, Sweden, and *NAGRA* Tec. Rep. (84-41), Baden, Switzerland.

Côme, B. and Chapman, N.A., 1985. First CEC Natural Analogue Working Group (NAWG), Brussels. (Nov. 5-7). EUR 10315 EN-FR, 223 pp.

Cullen, T.L., and Penna Franca, E., 1977. International symposium in areas of high natural radioactivity. *Academia Brasileira de Ciências*, Rio de Janeiro (pub), 191 pp.

Eisenbud, M., Krauskopf, K., Penna Franca, E., Lei, W., Ballad, R., Linsalata, P. and Fujimori, K., 1984. Natural analogues for the transuranic actinide elements: An investigation in Minas Gerais, Brazil. *Environ. Geol. Water Sci.*, 6, 1-9.

Ellert, R., 1959. Contribuição á geologica do maciço alcalino de Poços de Caldas. *Bol. Fac., Fil. Ciênc. Letras*, Univ. São Paulo, 237, Geol. 18, 5-63.

Frayha, R. 1962. Urânio e tório no planalto de Poços de Caldas. *Dep. Nac. Prod. Min., Bul.* No. 116, 75 pp.

IPT, 1984. Geology, hydrology, geochemistry and radioactivity of Morro do Ferro: a critical review of the literature. Unpublished report of Instituto de Pesquisas Tecnológicas do Estado de São Paulo.

Kawashita, K., deMahigues, M.M., and Ulbrich, H., 1984. Idades Rb/Sr de Nefelina Sienitos do Anel Norte do Maciço Alcalino de Poços de Caldas, MG-SP, 33rd *Congresso Brasilerio de Geologia*, Rio de Janeiro, Resumos e Breves Comunicações, p. 244.

KBS, 1983. Final storage of spent nuclear fuel – KBS-3. SKBF/KBS, Stockholm. (Five volumes).

Kertes, A.S., and Guillaumont, R., 1985. Solubility of UO_2: A comparative review, *Nuclear Chem. Waste Management*, 5, 215-219.

Linsalata, P., Penna Franca, E. and Eisenbud, M., 1986. Ingestion estimates of thorium and the light rare earth elements based on measurements of human faeces, *Health Physics* 50, 163-167.

Loureiro, F.E.L. and Santos, R.C., 1988. The intra-intrusive uranium deposits of Poços de Caldas, Brazil. *Ore Geol. Rev., 3, 227-240.*

NAGRA, 1985. Nukleare Entsorgung Schweiz: Konzept und Uebersicht über das Projekt Gewähr. NAGRA, Tec. Rep. (85-01 to 08), Baden, Switzerland.

Osmond, J.J., Cowart, J.B. and Ivanovich, M., 1983. Uranium isotopes in ground water as an indicator of anomalies. *J. Appl. Radiat. Isot.* 34(1), 283-308.

Parks, G.A., and Pohl, D.C., 1988. Hydrothermal solubility of uraninite. *Geochim. Cosmochim. Acta* 52, 863-875.

Sørensen, H., 1974. The alkaline rocks. (Ed. H. Sørensen). *London*: Wiley.

Thiel, K., Vorwerk, R., Saager, R., and Stupp, H.D., 1983. ^{235}U fission tracks and ^{238}U disequilibria as a means to study recent mobilisation of uranium in Archaean pyrite conglomerates. *Earth Planet. Sci. Letts.*, 65, 249-62.

Tolbert, G.E., 1955. Preliminary report on the Morro do Ferro thorium bearing rare-earth deposit. Poços de Caldas plateau, Brazil. Rep. to Conselho Nacional de Pesquisas, Rio de Janeiro (unpublished).

Ulbrich, H.H.G.J., and Gomes, C.B., 1981. Alkaline Rocks from Continental Brazil, *Earth Science Review*, Vol. 17, 135-154.

Ulbrich, H., 1985. The Ultramafic-Alkaline and Gabbroic Alkaline Lineages: Derivation by Fractionation of Ultrabasic Alkaline Magmas? *Academia Brasileira de Ciencias*, Resumos das Comunicações, 57(1).

Wedow, H., 1967. The Morro do Ferro thorium and rare earth ore deposit, Poços de Caldas District, Brazil. *U.S. Geol. Surv., Bull.* 1185-D, 35 pp.

CHAPTER 12. APPENDICES

Appendix 1:

Management structure of the project.

Appendix 2:

List of Progress Reports, publications and presentations for the duration of the Poços de Caldas Project (May 1986 – March 1990).

Appendix 1
Management structure of the project.

The Poços de Caldas project was a cooperative venture supported by CNEN, the Brazilian Nuclear Energy Commission; Nuclebrás (now Urânio do Brasil), the Brazilian Government Nuclear Development Company; NAGRA, the Swiss National Cooperative for the Disposal of Radioactive Waste; SKB, the Swedish Nuclear Fuel and Waste Management Company; UKDOE, the United Kingdom Department of the Environment, and (since June 1987) USDOE, the United States Department of Energy. The project ran for three years from June 1986 to May 1989, with an extension period from June 1986 to March 1990.

Project administration and financial management was provided by SKB, with Fred KARLSSON acting as *Project Manager.*

The objectives and management of the work were approved and guided by a *Steering Committee*, comprising:

Per-Eric AHLSTRÖM	SKB (chairman)
Fernando BIANCHINI	CNEN
Roberto ESTEVES	URÂNIO DO BRASIL
Nick HARRISON	UKDOE
Charles McCOMBIE	NAGRA
Ed PATERA / Michael FERRIGAN	USDOE

The Project Manager, Fred Karlsson (SKB), acted as secretary to the Steering Committee.

The routine scientific management of the project was provided by a *Technical Committee*, which defined the field and laboratory programme and monitored progress. This committee reported to the Steering Committee, and comprised:

Neil CHAPMAN	Intera Sciences (chairman)
Ian McKINLEY	NAGRA
Eduardo PENNA FRANCA	Fed. University of Rio de Janeiro
Mike SHEA	Battelle Memorial Institute
John SMELLIE	Conterra (secretary)

John Smellie also acted as *Project Coordinator* and, together with Eduardo Penna Franca, the *Local Coordinator*, managed the day-to-day field operation of the project.

The Steering Committee met when it was deemed necessary, while the Technical Committee met at least once a year (in practice, more frequently). Progress was reported quarterly by the Project Coordinator from the reports of each participating laboratory, and in an annual report which briefly reviewed the main findings and outlined proposed work for the forthcoming year.

Collaborating laboratories and principal investigators

Laboratory	Research area	Investigators
Federal University, Rio de Janeiro	Microbiology, R/W/NSR	E. Penna Franca
Catholic University, Rio de Janeiro	Colloids, R/W/REE, R/W/NSR	N. Miekeley H. Coutinho de Jesus C.-L. Porto da Silveira
Nuclebrás (Urânio do Brasil), Poços de Caldas	Geology Microbiology/W analyses	L. Barroso Magno Junior A. Vialta L. Gomiero L. Wiikmann W. Filho
University of São Paulo	Petrology/mineralogy	H. Schorscher
Cen. Ener. Nuc. Agric., Piracicaba	W stable isotopes W analyses	P. Ocheuze Trivelin P. Krug
Cen. Des. Tecno. Nuc., Belo Horizonte	W radioisotopes	C. Schayer Sabino
British Geological Survey, Keyworth	Hydrogeology Microbiology	D. Holmes, D. Noy J. West
Scott. Univ. Res. Reactor Cent., East Kilbride	R/NSR	A. MacKenzie R. Scott
New York Univ. Medic. Cent.	MdF R/W/REE, R/W/NSR.	P. Linsalata
University of Florida	W/NSR	K. Osmond
University of Chicago	R/W interactions/ R isotopes	M. Shea
University of Bern	Petrology/mineralogy/ geochem Geochem. modelling	T. Peters N. Waber P. Lichtner
Paul Scherrer Inst., Würenlingen	Chem. modelling Colloid properties	J. Eikenberg C. Degueldre
Roy. Inst. Tech., Stockholm	Transport modelling Thermodynamic Chem. modelling	L. Moreno L. Romero I. Neretnieks J. Bruno
U.S. Geol. Survey	W geochem. interpretation	K. Nordstrom
Los Alamos Scientific Lab.	R/W Tc/Np/Pu analyses	D. Curtis

Laboratory	Research area	Investigators
Stanford University	Colloid modelling	B. Honeyman
Cornell University	Thermal/chemical modelling	L. Cathles
University of East Anglia	Geomorphology	A. Pitty
Inst. für Hydrologie (GSF)	W Radio/stable isotopes	M. Wolf
Atkins ES	Transport modelling	D. Read
SKB, Stockholm	Chemical modelling	P. Sellin
UKAEA, Harwell	Transport modelling	J. Cross A. Haworth S. Sharland C. Tweed
McMaster University	Sr isotopes	R. McNutt
Studsvik AB	W. Geochem. modelling	I. Puigdomenech
Ohio State University	Geochronology	K. Foland
Krueger Enterprises	R stable isotopes	H. Krueger
Lucas Heights Res. Lab.	NSR extraction analyses	R. Edghill

KEY:
R = rock
W = groundwater
NSR = natural series radioisotopes
REE = rare-earth elements
MdF = Morro do Ferro

Appendix 2
List of Progress Reports, publications and presentations for the duration of the Poços de Caldas Project (May 1986 – March 1990).

- Proposed Programme of Investigation at Poços de Caldas, Minas Gerais, Brazil (SKB, Stockholm).
- Presentation of the Poços de Caldas project, and status, made at the Second CEC Natural Analogue Working Group (NAWG) Meeting held at Interlaken, Switzerland (June 17-19, 1986).
- Poços de Caldas Project, Progress Report (June 1986 – August 1986). SKB, Stockholm.
- Poços de Caldas Project, Progress Report (September 1986 – November 1986). SKB, Stockholm.
- Smellie, J.A.T., Barroso Magno Jr., Luiz, Chapman, N.A., McKinley, I.G. and Penna Franca, Eduardo, 1987. The Poços de Caldas Project Feasibility Study 1986-7. Presented at a Symposium on 'Natural Analogues in Radioactive Waste Disposal', Brussels, April 28-30.
- Poços de Caldas Project, Progress Report (December 1986 – February 1987). SKB, Stockholm.
- Poços de Caldas Project, Progress Report (March 1987 – May 1987). SKB, Stockholm.
- Poços de Caldas Project, Feasibility Study, Final Report (June 1986 – May 1987). SKB, Stockholm.
- Poços de Caldas Project, Progress Report (June 1987 – August 1987). SKB, Stockholm.
- Poços de Caldas Project, Progress Report (September 1987 – November 1987), SKB, Stockholm.
- Miekeley, N. and Kuechler, I.L., 1987. Interactions between thorium and humic compounds in surface waters. *Inorg. Chim. Acta*, 140, 315-319.
- Miekeley, N., Vale, M.G.R. and Porto da Silveira, C.L., 1987. Determination of isotopic and total uranium at ultra-trace level in water by alpha-spectroscopy and micro-injection ICP-AES. *Inorg. Chim. Acta*, 140, 321-325.
- Poços de Caldas Project, Progress Report (December 1987 – February 1988), SKB, Stockholm.
- Poços de Caldas Project, Progress Report (March 1988 – May 1988). SKB, Stockholm.

- Poços de Caldas Project, Second Year, Final Report (June 1987 – May 1988).
- Smellie, J.A.T., 1988. Poços de Caldas , Minas Gerais, Brazil: A Natural Analogue Study. Presented at the Third CEC Natural Analogue Working Group (NAWG) Meeting, held at Snowbird, Utah (June 15-17, 1988).
- Poços de Caldas Project, Progress Report (June 1988 – August 1988). SKB, Stockholm.
- Miekeley, N., Coutinho de Jesus, H., Porto da Silveira, C.L. and Kuechler, I.L., 1988. Colloid investigations in the Poços de Caldas natural analogue project. Scientific Basis for Nuclear Waste Management (XII). *Mat. Res. Soc. Proc.* 127, 831-842.
- Smellie, J.A.T., Chapman, N.A., McKinley, I.G., Penna Franca, E. and Shea, M., 1988. Testing safety assessment models using natural analogues in high natural-series groundwaters; a progress report on the second year of the Poços de Caldas project. Scientific Basis for Nuclear Waste Management (XII). *Mat. Res. Soc. Proc.* 127, 863-870.
- West, J.M., Vialta, A. and McKinley, I.G., 1988. The influence of microbial activity on the movement of uranium at the Osamu Utsumi mine, Poços de Caldas, Brazil. Scientific Basis for Nuclear Waste Management (XII). *Mat. Res. Soc. Proc.* 127, 771-777.
- Poços de Caldas Project, Progress Report (September 1988 – November 1988). SKB, Stockholm.
- Zhu, M., 1988. Simulation of redox front movement in the Poços de Caldas mine. In: Some aspects of modelling of the migration of chemical species in groundwater systems. *Licentiate Thesis* (January 1988). Royal Institute of Technology, Dept. Chem. Eng., Stockholm.
- Poços de Caldas Project, Progress Report (December 1988 – February 1989). SKB, Stockholm.
- Poços de Caldas Project, Progress Report (March 1989 – May 1989). SKB, Stockholm.
- Romero, L., Moreno, L. and Neretnieks, I., 1989. Preliminary 3-Dimensional Modelling of the Redox Front at the Osamu Utsumi Uranium Mine. Presented as Test Case 7 (Natural Analogues) at *INTRAVAL* (June 16-18), Helsinki, Finland.
- Coutinho de Jesus, H., 1989. Desequilibrios radioativos em águas e rochas e outros aspectos geoquímicos da mina de urânio Osamu Utsumi e do depósito torífero Morro do Ferro, Poços de Caldas, M.G. *M.Sc. Thesis* (Unpublished). Pontifical Universidade Catholica do Rio de Janeiro (PUC).
- Poços de Caldas Project, Progress Report (June 1989 – August 1989). SKB, Stockholm.

- Poços de Caldas Project, Progress Report (September 1989 – November 1989). SKB, Stockholm.